UNIVERSIDADE DE TAUBATÉ
PROGRAMA DE PÓS-GRADUAÇÃO EM CIÊNCIAS AMBIENTAIS
Revista Ambiente & Água
An Interdisciplinary Journal of Applied Science

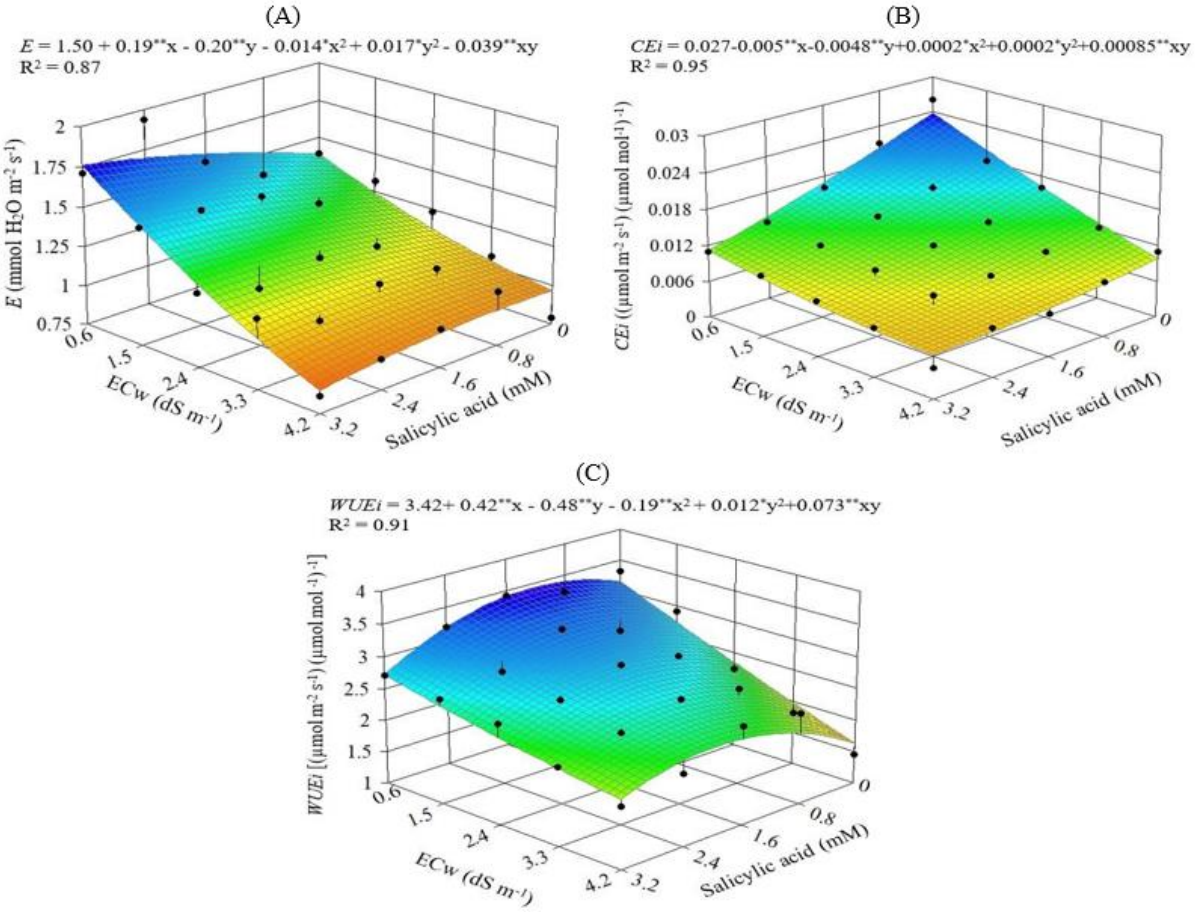

ISSN = 1980-993X (Online)
http://www.ambi-agua.net

EDITORIAL BOARD

Editors

Getulio Teixeira Batista (Emeritus Editor) Universidade de Taubaté - UNITAU, BR

Nelson Wellausen Dias (Editor-in-Chief), Fundação Instituto Brasileiro de Geografia e Estatística - IBGE, BR

	Associate Editors
Ana Aparecida da Silva Almeida	Universidade de Taubaté (UNITAU), BR
Marcelo dos Santos Targa	Universidade de Taubaté (UNITAU), BR
	Editorial Commission
Andrea Giuseppe Capodaglio	University of Pavia, ITALY
Arianna Callegari	Università degli Studi di Pavia, ITALY
Antonio Teixeira de Matos	Universidade Federal de Minas Gerais (UFMG), BR
Apostol Tiberiu	University Politechnica of Bucharest, Romênia
Claudia M. dos S. Cordovil	Centro de estudos de Engenharia Rural (CEER), Lisboa, Portugal
Dar Roberts	University of California, Santa Barbara, United States
Giordano Urbini	University of Insubria, Varese, Italy
Gustaf Olsson	Lund University, Lund, Sweden
Hélio Nobile Diniz	Inst. Geológico, Sec. do Meio Amb. do Est. de SP (IG/SMA), BR
Ignacio Morell Evangelista	University Jaume I- Pesticides and Water Research Institute, Spain
János Fehér	Debrecen University, Hungary
Julio Cesar Pascale Palhares	Embrapa Pecuária Sudeste, CPPSE, São Carlos, SP, BR
Luis Antonio Merino	Institute of Regional Medicine, National University of the Northeast, Corrientes, Argentina
Maria Cristina Collivignarelli	University of Pavia, Depart. of Civil Engineering and Architecture, Italy
Massimo Raboni	LIUC - University "Cattaneo", School of Industrial Engineering, Italy
Petr Hlavínek	Brno University of Technology República Tcheca
Richarde Marques da Silva	Universidade Federal da Paraíba (UFPB), BR
Stefan Stanko	Slovak Technical University in Bratislava Slovak, Eslováquia
Teresa Maria Reyna	Universidad Nacional de Córdoba, Argentina
Yosio Edemir Shimabukuro	Instituto Nacional de Pesquisas Espaciais (INPE), BR
Zhongliang Liu Beijing	University of Technology, China
Text Editor	Theodore D`Alessio, **FL, USA,** Maria Cristina Bean, **FL, USA**
Reference Editor	Liliane Castro, **Bibliotecária** - CRB/8-6748**, Taubaté, BR**
Peer-Reviewing Process	Marcelo Siqueira Targa, **UNITAU, BR**
System Analyst	Tiago dos Santos Agostinho, **UNITAU, BR**
Secretary and Communication	Luciana Gomes de Oliveira, **UNITAU, BR**

Library catalog entry by Liliane Castro CRB/8-6748

Revista Ambiente & Água - An Interdisciplinary Journal of Applied Science / Instituto de Pesquisas Ambientais em Bacias Hidrográficas. Taubaté. v. 17, n.3 (2006) - Taubaté: IPABHi, 2022.
Quadrimestral (2006 – 2013), Trimestral (2014 – 2016), Bimestral (2017), Publicação Contínua a partir de Janeiro de 2018.

Resumo em português e inglês.
ISSN 1980-993X

1. Ciências ambientais. 2. Recursos hídricos. I. Instituto de Pesquisas Ambientais em Bacias Hidrográficas.

CDD - 333.705
CDU - (03)556.18

TABLE OF CONTENTS

COVER:

This figure shows some of the results obtained from research developed in the Northeastern region of Brazil aimed at evaluating the effect of foliar application of salicylic acid at different concentrations in mitigating the deleterious effects of salt stress on gas exchange, growth, and quality of 'Paluma' guava seedlings. Figures A, B, and C show response curves for transpiration - *E* (A), instantaneous carboxylation efficiency -*CEi* (B) and instantaneous water use efficiency - *WUEi* (C) as a function of the interaction between water salinity - ECw and salicylic acid - SA concentrations in guava. Source: XAVIER, A.V.O. *et al*. Gas exchange, growth and quality of guava seedlings under salt stress and salicylic acid. **Rev. Ambient. Água, Taubaté, vol. 17 n. 3, p. 1-17, 2022.** ***doi:10.4136/ambi-agua.2816***

ARTICLES

Ambiente & Água - An Interdisciplinary Journal of Applied Science
ISSN 1980-993X – doi:10.4136/1980-993X
www.ambi-agua.net
E-mail: ambi.agua@gmail.com

Tannins from cashew tree (*Anacardium occidentale*) bark as a flocculant for water clarification

ARTICLES doi:10.4136/ambi-agua.2815

Received: 19 Nov. 2021; Accepted: 18 Apr. 2022

Bruna Ferreira dos Anjos[1]; Tatiane Kelly Barbosa de Azevêdo[2]; Bruna Rafaella Ferreira da Silva[3]; Renata Martins Braga[2]; Alexandre Santos Pimenta[2*]; Francisca Adriana Ferreira De Andrade[2]

[1]Programa de Pós Graduação em Agronomia. Departamento de Proteção Vegetal. Universidade Estadual Paulista "Júlio de Mesquita Filho" (UNESP), Avenida Universitária, n° 3780, CEP: 18610-034, Botucatu, SP, Brazil. E-mail: bruna.anjos07@gmail.com
[2]Programa de Pós-graduação em Ciências Florestais. Escola Agrícola de Jundiaí. Universidade Federal do Rio Grande do Norte (UFRN), RN 160, Km 03, s/n, CEP: 59280-000, Macaíba, RN, Brazil. E-mail: tatianekellyengenheira@hotmail.com, renatabraga.r@gmail.com, dricaandrade123@gmail.com
[3]Departamento de Ciências Florestais. Universidade Federal Rural de Pernambuco (UFRPE), Rua Dom Manuel de Medeiros, s/n, CEP: 52171-900, Recife, PE, Brazil. E-mail: brunarafaellaf@hotmail.com
[*]Corresponding author. E-mail: alexandre_spimenta@hotmail.com

ABSTRACT

Concern about the overexploitation of natural resources has increased in recent decades, especially involving water and its treatment. Paradoxically, one of the sources of water pollution is the treatment itself, due to the use of chemical flocculants, which end up generating sludge that may be highly aggressive to the environment. One of the ways to solve this problem is to use natural flocculants for this purpose, since they are biodegradable and do not harm nature. This study evaluated the efficiency of a natural flocculant produced from tannins extracted from the bark of the cashew tree (*Anacardium occidentale*) and compared it with two commercial coagulants, Tanfloc® and iron chloride. The water for treatment was collected from a weir. The cashew trees' bark was collected, ground, and submitted to hot-water extraction to yield the tannins, and the extraction product was cationized. The flocculation tests were carried out using the jar test with solutions having concentrations of 33.3, 66.7, and 100 mg L^{-1}. Turbidity and pH were analyzed before and after flocculation. Among the assessed flocculants, the cationized tannins produced the best responses both for removal of turbidity and final pH of the treated water. Tanfloc® also produced satisfactory results regarding turbidity removal. The iron chloride, besides not properly clarifying the water, left it very acidic. Since the cationized tannins practically did not change the pH and were effective in the removal of turbidity, they represent an interesting, sustainable alternative product to treat the water.

Keywords: cationized tannins, natural flocculating agente, removal of turbidity, water treatment.

Uso de taninos da casca de cajueiro (*Anacardium occidentale*) como floculante para remoção de turbidez de água

RESUMO

A preocupação com a exploração desenfreada dos recursos naturais tem aumentado nas

This is an Open Access article distributed under the terms of the Creative Commons Attribution License, which permits unrestricted use, distribution, and reproduction in any medium, provided the original work is properly cited.

últimas décadas, principalmente envolvendo a água e seu tratamento. Paradoxalmente, uma das fontes de poluição da água é justamente o seu tratamento, devido ao uso de floculantes químicos, que acabam gerando lodos que podem ser altamente agressivos ao meio ambiente. Uma das formas de resolver este problema é utilizar floculantes naturais para esta finalidade, uma vez que são biodegradáveis e não agridem a natureza. O objetivo deste trabalho foi avaliar a eficiência de um floculante natural produzido com taninos extraídos da casca do cajueiro (*Anacardium occidentale*) e compará-lo com dois coagulantes comerciais, Tanfloc® e cloreto de ferro. A água para tratamento foi coletada de um açude. A casca do cajueiro foi coletada, moída e submetida à extração em água quente para obtenção dos taninos, e o produto da extração foi cationizado. Os testes de floculação foram realizados utilizando-se o jar test com soluções nas concentrações de 33,3, 66,7 e 100 mg L^{-1}. A turbidez e o pH foram analisados antes e após a floculação. Dentre os floculantes avaliados, os taninos cationizados produziram as melhores respostas tanto para remoção de turbidez quanto para pH final da água tratada. O Tanfloc® também apresentou resultados satisfatórios quanto à remoção de turbidez. O cloreto de ferro, além de não clarificar adequadamente a água, a deixou muito ácida. Como os taninos cationizados praticamente não alteraram o pH e foram eficazes na remoção da turbidez, consistem em um produto interessante para o tratamento da água.

Palavras-chave: floculante natural, remoção de turbidez, taninos cationizados, tratamento de água.

1. INTRODUCTION

The high level of urbanization in the world is negatively affecting the quantity and quality of water supplies, making it increasingly difficult to satisfy societal needs. The treatment of water for human consumption, irrigation, and industrial use, among other activities, has prompted studies related to the reuse and/or recycling of water. However, this alternative requires a considerable increase in the use of flocculants for the removal of turbidity before the water is returned to the population (Sousa, 2018). The main water resources available to public supply are from the surface, whose quality is often degraded. In this respect, the employment of the traditional flocculants based on inorganic metallic salts, such as aluminum salts, is not always effective, and above all requires strict control of the residual aluminum in the water treated for human consumption. The presence of aluminum in treated water is undesirable because this element can damage the nervous system, as demonstrated by Kawamura (1991), among other researchers.

In this context, the use of natural products for water treatment has some advantages, such as renewable sources, the biodegradability of the residual sludge, low consumption of alkalis, and no release of metals after the water is treated (Yin, 2010). In the flocculation stage, flakes are formed due to the aggregation of neutralized particles (Béltran-Heredia *et al.*, 2011). According to Paula (2004), the formation of flakes can occur spontaneously as a result of successive collisions among the suspended particles, but only if energy is available for this process. According to Ioshimura (2016), sedimentation occurs due to the differential speed of decantation of the flakes. In all these steps, the consumption of energy and sedimentation time is reduced when flocculants are added to the water treatment. The use of tannins is an option that provides all the advantages cited above due to their ability to neutralize surface electrical charges of colloidal particles, promoting flocculation and sedimentation (Coral *et al.*, 2009). However, tannins in their original state do not have the cationic characteristics that enable their use as flocculants for the clarification of water. Thus, they have to go through a cationization reaction, where the substance becomes ionized when it dissolves in water, acquiring a positive charge and acting as a cation. In this form, cationized tannins can destabilize the colloidal system by neutralizing the charges of the particles that keep them in suspension in the untreated

water (Mangrich *et al.*, 2014).

Present in all forest plant species, mainly in the bark, condensed tannins are the most important class of tannins and have a broad range of applications in the pharmaceutical and food industries, leather making, adhesive production, and water treatment (Pizzi, 1994; Marques *et al.*, 2021). However, only a few studies have examined species from the dry forest of Northeast Brazil concerning their potential as sources of tannins for water treatment, mainly because they produce large amounts of bark. Some species of this biome have gained prominence, as is the case of *Anadenanthera colubrina* ('angico-vermelho') and *Mimosa tenuiflora* ('jurema preta'), both from the Fabaceae family.

The cashew tree (*Anacardium occidentale*) is native to Northeast Brazil. Besides the use of its pseudofruit as food (nuts and juice from the fruits), extracts also have medicinal therapeutic applications (Novaes and Novaes, 2021). The species is cultivated mainly in India, Vietnam, Côte d'Ivoire, Guinea-Bissau, Tanzania, Benin, Brazil, and other countries in East and West Central Africa and Southeast Asia, but plantations have also been established in South Africa and Australia (Global Cashew Council, 2021). World production of cashew nuts currently ranges between 720,000 and 790,000 metric tons (kernel basis) per year (seasons 2015/16-2019/20). India, with yearly output of 170,000-195,000 MT, ranks first, followed by Côte d'Ivoire, Vietnam, and Tanzania, with figures of 149,000; 82,000 and 53,000 MT, respectively (Oliveira *et al.*, 2020; Global Cashew Council, 2021).

The trunk of the cashew tree produces a yellow resin, known as cashew gum, which can replace the gum arabic used in the paper and pharmaceutical industries. The cashew tree wood is durable and pink in color and can be used in civil construction, cabinet making, joinery, etc. (Ceará, 2019). Pruning is one of the main management procedures applied to cashew trees. According to Embrapa (2021), young cashew orchards should be managed to form a compact canopy, with a large productive surface, free from entanglements and weed competition, in particular, to facilitate mechanized harvesting. Liming and fertilization (manual or mechanical) should be used as required, as well as inspection of the irrigation system when the crop is irrigated. In general, pruning is limited to removing parts of the tree attacked by insects or diseases, along with dry and broken branches. Since the fruiting of the cashew tree is peripheral, especially in the lower two-thirds of the plant, the elimination of the lower branches should be limited. In some cases, the strategy of canopy substitution can be successfully applied to unproductive and tall trees, where the crowns are removed and replaced by grafts of early-fruiting clones with small size and high production, keeping the root system and part of the trunk (Montenegro and Parente, 2018).

In all cases mentioned above, regular pruning and canopy substitution produce significant amounts of lignocellulosic material that is sold as firewood. Brazil has 439,200 ha cultivated with cashew trees (Novaes and Novaes, 2020), of which 99.5% are located in the country's Northeast region. Thus, every year thousands of tons of wood from cashew trees are used as firewood, mainly by brickyards. The bark is also burned as a source of energy. Nevertheless, despite these uses, a large amount of wood and bark waste is produced, so the development of other uses of these wastes has the potential to generate additional profits for growers. One option would be to find more uses of the condensed tannins from the bark and waste wood of cashew trees. The use of tannins for water clarification would achieve this goal.

To this aim, the present work assessed the technical viability of using tannins from cashew tree bark as flocculants for the clarification of water by coagulation and compared their performance with a commercial product and iron chloride. The novel aspect of this work is the employment of new raw material, more specifically, tannins from cashew tree bark, as a flocculant for water clarification.

2. MATERIAL AND METHODS

2.1. Tree selection and bark collection

For the experiments, 10 cashew trees (*Anacardium occidentale*) (around 15 years old) in good phytosanitary conditions were selected, considering the absence of pest attacks and diseases. The trees were located at the Forest Experimentation Unit (5°51′36″ S and 35°20′59″ W), Forest Engineering Department, Rio Grande do Norte Federal University (UFRN), in the municipality of Macaíba, Rio Grande do Norte State, Brazil. The local soil is classified as a sandy-textured yellow oxisol and the topography is flat (Beltrão *et al.*, 1975). The local climate is a transition between As and BSw, characterized as tropical rainy, according to the Köppen classification, with an annual average temperature of 27.1°C, average relative humidity of 76%, and total precipitation ranging from 863.7 to 1.070.7 mm (IDEMA, 2013).

After harvesting the trees, the bark was collected from the trunk and branches using a machete. The collected material was promptly packed in plastic bags to prevent moisture loss and stored for further processing. The bark was weighed and its natural moisture content was determined. The material was then dried outdoors in a sheltered shed. After the natural drying, the bark was chopped in a forage chopper (TRP-400 model, TRAPP, São Paulo-SP, Brazil). After this, the granulometry of the material was reduced by grinding in a Wiley mill (TE-650/1 model, CASALAB, Belo Horizonte-MG, Brazil).

2.2. Tannin extraction and quantification

For the tannin extraction and quantification, five 25 g dry samples were employed. The samples were transferred to 500 mL flat-bottomed glass flasks and 250 mL of deionized water was added to each one (1:10 weight/weight ratio). The samples were heated until boiling and kept under reflux for 2 hours. Each sample was double extracted to ensure the complete removal of the hot-water fraction. This way, the final bark/water ratio became 1:20 (w/w). After extraction, the solutions were filtered through flannel and a 150-mesh sieve to remove the fine particles. Then the extracts were filtered through a number-2 sintered glass filter. The extracts were concentrated by evaporation using a Soxhlet apparatus until a final volume of 50 mL. Two samples were employed for the determination of the total condensed tannins content (TTC) and one was evaporated until dry at 103 ± 2°C for 48 hours to determine the total solids content (TSC). The TSC was calculated using Equation 1.

$$TSC\ (\%) = \left(\frac{M1-M2}{M2}\right) x\ 100 \quad (1)$$

Where:

TSC = total solids content (%);

M_1 = Initial mass (g);

M_2 = Final mass (g).

For the determination of TTC, the Stiasny method was employed as described by Guangcheng *et al.* (1991) with three replicates. For this, 4 mL of formaldehyde (37% w/w) and 1 mL of hydrochloric acid were added to 50 mL of the raw extract. Each replicate was boiled under reflux for 30 min. After cooling, the precipitated tannins were separated by simple filtering through filter paper (Whatman Number 1) by using a 10 cm diameter Büchner funnel. The solids retained in the filter paper were oven-dried at 103 ± 2°C for 24 hours, weighed and the Stiasny number was calculated.

All the analyses were carried out in triplicate according to the methods recommended by Paes *et al.* (2006a; 2006b). The Stiasny number was obtained by Equation 2.

$$I\ (\%) = \left(\frac{M2}{M1}\right) x\ 100 \quad (2)$$

Where:

I = Stiasny number (%);

M_1 = Mass of solids in 50 mL of hot-water extract;

M_2 = Mass of precipitated tannins.

The total condensed tannins content of each sample was calculated by Equation 3.

$$TCT\ (\%) = \frac{TSC\ x\ I}{100} \quad (3)$$

2.3. Cationization and flocculation assays

Before use as a flocculating agent, the tannins' structure was modified by cationization. This process was carried out in three steps based on the reaction of Mannich reported by Konrath and Fava (2006). Initially, 5.4 g of aluminum chloride and 24.4 g of formaldehyde were placed in a reaction flask. The mixture was heated to 80 – 90°C for 2 hours. The effectiveness of the reaction between the reactants was checked until the mixture reached a pale-yellow color. Then the reaction product was stirred together with 28.0 g of an aqueous solution of tannins (50% weight/weight) for 30 min at 50 – 60°C. Next, the product of this second step was mixed with 0.2 g of monoethanolamine and left to react for 3 hours at 50 – 60°C.

The water employed in the flocculation assays was collected from a reservoir located at the Jundiaí School of Agriculture, Rio Grande do Norte Federal University (UFRN). Ten samples of 5 L were collected and stored under refrigeration until further use. For the flocculation assays, the jar test was used, with 1.5 L of water in each jar. Before the assays, the pH (HI9813-6N Grochek pH/EC/TDS/C Portable Meter w/ Cal Check, Hanna Instruments) and turbidity (portable turbidimeter, LaMotte model LTC-3000 we/wi) were determined. The performance of the cationized tannins as flocculating agents was compared with two commercial products: ferric chloride (iron-III chloride, Sigma-Aldrich) and Tanfloc® powder (Tanac, Montenegro, RS, Brazil). Tanfloc® is an organic flocculant produced with tannins from the bark of black wattle (*Acacia mearnsii*). As defined in preliminary tests and based on the study of Silva (2021), for all three flocculation agents we employed concentrations of 33.3, 66.7, and 100 mg L^{-1}, with two stirring speeds/times: 30 rpm for 30 min and 130 rpm for 2 min (slow and fast mixing). Those values were established based on the works of Beltrán-Heredia *et al.* (2009) and Sousa (2015). One hour after stirring, the final pH and turbidity of the water were determined. After each flocculant was applied in the water, the values of turbidity were determined in NTUs (nephelometric turbidity units) at intervals of 10 min until 60 min. The initial turbidity of the water samples was 150 NTUs. All assays were performed with this turbidity value as a starting point.

2.4. FTIR analysis

The tannins were analyzed by FTIR before and after cationization. The samples were oven-dried at 60°C for three hours. Then they were immobilized in KBr pellets and analyzed with a Shimadzu model IRA Affinity-1 spectrophotometer. The FTIR spectra were acquired by attenuated total reflectance (ATR). Each spectrum was acquired with 32 scans with a resolution of 4 cm^{-1} from 4,000 to 500 cm^{-1}.

3. RESULTS AND DISCUSSION

3.1. Tannin extraction and quantification

Table 1 reports the mean values found for total solids content (TSC), Stiasny number (I), and total condensed tannins content (TCT) in the hot-water extracts of cashew tree bark. The results found for the hot-water extraction and the tannin parameters were similar to those

determined in previous research works (Paes *et al.*, 2006a; 2006b).

Table 1. Means of total solids content (TSC), Stiasny number (I), and the total condensed tannins content (TCT) found in the hot-water extracts of cashew tree bark.

Source	TSC (%)	I (%)	TTC (%)
Cashew tree bark	33.4	59.5	19.8

3.2. Flocculation assays

Table 2 compares the performance of the three flocculants for the reduction of water turbidity. Mean values (from three replicates) of each assessed flocculant for the removal of turbidity are presented according to the time of sedimentation.

Table 2. Means of final turbidity obtained with increasing sedimentation times as a function of flocculant concentration.

Time of sedimentation (min)	Final turbidity (NTU) (with 33.3 mg L^{-1})	Final turbidity (NTU) (with 66.7 mg L^{-1})	Final turbidity (NTU) (with 100 mg L^{-1})
Cashew Bark Tannins			
10	40.33	22.66	19.00
20	26.33	8.13	3.10
30	22.00	6.50	2.53
40	2190	6.40	2.25
50	21.06	6.03	2.25
60	21.06	5.60	2.23
Tanfloc®			
10	11.53	25.00	34.66
20	3.66	7.93	22.00
30	2.73	7.76	20.00
40	2.43	7.73	19.33
50	2.43	7.73	18.33
60	2.36	7.43	18.00
Iron chloride			
10	39.66	51.66	63.33
20	30.33	41.33	41.33
30	30.00	40.33	39.66
40	28.66	40.33	39.33
50	28.33	40.00	39.00
60	28.33	39.66	39.00

*For each sedimentation time, the values of turbidity are the means of three replicates

As displayed in Table 2, the cationized cashew bark tannins presented the best removal of turbidity when the concentration of 100 mg L^{-1} was employed, since this parameter decreased from the initial value to 2.23 NTUs. For this flocculant, the best sedimentation time was 60 min with a concentration of 100 mg L^{-1}. Different behavior was observed for Tanfloc®, since the best removal of turbidity (18.00 NTUs) was achieved at the lowest concentration (33.3 mg L^{-1}), but also at 60 min of sedimentation. The iron chloride had behavior similar to Tanfloc®, with the best performance at the same concentration but after sedimentation for 40

min. However, it is important to highlight that the final turbidity value achieved for Tanfloc® was 8 times greater than the value found for the cashew bark tannins. For iron chloride, the value of this parameter was 17.4 times higher. These results indicate the good performance of the cationized cashew bark tannins for the removal of water turbidity. The products Tanfloc® and iron chloride had the advantage of requiring lower concentration to produce their best results, only 33.3 mg L^{-1}. Iron chloride did not present satisfactory results, since the final turbidity for all concentrations was higher than that achieved with the organic flocculants (cashew bark tannins and Tanfloc®). As mentioned before, Tanfloc® is a commercial product derived from tannins from the bark of *Acacia mearnsii* trees.

Table 3 reports the final pH of the treated water samples of the three flocculants. As can be observed, only slight alterations between the initial and the final values of pH were found in the water treated with the cashew bark tannins and Tanfloc, while for iron chloride, a significant change was determined, with the pH becoming less acidic with increased concentration.

Table 3. Effect of the type of flocculant on the final pH of the treated water.

Type of Flocculant	Concentration (mg L^{-1})	Initial pH	Final pH
Cashew bark tannins	33.3	6.80	7.14
	66.7	6.79	7.01
	100	7.02	6.88
Tanfloc®	33.3	7.84	7.10
	66.7	6.76	6.80
	100	6.97	6.70
Iron chloride	33.3	7.34	4.10
	66.7	7.05	3.20
	100	6.89	3.00

Good results with high concentrations of a flocculant based on cationized black wattle tannins to remove water turbidity were reported by Béltran-Heredia *et al.* (2011). Also, Silva (2021), employing a concentration of 33.3 mg L^{-1} of tannins from the bark of *Stryphnodendron adstringens* (‘barbatimão’) trees, achieved 75% turbidity reduction, while with the concentration of 100 mg L^{-1}, that parameter increased to 96%. Concerning the alteration of the pH of water after flocculation, Sousa (2018) studied the employment of tannins from *Anadenanthera peregrina* and *Tachigali aurea*, comparing them with iron chloride and aluminum sulfate. They reported only slight changes in pH after their use, and good efficiency even when mixed with the chemical flocculants, corroborating the relevance of natural products. As previously noted, the cationized cashew tannins assessed in this work promoted only a small change in pH of the treated water after the product was applied.

Comparison of the pH values showed that iron chloride did not comply with the regulations of the Brazilian National Environmental Council (CONAMA, 2011), which establishes that the value of this parameter must be in the range of 5 to 9. Coral *et al.* (2009), working with natural and chemical flocculant agents, also found results similar to ours, since the pH remained constant for Tanfloc® and decreased strongly with the use of aluminum sulfate. The same pattern was observed in our work for iron chloride.

3.3. FTIR analyses

The FTIR spectra of the cashew tree bark tannins in their pristine state and after cationization are presented in Figure 1.

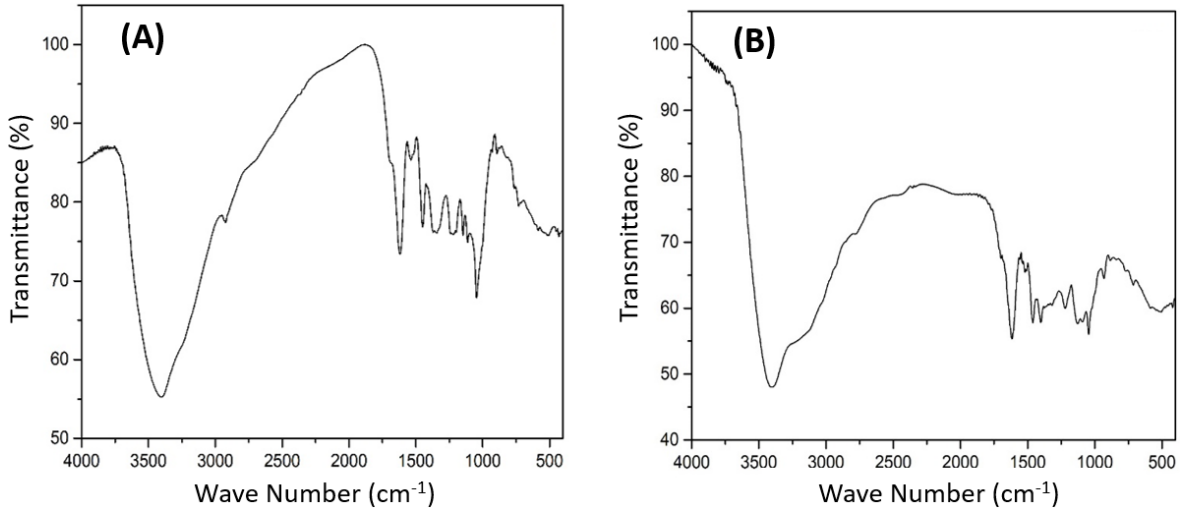

Figure 1. FTIR spectra of the cashew tree bark tannins, (A) original state and (B) after cationization.

Regarding the alterations in the chemical structure of the cashew bark tannins achieved after cationization, the spectra of the original product contained stretching bands related to hydroxyl groups (-OH) bonded to phenolic units and aliphatic chains at 3,400 cm^{-1}, with a transmittance of 85%, while for the cationized tannins, the transmittance was 100%. This result is in the same range as found by Marques *et al.* (2021), who determined the same responses for tannins from the bark of *Acacia mangium* (3,418 cm^{-1}), *Azadirachta indica* (3,452 cm^{-1}), *Mimosa tenuiflora* (3,418 cm^{-1}), and *Mimosa caesalpiniifolia* (3,429 cm^{-1}). Also, Silva (2021) found the same stretching band at 3,199 cm^{-1} for *Stryphnodendron adstringens* ('barbatimão'). The stretchings at 3,100 cm^{-1} found here for the cationized tannins can be attributed to primary amines (Silverstein *et al.*, 2019), indicating that N-H bonds were formed after the chemical modification of the tannins since they were not present in the product in its pristine form. The higher content of hydroxyl groups in the modified tannins is due to the reaction with formaldehyde (Ramires and Frollini, 2012).

Stretching related to C-H bonds from aromatic compounds was observed at 3,000 cm^{-1} for the original tannins. However, in the cationized versions, this stretching was not observed. For both types of tannins (before and after cationization), the spectral bands from 1,580 to 1,615; and 1,450 to 1,510 cm^{-1} of aromatic stretching (C=C from aromatic rings) were observed with peaks of strong and medium intensities. According to Ntenga *et al.* (2017), intense peaks of aromatic C=C bonds combined with a high Stiasny number can be considered an indicator of the purity of tannic extracts. However, despite the presence of similar strong peaks in the spectra of the cashew tree bark observed in Figure 1, high purity was not detected, since the Stiasny number in the hot-water extracts was 59.5% (Table 1).

For the cationized tannins, the peaks at 1,520 and 1,300 cm^{-1} disappeared, which was a result of the Mannich reaction. In the modified tannins, peaks appeared at 600 and 900 cm^{-1}. The first peak can be attributed to the out-of-plane stretching of the aromatic rings, most likely due to the action of the ammonium chloride employed in the cationization reaction, as stated by Faris *et al.* (2016). The same authors highlight that the second one can be attributed to the movements of -OH from aromatic alcohols and out-of-plane bending of aromatic CH.

Regarding the presence of formaldehyde in the water after treatment with the cationized tannins, the results of the analysis were negative, or at least when present, this compound was under the limits of detection of the method employed, of 0.001 mg L^{-1}. This quantification is important since several studies have proven the negative effects of formaldehyde on people exposed to it in water (Silva, 2021).

Concerning products for water clarification based on condensed tannins from the bark of

forest species, as cited above, several research works have been published. Tanfloc® is an example of a successful commercial product based on trees' bark tannins. Also, patents have been registered with innovative products. Still, Beltrán-Heredia *et al.* (2011) described in a scientific article a process to produce a flocculant based on trees' bark tannins. However, neither articles nor patents have been published or registered that employ tannins from the bark of cashew trees as raw material. The use of this material as a basis for producing a flocculant is therefore a clear novelty of the present work.

Brazilian patent BR 102015005684-2 A2 (Klein and Forte, 2015), titled "Process for obtaining a biodegradable flocculant from cashew tree gum and its use for the treatment of effluent waters", regards the obtention of a flocculant with the same end-use as the product whose application is depicted herein. However, in the cited patent, the flocculant is obtained from cashew tree gum. Such gum is mainly composed of polysaccharides and it is produced by the stem in a process named gummosis, partially as a natural phenomenon, partially in response to heat, drought stress, mechanical injuries, and fungal or bacterial attack (Cunha *et al.*, 2007; Pinto *et al.*, 2018). On the other hand, condensed tannins from cashew trees are polyphenolic products that are a constituent part of the bark. Therefore, the products cited above are rather different both in origin and chemical composition. The process described in this study is innovative in its entirety because it deals with the production of flocculant from a raw material derived from cashew bark, which has not been used in any previous process as a basis for the production of flocculant.

4. CONCLUSIONS

The flocculant agent produced through cationization of the cashew tree tannins presented better results for the removal of turbidity than the commercial products Tanfloc® and iron chloride. The use of Tanfloc®, for instance, brought about in final turbidity of 2.36 NTU, while after the application of the tannins this parameter reached 2.23 NTU. Similar to the Tanfloc®, the cashew tree tannins virtually did not modify the final pH of the treated water. On the other hand, the iron chloride made the water acidic after the removal of turbidity, reaching a final pH of 4.10 in the best condition of clarification (33.3 mg L^{-1}). Thus, the cationized tannins can be used as flocculant agents and their extraction from waste wood of cashew trees could be an interesting option to add value to the productive chain. The FTIR analyses showed the efficacy of the cationization of the tannins, since new bands of absorbance appeared in the spectra of the product after the chemical modification. The addition of new functional groups in the chemical structure of the cashew bark tannins explains the efficiency of the modified product for clarification of water.

5. ACKNOWLEDGEMENTS

This study was supported by the Office to Coordinate Improvement of Higher Education Personnel (CAPES) – Finance code 001. We are thankful to the NUPPRAR - Núcleo de Processamento Primário e Reuso de Água Produzida e Resíduos for assisting us in the analyses and interpretation of the experimental results.

6. REFERENCES

BELTRÁN-HEREDIA, J.; SÁNCHEZ-MARTÍN, J.; DÁVILA-ACEDO, M. A. Optimization of the synthesis of a new coagulant from a tannin extract. **Journal of Hazardous Materials**, v. 186, n. 2-3, p. 1704-1712, 2011. https://doi.org/10.1016/j.jhazmat.2010.12.075

BELTRÃO, V. A.; FREIRE, L. C. M.; SANTOS, M. F. **Levantamento Sem detalhado da Área do Colégio 379 Agrícola de Jundiaí – Macaíba/RN**. Recife: SUDENE, 1975. 380 p.

CEARÁ. **Potencial da madeira de cajueiro**. Available at https://www.ceara.gov.br/2019/06/05/projeto-cearense-descobre-o-potencial-inexplorado-da-madeira-de-cajueiros/. 2019. Accessed on November 16, 2021.

CORAL, L. A.; BERGAMASCO, R. B.; BASSETTIC, F. J. Estudo da viabilidade de utilização do polímero natural (TANFLOC) em substituição ao sulfato de alumínio no tratamento de águas para consumo. *In:* INTERNATIONAL WORKSHOP | ADVANCES IN CLEANER PRODUCTION, 2., May 20 th -22 nd, 2009, São Paulo-SP, Brazil. **Proceedings[…]** São Paulo: UNIP, 2009. Theme: Key Elements for a Sustainable World: Energy, water and climate change. Available at http://www.advancesincleanerproduction.net/second/files/sessoes/4a/4/F.%20J.%20Bassetti%20-%20Resumo%20Exp.pdf. Accessed on November 16, 2021.

CUNHA, P. L. R.; MACIEL, J. S.; SIERAKOWSKI, M. R.; PAULA, R. C. M.; FEITOSA, J. P. A. Oxidation of cashew tree gum exudate polysaccharide with TEMPO reagent. **Journal of the Brazilian Chemical Society**, v. 18, n. 1, 2007. https://doi.org/10.1590/S0103-50532007000100009

EMBRAPA. **Cultivation of the cashew tree**. 2021. Available at https://www.agencia.cnptia.embrapa.br/gestor/caju/arvore/CONT000fiekra6m02wyiv80z4s473fubzdpp.html. Accessed on November 10, 2021.

FARIS, A. H.; IBRAHIM, M. N. M.; RAHIM, A. A. Preparation and characterization of green adhesives using modified tannin and hyperbranched poly (amine-ester). **International Journal of Adhesion and Adhesives**, n. 71, p. 39-47, 2016. https://doi.org/10.1016/j.ijadhadh.2016.08.009

GLOBAL CASHEW COUNCIL. **Cashew nut annual report**. 2021. Available at https://www.cashews.org/en/cashew-information. Accessed on November 11, 2021.

GUANGCHENG, Z.; YUNLU, L.; YAZAKI, Y. Extractive yields, Stiasny values, and polyflavonoid contents in barks from six acacia species in Australia. **Australian Forestry**, v. 554, n. 2, p. 154-156, 1991. https://doi.org/10.1080/00049158.1991.10674572

IDEMA. **Perfil do seu município: Macaíba-RN, Brazil**. Natal, 2013.

IOSHIMURA, R. A. **Estudo da eficiência granulométrica no processo de filtração direta com aplicação de coagulantes no tratamento de água**. 2016. 63 f. Trabalho de Conclusão de Curso (Graduação) - Universidade Tecnológica Federal do Paraná, Londrina, 2016.

KAWAMURA, S. Effectiveness of natural polyelectrolytes in water treatment. **Journal American Water Works Association**, v. 83, n. 10, p. 88-91, 1991. https://doi.org/10.1002/j.1551-8833.1991.tb07236.x

KLEIN, J. M.; FORTE, M. M. C. **Process for obtaining a biodegradable flocculant from cashew tree gum and its use for the treatment of effluent waters**. Deposited: Instituto Nacional da Propriedade Industrial – INPI. BR 102015005684-2 A2. Depósito: 2015.

KONRATH, R. A.; FAVA, F. J. **Processo de preparação de um agente floculante à base de extrato vegetal**. Deposited: Instituto Nacional da Propriedade Industrial – INPI. BR PI0500471-3 A. Depósito: 2006.

MANGRICH, A. S.; DOUMER, M. E.; MALLMANN, A. S.; WOLF, C. R. Química verde no tratamento de águas: Uso de coagulante derivado de tanino de *Acácia mearnsii*. **Revista Virtual de Química**, v. 6, n.1, p. 2–15, 2014. http://dx.doi.org/10.5935/1984-6835.20140002

MARQUES, S. R. R.; AZEVÊDO, T. K. B; CASTILHO, A. R. F.; BRAGA, R. M.; PIMENTA, A. S. Extraction, quantification, and FTIR characterization of bark tannins of four forest species grown in Northeast Brazil. **Revista Árvore**, v. 45, e4541, 2021. http://dx.doi.org/10.1590/1806-908820210000041

MONTENEGRO, A. A. T.; PARENTE, J. I. G. **Método para estimar a oferta de lenha na substituição de copa em cajueiros**. Fortaleza: EMBRAPA , 2018. 6 p.

NOVAES, T. E. R.; NOVAES, A. S. R. Analysis of the medicinal potential of cashew tree (*Anacardium occidentale* Linn): a brief review. **Research, Society and Development**, v. 10, n. 1, e4180111838, 2021. http://dx.doi.org/10.33448/rsd-v10i1.11838

NTENGA, R.; PAGORE, F. D.; PIZZI, A.; MFOUMOU, E.; OHANDJA, L. M. A. Characterization of tannin-based resins from the barks of *Ficus platyphylla* and of *Vitellaria paradoxa*: composites' performances and applications. **Materials Sciences and Applications**, v. 8, n. 12, p. 899-917, 2017. http://dx.doi.org/10.4236/msa.2017.812066

OLIVEIRA, N. N.; MOTHÉ, C. G.; MOTHÉ, M. G.; OLIVEIRA, L. G. Cashew nut and cashew apple: a scientific and technological monitoring worldwide review. **Journal of Food and Science Technology**, v. 57, n. 1, p. 12-21, 2020. http://dx.doi.org/10.1007/s13197-01904051-7

PAES, J. B.; LIMA, C. R.; DINIZ, C. E. F.; MARINHO, I. V. Avaliação do potencial tanífero de seis espécies florestais de ocorrência no Semiárido brasileiro. **Revista Cerne**, n. 12, p. 232-238, 2006a.

PAES, J. B.; MARINHO, I. V.; LIMA, R. A.; LIMA, C. R.; AZEVEDO, T. K. B. Viabilidade técnica dos taninos de quatro espécies florestais de ocorrência no semiárido brasileiro no curtimento de peles. **Revista Ciência Florestal**, n. 16, 453-462, 2006b. https://doi.org/10.5902/198050981927

PAULA, S. L. **Clarificação do extrato aquoso de Stevia Rebaudiana (Bert.) Bertoni, utilizando polímeros naturais**. 2004. Dissertação (Mestrado em Engenharia Química) – Universidade Estadual de Maringá, Maringá, 2004.

PINTO, A. P. S.; SILVA, K. G. H.; MANSUR, C. R. E. Evaluation of the application of cashew gum as an excipient to produce tablets. **Polímeros**, v. 28, n. 4, 2018. https://doi.org/10.1590/0104-1428.04117

PIZZI, A. **Advanced wood adhesives technology**. New York: M. Dekker, 1994. 289 p.

RAMIRES, E. C.; FROLLINI, E. Tannin—phenolic resins: synthesis, characterization, and application as a matrix in biobased composites reinforced with sisal fibers. **Composites Part B**, n. 43, p. 2851–2860, 2012. https://doi.org/10.1016/j.compositesb.2012.04.049

SILVA, B. R. F. **Aplicação dos taninos de *Stryphnodendron adstringens* e *Mimosa tenuiflora* como coagulantes no tratamento de água para abastecimento**. Master dissertation (Graduate Program in Wood Science and Technology) - Universidade Federal de Lavras, Lavras, 2021. 70 p.

SILVERSTEIN, R. M.; WEBSTER, F.; KIEMLE, D.; BRYCE, D. **Spectrometric identification of organic compounds**. New York: John Wiley & Sons, 2019.

SOUSA, T. B. **Uso de taninos de espécies florestais no tratamento de água para abastecimento**. Master Dissertation (Graduate Program in Wood Science and Technology) - Universidade Federal de Lavras, Lavras, 2015. 96 p.

SOUSA, T. B. **Caracterização de cascas de espécies florestais brasileiras e uso de seus taninos na clarificação da água**. Doctoral thesis (Graduate Program in Engineering of Biomaterials) Universidade Federal de Lavras, Lavras, 2018. 75 p.

YIN, C. Y. Emerging usage of plant-based coagulants for water and waste treatment. **Process Biochemistry**, v. 45, n. 9, p. 1437–1444, 2010. https://doi.org/10.1016/j.procbio.2010.05.030

Ambiente & Água - An Interdisciplinary Journal of Applied Science
ISSN 1980-993X – doi:10.4136/1980-993X
www.ambi-agua.net
E-mail: ambi.agua@gmail.com

Gas exchange, growth and quality of guava seedlings under salt stress and salicylic acid

ARTICLES doi:10.4136/ambi-agua.2816

Received: 23 Nov. 2021; Accepted: 18 Apr. 2022

Adnelba Vitória Oliveira Xavier[1]; Geovani Soares de Lima[1*]; Hans Raj Gheyi[1]; André Alisson Rodrigues da Silva[1]; Lauriane Almeida dos Anjos Soares[2]; Cassiano Nogueira de Lacerda[1]

[1]Programa de Pós-Graduação em Engenharia Agrícola. Universidade Federal de Campina Grande (UFCG), Avenida Aprígio Veloso, n° 882, CEP: 58429-140, Campina Grande, PB, Brazil.
E-mail: adnelba_vitoria@hotmail.com, hgheyi@gmail.com, andrealisson_cgpb@hotmail.com, cassianonogueiraagro@gmail.com
[2]Unidade Acadêmica de Ciências Agrárias. Universidade Federal de Campina Grande (UFCG), Rua Jario Vieira Feitosa, n° 1770, CEP: 58840-000, Pombal, PB, Brazil. E-mail: laurispo.agronomia@gmail.com
[*]Corresponding author. E-mail: geovanisoareslima@gmail.com

ABSTRACT

Guava is a popular Brazilian fruit that is widely produced in Northeastern Brazil, a region with water sources that commonly have high concentrations of salts. Thus, searching for techniques that allow the management of these waters is extremely important for the expansion of irrigated agriculture. In this context, salicylic acid is a phytohormone that can contribute to reducing the effects of salt stress on plants. Given the above, this study evaluated the effect of foliar application of salicylic acid at different concentrations in the mitigation of salt stress on gas exchange, growth, and quality of 'Paluma' guava seedlings. The experiment was conducted in a greenhouse, in Campina Grande - PB, Brazil, using a randomized block design in a 5 × 5 factorial arrangement, corresponding to five levels of electrical conductivity of water (0.6, 1.5, 2.4, 3.3, and 4.2 dS m^{-1}) and five concentrations of salicylic acid (0 - Control; 0.8, 1.6, 2.4, and 3.2 mM), with four replicates and two plants per plot. Foliar application of salicylic acid at a concentration of up to 1.4 mM reduced the deleterious effects of salt stress on the instantaneous water use efficiency of 'Paluma' guava seedlings at 180 days after sowing. The concentrations of salicylic acid applied via foliar did not mitigate the harmful effects of irrigation water salinity on the growth and quality of 'Paluma' guava seedlings.

Keywords: Abiotic stress, *Psidium guajava* L., water scarcity.

Trocas gasosas, crescimento e qualidade de mudas de goiabeira sob estresse salino e ácido salicílico

RESUMO

A goiaba é uma fruta de grande aceitação pelos brasileiros e é largamente produzida no Nordeste do Brasil, região com a presença de fontes de água que comumente apresentam elevadas concentrações de sais. Assim, a busca por técnicas que permitam o manejo dessas águas é de extrema importância para expansão da agricultura irrigada. Neste contexto, o ácido salicílico é um fitohormônio que pode contribuir na diminuição dos efeitos do estresse salino

This is an Open Access article distributed under the terms of the Creative Commons Attribution License, which permits unrestricted use, distribution, and reproduction in any medium, provided the original work is properly cited.

nas plantas. Diante do exposto, objetivou-se com este estudo avaliar o efeito da aplicação foliar de ácido salicílico em diferentes concentrações na mitigação do estresse salino sobre as trocas gasosas, o crescimento e a qualidade de mudas de goiabeira 'Paluma'. O experimento foi conduzido em casa de vegetação, em Campina Grande – PB, utilizando-se o delineamento de blocos casualizados em arranjo fatorial 5 × 5, sendo cinco níveis de condutividade elétrica da água (0,6; 1,5; 2,4; 3,3 e 4,2 dS m^{-1}) e cinco concentrações de ácido salicílico (0 - Controle; 0,8; 1,6; 2,4 e 3,2 mM), com quatro repetições e duas plantas por parcela. A aplicação foliar de ácido salicílico na concentração de até 1,4 mM reduziu os efeitos deletérios do estresse salino sobre a eficiência instantânea no uso da água das mudas de goiabeira 'Paluma' aos 180 dias após o semeio. As concentrações de ácido salicílico aplicadas via foliar não mitigaram os efeitos nocivos da salinidade da água de irrigação sobre o crescimento e a qualidade das mudas de goiabeira 'Paluma'.

Palavras-chave: escassez hídrica, estresse abiótico, *Psidium guajava* L.

1. INTRODUCTION

Guava (*Psidium guajava* L.) is a tropical fruit found throughout Brazil, with emphasis on the cultivar Paluma for the great acceptance of its fruit by consumers, being consumed *in natura* or as processed products (Montes *et al.*, 2016). The fruit is easily found in open markets and supermarkets because it is the most cultivated in Brazil (Manica *et al.*, 2001; Dias *et al.*, 2012). The Northeast and Southeast regions of Brazil stand out as the largest guava producers in the country, respectively, accounting for 47.95 and 40.56% of the 22,128 hectares harvested. The state of Paraíba is responsible for 3.01% of guava production in the Northeast (IBGE, 2019).

The semi-arid region of Northeastern Brazil is characterized by high evapotranspiration rates, irregular rainfall and inadequate soil drainage, and well water most often has an electrical conductivity greater than 1.5 dS m^{-1}, standing out as a limiting factor for the production of various crops (Bezerra *et al.*, 2019). The salinity of irrigation water causes damage to agricultural production, inhibiting crop growth due to the reduction in water availability to plants because of a decrease in the osmotic potential of the soil solution, leading to stomatal closure and compromising transpiration and photosynthesis (Dias *et al.*, 2019).

Given the growing need to increase irrigated area studies that enable the use of saline water sources have become essential, especially in semi-arid regions (Silva *et al.*, 2021a). Thus, the use of elicitor substances such as salicylic acid (SA) has emerged as a promising alternative to minimize the harmful effects caused by biotic and abiotic stresses, including salinity (Nazar *et al.*, 2015).

Salicylic acid is a phenolic compound and acts as a growth regulator, playing an exclusive role in several physiological and biochemical processes, such as plant growth, floral induction, stomatal opening and closing, ion absorption, photosynthesis, and transpiration (Jini and Joseph, 2017; Silva *et al.*, 2020). Treatment with SA also reduces lipid peroxidation and may interact with other plant hormones to increase plant tolerance to salt stress (Souana *et al.*, 2020).

Some studies have reported that the exogenous application of SA increases the tolerance to salt stress in soursop (Silva *et al.*, 2020), almond (Mohammadi *et al.*, 2020), West Indian cherry (Dantas *et al.*, 2021), and tomato (Silva *et al.*, 2022). However, information on the use of salicylic acid in the production of guava rootstock under irrigation with saline water in the semi-arid region of the Northeast is scarce. In this context, this study evaluated the effect of foliar application of salicylic acid at different concentrations in mitigating the deleterious effects of salt stress on gas exchange, growth, and quality of 'Paluma' guava seedlings.

2. MATERIAL AND METHODS

The experiment was conducted from October 2020 to April 2021 in a greenhouse

belonging to the Academic Unit of Agricultural Engineering of the Federal University of Campina Grande (UFCG), in Campina Grande, PB, Brazil (07°15'18" S latitude, 35°52'28" W longitude and an average altitude of 550 m). The greenhouse used was of the arch type, 30 m long and 21 m wide, with a ceiling height of 3.0 m, with a low-density polyethylene cover (150 microns). The data of air temperature (maximum and minimum) and mean relative humidity of air during the experimental period are presented in Figure 1.

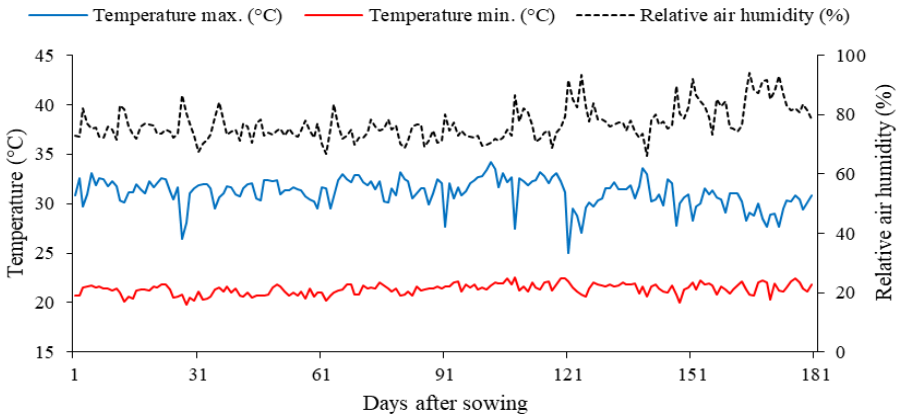

Figure 1. Mean values of air temperature (maximum and minimum) and relative humidity of air observed in the internal area of the greenhouse during the experimental period.

Treatments consisted of the combination of five levels of electrical conductivity of irrigation water - ECw (0.6 – Control, 1.5, 2.4, 3.3, and 4.2 dS m^{-1}) and five concentrations of salicylic acid - SA (0 – Control, 0.8, 1.6, 2.4, and 3.2 mM), distributed in randomized blocks in a 5 × 5 factorial arrangement with four replicates and two plants per plot. The levels of electrical conductivity of irrigation water were established considering the study conducted by Bezerra *et al.* (2019). The concentrations of SA were adapted according to Silva *et al.* (2020).

'Paluma' was the guava cultivar used in the experiment. It is a vigorous cultivar with easy propagation and tolerance to pests and diseases, especially rust (*Puccinia psidii* Wint.). The seeds used in the experiment were obtained from a guava orchard located in the experimental area of the Center of Science and Agri-Food Technology (CCTA), at the Pombal Campus belonging to UFCG, being manually extracted from the fruit pulp and subsequently air-dried in an open environment.

Irrigation waters with different electrical conductivities were prepared by dissolving NaCl, $CaCl_2.2H_2O$, and $MgCl_2.6H_2O$ in local-supply water (ECw= 0.28 dS m^{-1}) following the equivalent ratio commonly found in the Brazilian Northeast of 7:2:1 for Na^+, Ca^{2+}, and Mg^{2+} (Medeiros, 1992); the quantities of salts were determined considering the relationship between ECw and the salt concentration (Richards, 1954), according to Equation 1.

$$Q = 10 \, x \, ECw \quad (1)$$

Where:

Q = Quantity of salts to be added ($mmol_c$ L^{-1});

ECw = Electrical conductivity of water (dS m^{-1})

Salicylic acid concentrations were obtained by dissolving the acid in 30% ethyl alcohol. The solution was always prepared on the days of biweekly application events, with the addition of the Wil fix spreader (0.5 mL L^{-1}) to assist in the fixation of SA on the leaves by breaking the surface tension. Spraying on the adaxial and abaxial sides was performed with a manual sprayer between 17:00 and 18:00 hours. To minimize the evaporation of the solution from the leaf

surface, each plant before application was removed from the proximity of the others for spraying, avoiding cross-application of different concentrations of SA in each plot and returned to its location after spraying. Throughout the assay, a total of eight spraying operations were carried out with an average volume of 50 mL of SA applied per plant in each event.

The seedlings were grown in plastic bags with dimensions of 10 × 20 cm, filled with 1.6 kg of the substrate in the proportion of 3:1 (v/v basis) of a soil classified as *Neossolo Regolítico* (Entisol) with sandy loam texture, from the municipality of Lagoa Seca, PB, collected at 0-20 cm depth (A horizon), whose chemical and physical characteristics are shown in Table 1.

Table 1. Chemical and physical attributes of the soil used in the experiment, before application of the treatments.

Chemical characteristics								
pH (H_2O)	OM	P	K^+	Na^+	Ca^{2+}	Mg^{2+}	Al^{3+}	H^+
(1:2.5)	(g dm^{-3})	(mg dm^{-3})	cmol$_c$ kg^{-1}					
6.50	8.10	79.00	0.24	0.51	14.90	5.40	0.00	0.90

Chemical characteristics			Physical characteristics					
EC_{se} (dS m^{-1})	CEC (cmol$_c$ kg^{-1})	SAR_{se} (mmol L^{-1})$^{0.5}$	ESP	Particle-Size Fraction (g kg^{-1})			Moisture (dag kg^{-1})	
				Sand	Silt	Clay	FC[1]	PWP[2]
2.15	21.44	0.16	3.08	572.7	100.7	326.6	25.91	12.96

OM – Organic matter: Walkley-Black Wet Digestion; Ca^{2+} and Mg^{2+} extracted with 1 M KCl at pH 7.0; Na^+ and K^+ extracted with 1 M NH_4OAc at pH 7.0; Al^{3+} and H^+ extracted with 0.5 M calcium acetate at pH 7.0; ESP- Exchangeable sodium percentage; ECse – Electrical conductivity of saturation extract; SAR_{se} – Sodium adsorption ratio of soil saturation extract; [1]Field capacity tension of 33.42 kPA; [2]Permanent wilting point tension of 1519.50 kPa.

On the day prior to sowing, the soil moisture content was increased to the level corresponding to the maximum retention capacity with water of lowest level of electrical conductivity (ECw = 0.6 dS m^{-1}). Sowing was performed by placing 4 seeds per bag distributed equidistantly at a depth of 2 cm. After sowing, irrigation was carried out daily at 16 h, applying in each bag the volume corresponding to that obtained by the water balance, determined by Equation 2:

$$VI = \frac{(Va - Vd)}{(1 - LF)} \quad (2)$$

Where:

VI - volume of water to be used in the next irrigation event (mL);

Va - volume applied in the previous irrigation event (mL);

Vd - volume drained (mL); and

LF = leaching fraction (0.15).

Seedling emergence began at 20 days after sowing (DAS). After establishment of emergence, fertilization with nitrogen, phosphorus and potassium began as recommended by Novais *et al.* (1991), applying the equivalent to 100, 300, and 150 mg kg-1 of soil of N, P_2O_5, and K_2O, respectively, with the local-supply water (0.28 dS m^{-1}) split into nine applications from 40 DAS at intervals of 15 days up to 160 DAS. Applications with micronutrients were performed at the concentration of 2.5 g of Ubyfol® L^{-1} [(N (15%); P_2O_5 (15%); K_2O (15%);

Ca (1%); Mg (1.4%); S (2.7%); Zn (0.5%); B (0.05%); Fe (0.5%); Mn (0.05%); Cu (0.5%); Mo (0.02%)] through the leaves on their adaxial and abaxial sides, applied every two weeks to meet micronutrient needs.

Salicylic acid concentrations began to be applied at 67 DAS, when the plants showed uniform growth, and the other applications were performed every two weeks until 165 DAS. Irrigation with the different levels of water salinity started at 75 DAS, at daily intervals.

Plant growth was evaluated at 104 and 180 DAS through stem diameter (SD), measured with a digital caliper, plant height (PH), measured with a graduated ruler, and total leaf area (LA), obtained according to Lima *et al.* (2012) as shown in Equation 3:

$$LA = \sum 0.3205 \times L^{2.0412} \quad (3)$$

Where:

LA = total leaf area (cm^2);

L = leaf midrib length (cm).

The relative growth rates in plant height (RGR_{PH}), stem diameter (RGR_{SD}) and leaf area (RGR_{LA}) in the period from 104 to 180 DAS were obtained according to Benincasa (2003), as shown in Equation 4:

$$RGR = \frac{(lnA_2 - lnA_1)}{(t_2 - t_1)} \quad (4)$$

Where:

RGR = relative growth rate;

A_1 = plant growth at time t_1;

A_2 = plant growth at time t_2;

$t_2 - t_1$ = time difference between evaluations; and

ln = natural logarithm.

At 180 DAS, gas exchange was measured through stomatal conductance - *gs* (mol H_2O m^{-2} s^{-1}), transpiration - *E* (mmol H_2O m^{-2} s^{-1}), CO_2 assimilation rate – *A* (µmol CO_2 m^{-2} s^{-1}), internal CO_2 concentration – *Ci* (µmol m^{-2} s^{-1}), instantaneous carboxylation efficiency - *CEi* [(µmol m^{-2} S^{-1}) (µmol mol^{-1})$^{-1}$] and instantaneous water use efficiency - *WUEi* [(µmol m^{-2} s^{-1}) (mmol H_2O m^{-2} s^{-1})$^{-1}$]. Gas exchange was determined on the third leaf counted from the apex using the portable photosynthesis meter LCPro+ from ADC BioScientific Ltda. The obtained data were then used to quantify water use efficiency (*WUEi*) (A/E) [(µmol m^{-2} s^{-1}) (mmol H_2O m^{-2} s^{-1})$^{-1}$] and instantaneous carboxylation efficiency (*CEi*) (A/Ci) [(µmol m^{-2} s^{-1}) (µmol mol^{-1})$^{-1}$].

In the last evaluation (at 180 DAS), dry mass of leaf (LDM), stem (StDM), root (RDM), total dry mass (TDM) and Dickson quality index (DQI) of the seedlings were evaluated. The dry mass accumulation of each plant was obtained by oven drying for 48 hours and subsequent weighing on a semi-analytical scale, and TDM was obtained by the sum of dry mass of leaf, stem and root. Shoot dry mass (ShDM) was quantified by the sum of LDM and StDM.

Seedling quality was determined using the Dickson Quality Index - DQI (Dickson *et al.*, 1960), according to Equation 5:

$$DQI = (TDM)/[\left(\frac{PH}{SD}\right) + \left(\frac{ShDM}{RDM}\right)] \quad (5)$$

Where:

DQI= Dickson quality index;
PH = plant height (cm);
SD = stem diameter (mm);
TDM = total dry mass (g per plant),
ShDM = shoot dry mass (g per plant); and
RDM = root dry mass (g per plant).

The data obtained were subjected to analysis of variance by the F test, and when significance was observed, linear and quadratic polynomial regression analysis was performed for water salinity levels and salicylic acid concentrations ($p \leq 0.05$), using the statistical program SISVAR-ESAL version 5.6 (Ferreira, 2019).

3. RESULTS AND DISCUSSION

The interaction between saline levels (NS) and salicylic acid concentrations significantly influenced transpiration (E), instantaneous carboxylation efficiency (*CEi*), and instantaneous water use efficiency (*WUEi*), at 180 DAS (Table 2). On the other hand, saline levels significantly affected ($p \leq 0.01$) all gas exchange variables, except *WUEi*. The salicylic acid concentrations analyzed in isolation did not significantly influence the gas exchange variables of 'Paluma' guava.

Table 2. Summary of the analysis of variance for stomatal conductance (*gs*), internal CO_2 concentration (*Ci*), CO_2 assimilation rate (*A*), transpiration (*E*), instantaneous carboxylation efficiency (*CEi*) and instantaneous water use efficiency (*WUEi*) of 'Paluma' guava irrigated with different levels of salinity and subjected to exogenous application of salicylic acid at 180 days after sowing.

Source of variation	DF	Mean squares					
		gs	*Ci*	*A*	*E*	*CEi*	*WUEi*
Salinity level (SL)	4	0.004^{**}	4094.12^{*}	7.04^{*}	1.30^{**}	0.000248^{**}	0.98^{ns}
Linear regression	1	0.009^{**}	10522.22^{*}	2.90^{ns}	3.25^{**}	0.000165^{*}	1.91^{ns}
Quadratic regression	1	0.004^{**}	1487.14^{ns}	13.37^{*}	1.35^{**}	0.000477^{**}	1.38^{ns}
Salicylic acid (SA)	4	0.001^{ns}	2427.70^{ns}	0.49^{ns}	0.06^{ns}	0.000016^{ns}	0.53^{ns}
Linear regression	1	0.000^{ns}	582.60^{ns}	0.00^{ns}	0.21^{ns}	0.000014^{ns}	0.24^{ns}
Quadratic regression	1	0.002^{*}	6528.32^{*}	0.68^{ns}	0.01^{ns}	0.000008^{ns}	1.21^{ns}
Interaction (SL × SA)	16	0.001^{ns}	1181.05^{ns}	2.41^{ns}	0.14^{*}	0.000078^{**}	1.99^{*}
Blocks	3	0.001^{*}	3901.04^{ns}	1.83^{ns}	0.04^{ns}	0.000054^{ns}	1.55^{ns}
Residue	72	0.000	1653.02	2.33	0.07	0.000027	1.01
CV %		38.63	14.64	48.10	21.92	38.39	39.14

ns, *, ** respectively not significant, significant at $p \leq 0.05$ and $p \leq 0.01$; DF - degree of freedom; CV (%) - coefficient of variation.

The stomatal conductance of 'Paluma' guava seedlings was negatively affected by the increase in the electrical conductivity of the irrigation water up to 3.2 dS m^{-1} (Figure 2A). It is observed that plants irrigated with ECw of 3.2 dS m^{-1} obtained the lowest gs value (0.0488 mol H_2O m^{-2} s^{-1}), corresponding to a reduction of 40.0% (0.0325 mol H_2O m^{-2} s^{-1}), in relation to

plants irrigated with ECw of 0.6 dS m^{-1}. Stomatal closure with the increase in ECw is a response to the osmotic stress caused by excess salts, being an important strategy against dehydration, maintaining a high cell water potential (Dias *et al.*, 2020). Reduction in stomatal conductance of plants due to the increase in ECw was also observed by Dias *et al.* (2019), in a study with West Indian cherry cv. 'BRS 366 Jaburu' subjected to water salinity (0.8 and 3.8 dS m^{-1}).

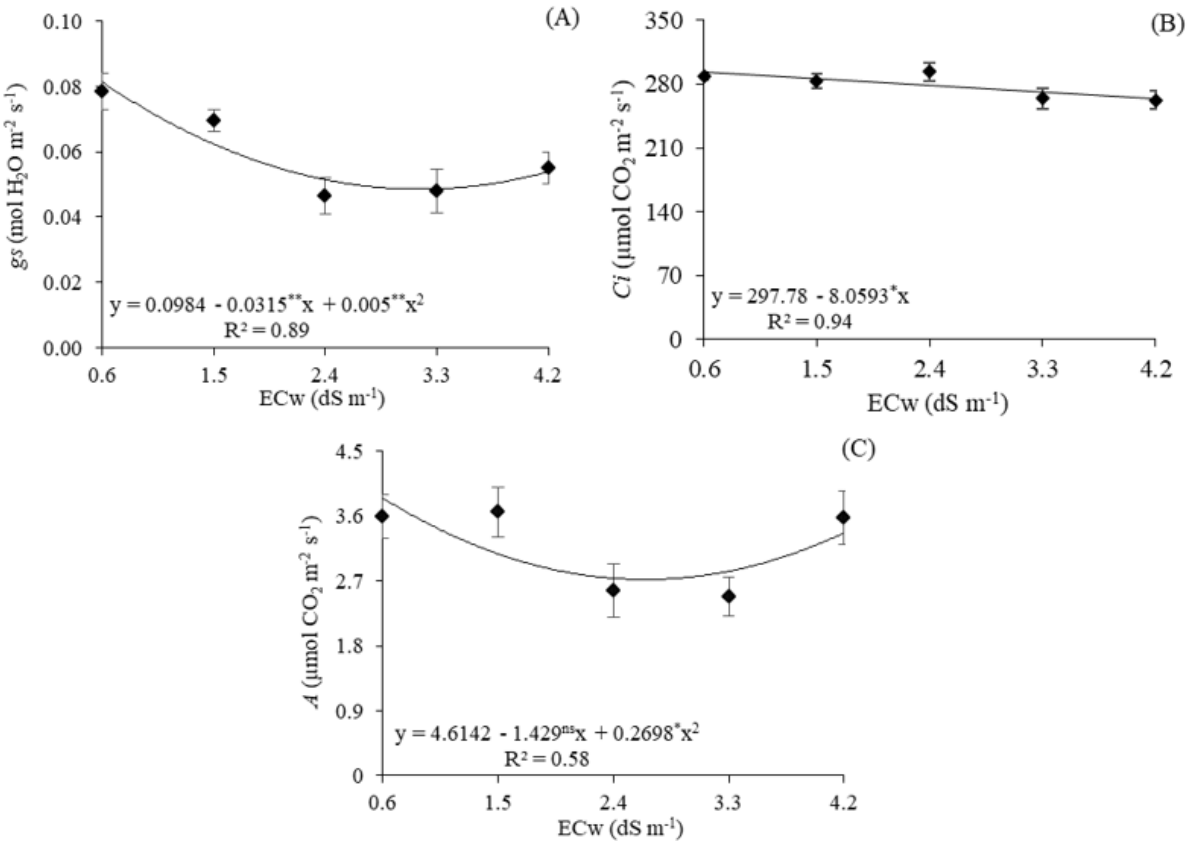

Figure 2. Stomatal conductance - *gs* (A), internal CO_2 concentration - *Ci* (B), and CO_2 assimilation rate - *A* (C) of 'Paluma' guava seedlings, as a function of the levels of irrigation water salinity - ECw and exogenous application of salicylic acid, at 180 days after sowing.
Vertical bar represents the standard error of the mean (n=4); *, ** respectively not significant, significant at $p \leq 0.05$ and $p \leq 0.01$.

The internal CO_2 concentration of the 'Paluma' guava was linearly reduced with the increase in the electrical conductivity of the irrigation water (Figure 2B), with a reduction of 2.71% per unit increase in ECw. When comparing the Ci of plants irrigated with water of higher salinity (4.2 dS m^{-1}) to those cultivated under the lowest salinity level (0.6 dS m^{-1}), a reduction of 10.0% is observed (29.01 µmol CO_2 m^{-2} s^{-1}). Corroborating the present study, Lacerda *et al.* (2022) in a study carried out with 'Paluma' guava under saline stress (0.6 and 3.2 dS m^{-1}) found a reduction of 9.51% (25.43 µmol CO_2 m^{-2} s^{-1}) in the Ci of plants irrigated with ECw of 3.2 dS m^{-1} compared to those cultivated under ECw of 0.6 dS m^{-1}. The reduction in *Ci* can be seen as a consequence of stomatal closure and is one of the main mechanisms responsible for the reduction in CO_2 assimilation rate (Lima *et al.*, 2021).

Analyzing the regression equation in Figure 2C, referring to the CO_2 assimilation rate, it appears that the guava seedlings had a reduction in A when irrigated with ECw of up to 2.65 dS m^{-1}. When comparing seedlings irrigated with ECw of 2.65 dS m^{-1} to plants cultivated under ECw of 0.6 dS m^{-1}, a reduction of 25.3% (0.92 µmol CO_2 m^{-2} s^{-1}) was observed. Reduction in CO_2 assimilation rate is directly related to stomatal closure, leading to a consequent reduction in leaf transpiration and a decrease in the internal CO_2 concentration in leaves (Altuntas *et al.*,

2018). Another factor to be considered that leads to reduction in *A* is the increase in mesophyll resistance to the entry of atmospheric CO_2 caused by salinity, which can also reduce enzymatic activities that are related to photosynthetic carbon metabolism (Soares *et al.*, 2021).

The increase in salicylic acid concentrations increased the transpiration of 'Paluma' guava seedlings when irrigated with ECw of up to 3.7 dS m^{-1} (Figure 3A). However, the maximum value of E (1.78 mmol H_2O m^{-2} s^{-1}) was recorded in plants irrigated with ECw of 0.6 dS m^{-1} and sprayed with a concentration of 3.2 mM of SA, corresponding to an increase of 21.9% (0.39 mmol H_2O m^{-2} s^{-1}) compared to those grown under the same ECw (0.6 dS m^{-1}) and without SA application (0 mM). Similar results were obtained by Silva *et al.* (2021a) in soursop plants under saline stress (ECw ranging from 0.8 to 4.0 dS m^{-1}), the authors found that foliar application of salicylic acid at a concentration of 1.4 mM promoted an increase in E regardless of the electrical conductivity of irrigation water.

According to Dantas *et al.* (2021), the increase in transpiration due to the application of salicylic acid may be related to its role in the regulation of stomatal opening, promoting the entry of water and CO_2 into the cells. In addition, under stressful conditions, salicylic acid helps to protect and increase the activity of antioxidant enzymes, increasing plant tolerance (Rajeshwari and Bhuvaneshwari, 2017).

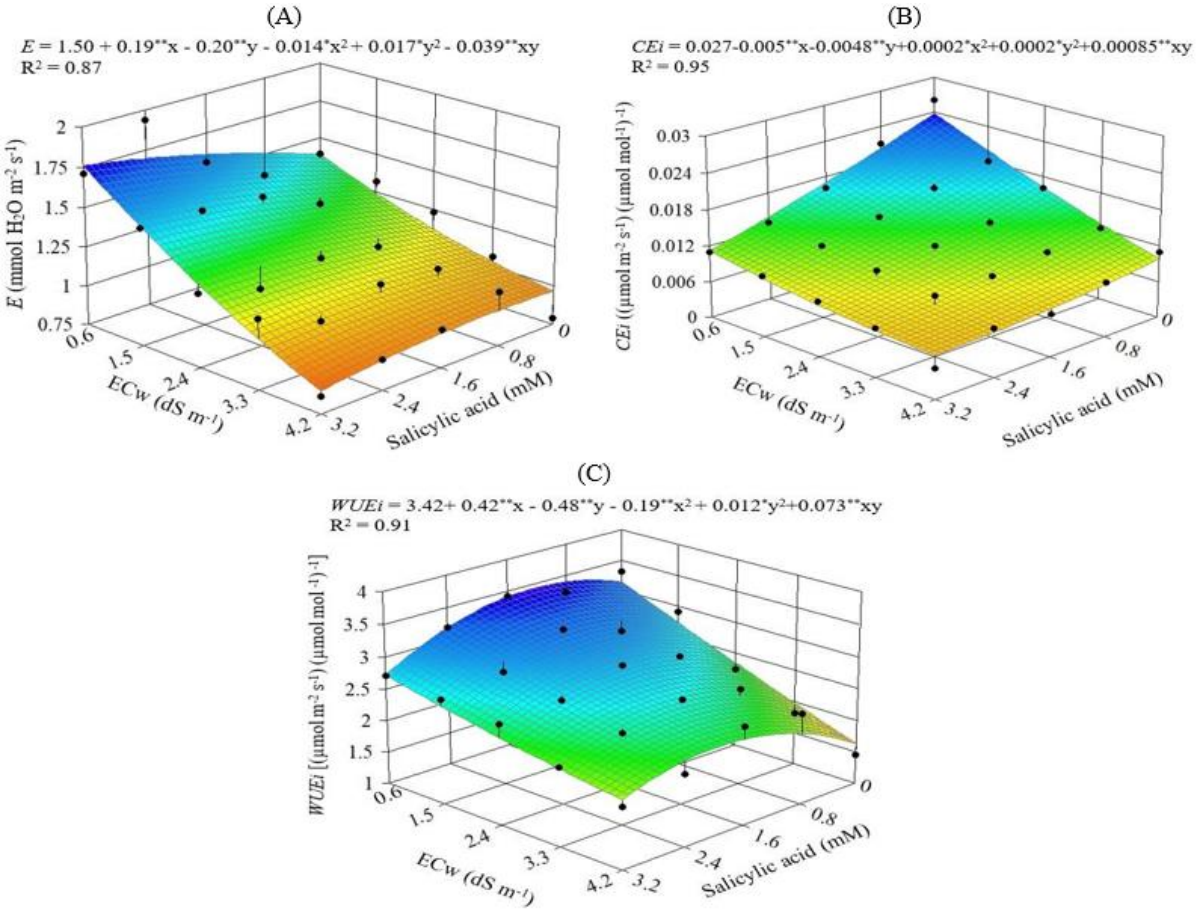

Figure 3. Response surface for transpiration - *E* (A), instantaneous carboxylation efficiency -*CEi* (B) and instantaneous water use efficiency - *WUEi* (C) as a function of the interaction between water salinity - ECw and salicylic acid - SA concentrations in guava cv. 'Paluma' at 180 days after sowing. X and Y - SA concentration and ECw, respectively; *, ** significant at $p \leq 0.05$ and $p \leq 0.01$, respectively. Point and vertical lines represent the mean and the standard error (n=4).

The instantaneous efficiency of carboxylation was negatively affected by the increase in the electrical conductivity of the irrigation water, regardless of the salicylic acid concentration.

The guava plants irrigated with ECw of 0.6 dS m^{-1} and submitted to a concentration of 0 mM of SA, stood out with the highest *CEi* value [0.0242 (μmol m^{-2} s^{-1}) (μmol mol^{-1})$^{-1}$]. The lowest *CEi* value [0.0078 (μmol m^{-2} s^{-1}) (μmol mol^{-1})$^{-1}$] was recorded in plants irrigated with ECw of 4.2 dS m^{-1} and subjected to a concentration of 3.2 mM SA. The decrease in instantaneous carboxylation efficiency due to salt stress may be associated with metabolic restrictions in the Calvin cycle and the occurrence of non-stomatal factors that act on the photosynthetic apparatus, such as inhibition of RuBisCO enzyme activity due to the reduction in the availability of ATP and NADPH (Lima *et al.*, 2020).

Foliar application of SA up to an estimated concentration of 1.4 mM promoted an increase in *WUEi*, regardless of the electrical conductivity of the irrigation water (Figure 3C). According to the regression equation, it appears that plants irrigated with ECw of 0.6 dS m^{-1} and submitted to a concentration of 1.4 mM of SA reached the highest *WUEi* value [3.42 (μmol m^{-2} s^{-1}) (μmol mol^{-1})$^{-1}$], corresponding to an increase of 8.9% [0.28 (μmol m^{-2} s^{-1}) (μmol mol^{-1})$^{-1}$] in relation to plants irrigated with the same ECw and without SA application (0 mM). On the other hand, the lowest *WUEi* value [1.62 (μmol m^{-2} s^{-1}) (μmol mol^{-1})$^{-1}$] was obtained from plants irrigated with ECw of 4.2 dS m^{-1} and without application of SA (0 mM).

Agami *et al.* (2019), in research carried out with wheat plants under water stress, also found that salicylic acid (0.1 mM) was able to increase the efficiency of water use, even in plants under stress. Salicylic acid is an endogenous phenolic-type regulator, which regulates the physiological and biochemical processes of plants to alleviate the deleterious effects caused by various stresses, including saline stress (Ghassemi-Golezani *et al.*, 2018).

According to the summary of the analysis of variance (Table 3), it can be seen that the interaction between the factors under study (SL × SA) did not significantly affect any of the analyzed variables. The saline levels analyzed in isolation significantly influenced all the variables under study. Furthermore, salicylic acid concentrations promoted a significant effect ($p \leq 0.05$) for RDM, TDM, and DQI.

The relative growth rates in plant height (RGR_{PH}), stem diameter (RGR_{SD}), and leaf area (RGR_{LA}) were negatively affected by the increase in the electrical conductivity of the irrigation water (Figure 4). A decreasing linear effect can be observed, with decreases per unit increment of ECw of 2.16, 9.09, and 6.15% in RGR_{PH}, RGR_{SD}, and RGR_{LA}, respectively. Comparison of 'Paluma' guava seedlings irrigated with an ECw of 4.2 dS m^{-1} with those grown under an ECw of 0.6 dS m^{-1}, indicated a reduction of 7.87% (0.0011 cm cm^{-1} day^{-1}) in the RGR_{PH}, 34.62% (0.0036 nm mm^{-1} day^{-1}) in the RGR_{SD} and 23% (0.0043 cm^2 cm^{-2} day^{-1}) in the RGR_{LA}, in the period from 104 to 180 DAS.

Similar results were observed by Bezerra *et al.* (2018a) in a study carried out with 'Paluma' guava under saline stress (ECw ranging from 0.3 to 3.5 dS m^{-1}), where they found that the increase in the electrical conductivity of irrigation water negatively affected the absolute and relative growth rates of plants. Reduction in growth of plant height and stem diameter is the result of changes in soil water potential caused by excess salts, which restricts water absorption, decreasing turgor pressure and cell activity of plants, by inhibiting cell expansion and elongation (Lopes *et al.*, 2019). Reduction in leaf area (Figure 4C) can be considered a mechanism to protect plants from salt stress, since it leads to a decrease in the absorption of water and toxic ions that would result in damage to essential biochemical processes (Dias *et al.*, 2020).

The increase in water salinity negatively affected the dry mass of leaf and stem accumulation of guava plants (Figure 5A and 5B), the reductions were 14.23% and 15.72% per unit increase, respectively. When comparing the LDM and StDM of plants irrigated with the highest salinity level (ECw=4.2 dS m^{-1}) to those of plants subjected to ECw of 0.6 dS m^{-1}, there were reductions of 56.01% and 62.48%, respectively.

Table 3. Summary of the analysis of variance for relative growth rates in plant height (RGR_{PH}), stem diameter (RGR_{SD}), and leaf area (RGR_{LA}) during the period 104 to 180 days after sowing (DAS), and dry mass of leaf (LDM), stem (StDM), and root (RDM), total dry mass (TDM) and Dickson quality index (DQI) of 'Paluma' guava plants irrigated with different levels of salinity and subjected to exogenous application of salicylic acid, at 180 days after sowing.

Source of variation	DF	Mean squares							
		RGR_{PH}	RGR_{SD}	RGR_{LA}	LDM	StDM	RDM	TDM	DQI
Salinity levels (SL)	4	0.000014^{**}	0.000047^{**}	0.000082^{*}	34.70^{**}	44.22^{**}	43.50^{**}	362.98^{**}	3.09^{**}
Linear regression	1	0.000019^{*}	0.000174^{**}	0.000232^{**}	137.35^{**}	173.99^{**}	671.79^{**}	1407.20^{**}	11.47^{**}
Quadratic regression	1	0.000000^{ns}	0.000001^{ns}	0.000008^{ns}	0.15^{ns}	1.39^{ns}	31.10^{**}	18.36^{ns}	0.47^{**}
Salicylic acid (SA)	4	0.000005^{ns}	0.000003^{ns}	0.000052^{ns}	2.43^{ns}	2.27^{ns}	0.66^{*}	14.04^{*}	0.07^{*}
Linear regression	1	0.000001^{ns}	0.000011^{*}	0.000132^{*}	0.65^{ns}	2.84^{ns}	2.02^{ns}	10.12^{ns}	0.01^{ns}
Quadratic regression	1	0.000017^{*}	0.000001^{ns}	0.000067^{ns}	4.89^{**}	1.54^{ns}	7.51^{**}	22.88^{*}	0.24^{**}
Interaction (SL × SA)	16	0.000002^{ns}	0.000003^{ns}	0.000043^{ns}	1.06^{ns}	0.69^{ns}	0.33^{ns}	4.29^{ns}	0.03^{ns}
Blocks	3	0.000024^{**}	0.000062^{**}	0.000025^{**}	4.77^{**}	14.07^{**}	1.13^{**}	25.77^{**}	0.01^{ns}
Residue	72	0.000004	0.000002	0.000025	1.09	1.02	0.24	4.19	0.02
CV %		14.81	17.00	30.11	24.51	24.68	18.70	20.20	19.25

^{ns}, *, ** respectively not significant, significant at $p \leq 0.05$ and $p \leq 0.01$; DF - degree of freedom; CV (%) - coefficient of variation.

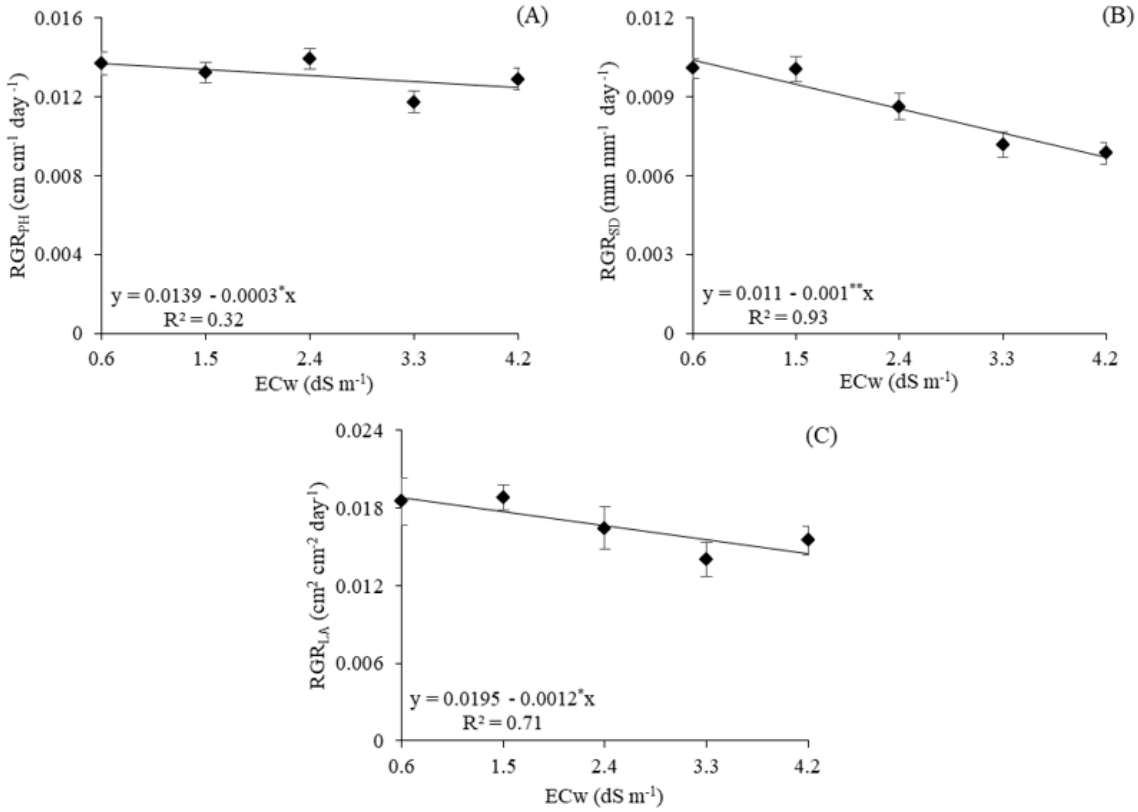

Figure 4. Relative growth rates in plant height - RGR_{PH} (A), stem diameter - RGR_{SD} (B) and leaf area - RGR_{LA} (C) of 'Paluma' guava, as a function of water salinity levels - ECw, during the period 104 to 180 days after sowing.
Vertical bar represents the standard error of the mean (n=4); *, ** respectively, significant at $p \leq 0.05$ and $p \leq 0.01$.

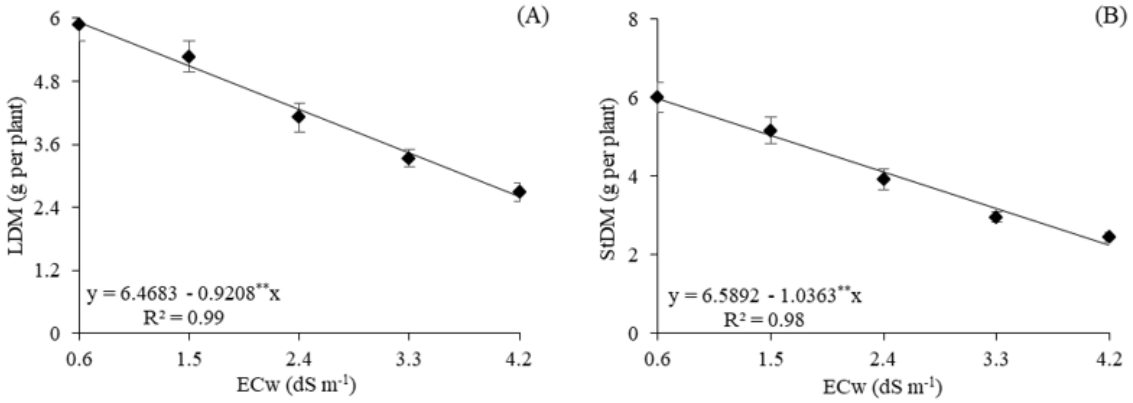

Figure 5. Dry mass of leaf - LDM (A) and stem - StDM (B) of 'Paluma' guava plants, as a function of water salinity levels - ECw, at 180 days after sowing.
Vertical bar represents the standard error of the mean (n=4); **, significant at $p \leq 0.01$.

The energy expenditure for maintaining metabolic activities induces changes in plant growth, as observed through the reduction in RGR_{PH}, RGR_{SD} and RGR_{LA}; and when plants absorb water with excess salts (mainly Na^+ and Cl^-), these ions get accumulated in cell tissues, causing stomatal closure, reduction in gas exchange and damage to photosynthetic apparatus, which results in lower CO_2 assimilation, nutritional imbalances, decrease in turgor, and reduction in cell expansion and division, causing lower growth and consequent biomass accumulation (Bonacina *et al.*, 2022).

Bezerra *et al.* (2018b) in a study evaluating the growth of grafted plants of 'Paluma' guava subjected to different levels of irrigation water salinity (ECw between 0.3 and 3.5 dS m^{-1}) and doses of nitrogen fertilization (70, 100, 130, and 160% of the recommended dose for the crop), found that salinity in irrigation water negatively affected the leaf area, stem diameter, and shoot dry mass of 'Paluma' guava plants.

The salinity of irrigation water caused reduction in the accumulation of root dry mass (Figure 6A), with decreases of 19.95% per unit increment in ECw. When the RDM of plants grown under electrical conductivity of 4.2 dS m^{-1} was compared to that of plants under the lowest salinity level (0.6 dS m^{-1}), there was a reduction of 81.65% (3.56 g per plant). It is also observed that water salinity caused a reduction in the total dry mass (Figure 6B), 16.32% per unit increase in ECw, and the TDM of plants irrigated with water of highest salinity (4.2 dS m^{-1}) was reduced by 65.17% (10.61 g per plant) compared to control treatment (0.6 dS m^{-1}).

The reduction in biomass may be associated with the deleterious effects of salinity on plants, which reduces water absorption capacity and causes immediate interference in CO_2 assimilation processes and energy diversion to other processes, such as osmotic adjustment, maintenance of basic metabolic processes and repair of damage caused by salt stress (Silva *et al.*, 2021b). In a study conducted by Souza *et al.* (2017), evaluating the influence of irrigation with different salinity levels (ECw between 0.3 and 3.5 dS m^{-1}) on 'Paluma' guava rootstock, the authors also verified a linear reduction in the RDM of plants with the increase in irrigation ECw.

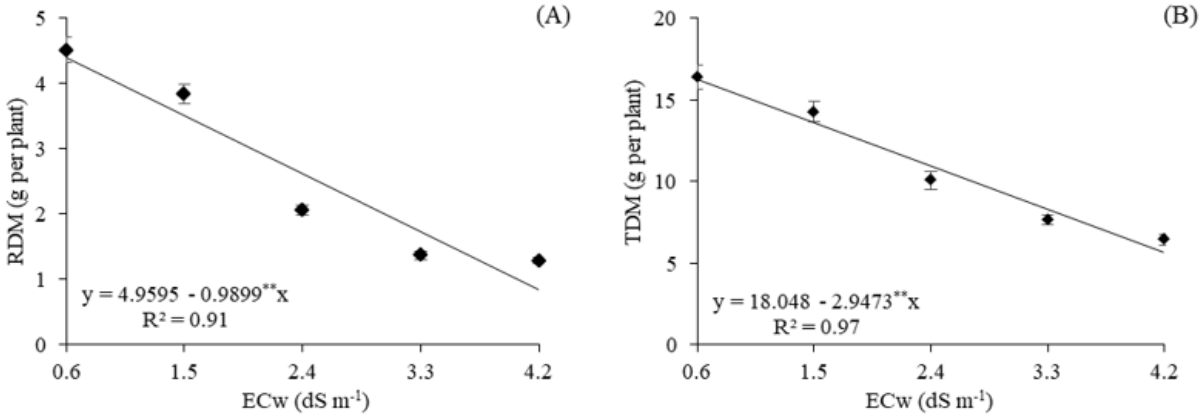

Figure 6. Root dry mass - RDM (A) and total dry mass - TDM (B) of 'Paluma' guava seedlings, as a function of water salinity levels - ECw, at 180 days after sowing.
Vertical bar represents the standard error of the mean (n=4); **, significant at $p \leq 0.01$.

Salicylic acid concentrations caused a significant effect on the RDM and TDM (Figure 7A and 7B) of 'Paluma' guava seedlings. According to the regression equation (Figure 7A), plants that did not receive exogenous application of SA (0 mM) obtained the highest value of RDM (2.87 g per plant), while those subjected to SA concentration of 1.84 mM had the lowest value (2.45 g per plant). Salicylic acid concentrations negatively influenced the production of total dry mass (Figure 7B). Plants subjected to the highest concentration of salicylic acid (3.2 mM) reduced their TDM by 66.13% (10.92 g per plant) compared to those in the control treatment (0 mM).

Salicylic acid is an important compound capable of mitigating the effects of salt stress and is present in several physiological processes of plants (Silva *et al.*, 2018). In the present study, the negative effect of SA on TDM may be associated with the method of application and the concentration used, since its use as a mitigator of salt stress depends on other factors such as species and/or genotype and environmental factors, as well as abiotic factors (El-Esawi *et al.*, 2017).

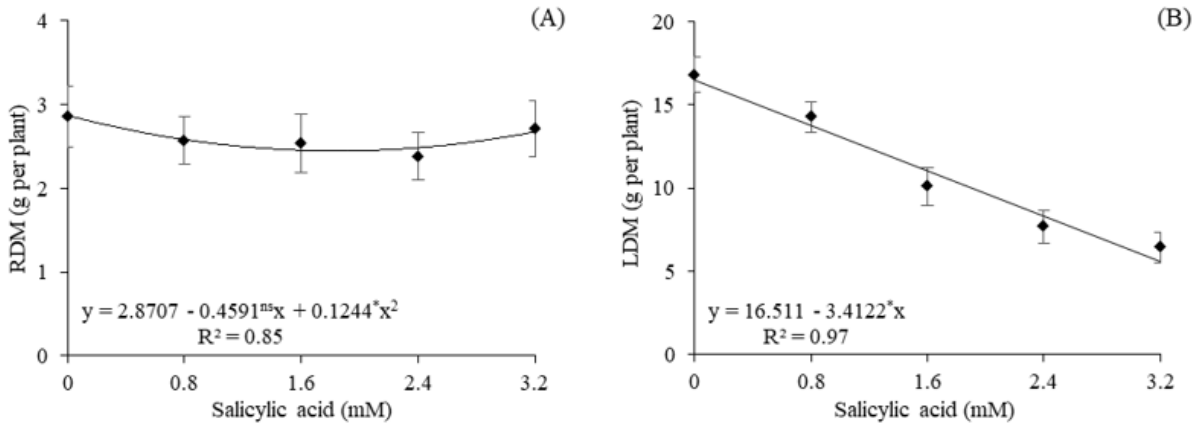

Figure 7. Root dry mass - RDM (A) and total dry mass - TDM (B) of 'Paluma' guava seedlings, as a function of salicylic acid concentrations – SA, at 180 days after sowing.
Vertical bar represents the standard error of the mean (n=4); ^{ns}, * respectively not significant and significant at $p \leq 0.05$.

Dickson's quality index (DQI) was reduced linearly with the increase in electrical conductivity levels of irrigation water (Figure 8A), by 18.58% per unit increase in ECw. Plants grown under water salinity of 4.2 dS m^{-1} reduced their DQI by 75.29% compared to those irrigated with ECw of 0.6 dS m^{-1}. DQI is an integrated morphological measure that, for relating robustness (plant height and stem diameter) to biomass distribution balance, is considered a good indicator of quality of seedlings to be used in the field (Lima *et al.*, 2021).

Lima *et al.* (2021), in a study evaluating the gas exchange, growth and quality of passion fruit cultivars 'BRS Sol do Cerrado' and 'Guinezinho' irrigated with saline waters (0.3 to 3.5 dS m^{-1}), also observed reductions in DQI of 44.83% and 62.18%, respectively, when comparing the lowest and highest levels of ECw.

Regarding the effects of SA concentrations on Dickson quality index (Figure 8B), it was verified that the maximum estimated value (0.8625) was obtained in plants subjected to SA concentration of 0 mM, while the lowest estimated value (0.7415) was obtained under the concentration of 1.82 mM according to the regression equation. The reduction in DQI with the increase in SA concentration may be related to the reduction observed in TDM (Figure 7B) since this is one of the variables used to determine the DQI. Despite the reduction in DQI, the values obtained in this study ranged from 0.31 to 1.27, which indicate seedlings with acceptable quality for transplanting to the field (Dickson *et al.*, 1960).

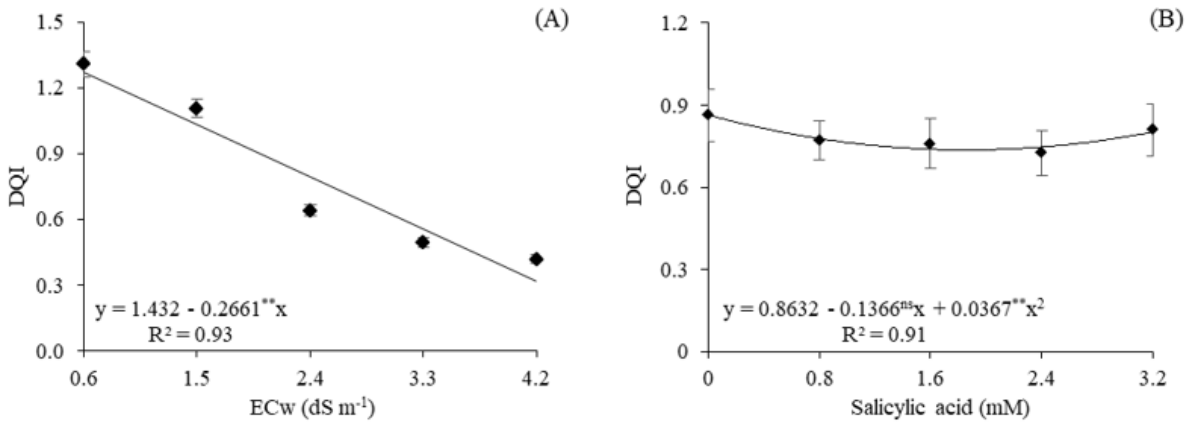

Figure 8. Dickson Quality Index (DQI) of 'Paluma' guava seedlings as a function of irrigation water salinity levels - ECw (A) and salicylic acid concentrations - SA (B) at 180 days after sowing.
Vertical bar represents the standard error of the mean (n=4); ^{ns}, **, respectively not significant and significant at $p \leq 0.01$.

In general, in the present study, it was observed that the foliar application of salicylic acid did not induce the tolerance of plants to salt stress, this fact may be related to the frequency of application (15 days), with only seven applications being carried out during the research. In addition, the beneficial effect of salicylic acid depends on several factors, including concentration, plant species, stage of crop development, and mode of application (Semida *et al.*, 2017); therefore, further research is needed to better understand the effects of SA on guava.

4. CONCLUSIONS

Foliar application of salicylic acid at a concentration of up to 1.4 mM reduces the deleterious effects of saline stress on the instantaneous water use efficiency of 'Paluma' guava seedlings at 180 days after sowing.

The transpiration of guava seedlings irrigated with electrical conductivity of up to 3.7 dS m^{-1} is benefited by the foliar application of salicylic acid at a concentration of 3.2 mM.

The concentrations of salicylic acid applied via foliar did not mitigate the harmful effects of irrigation water salinity on the growth and quality of 'Paluma' guava seedlings.

5. REFERENCES

ALTUNTAS, O.; DASGAN, H. Y.; AKHOUNDNEJAD, Y. Silicon-induced salinity tolerance improves photosynthesis, leaf water status, membrane stability, and growth in pepper (*Capsicum annuum* L.). **HortScience**, v. 53, n. 12, p. 1820-1826, 2018. https://doi.org/10.21273/HORTSCI13411-18

AGAMI, R. A.; ALAMRI, S. A.; ABD EL-MAGEED, T. A.; ABOUSEKKEN, M. S. M.; HASHEM, M. Salicylic acid and proline enhance water use efficiency, antioxidant defense system and tissues' anatomy of wheat plants under field deficit irrigation stress. **Journal of Applied Botany and Food Quality**, v. 92, n. 1, p. 360-370, 2019.

BENINCASA, M. M. P. **Análise de crescimento de plantas**: noções básicas. 2. ed. Jaboticabal: FUNEP, 2003. 42 p.

BEZERRA, I. L.; GHEYI, H. R.; NOBRE, R. G.; LIMA, G. S. DE; LACERDA, C. F. DE; LIMA, B. G. F. *et al.* Water salinity and nitrogen fertilization in the production and quality of guava fruits. **Bioscience Journal**, v. 35, n. 3, p. 837-848, 2019.

BEZERRA, I. L.; NOBRE, R. G.; GHEYI, H. R.; LIMA, G. S. DE; BARBOSA, J. L. Physiological indices and growth of `Paluma' guava under saline water irrigation and nitrogen fertigation. **Revista Caatinga**, v. 31, n.4, p.808-816, 2018a. https://doi.org/10.1590/1983-21252018v31n402rc

BEZERRA, I. L.; NOBRE, R. G; GHEYI, H. R.; SOUZA, L. DE P.; PINHEIRO, F. W. A.; LIMA, G. S. de. Morphophysiology of guava under saline water irrigation and nitrogen fertilization. **Revista Brasileira de Engenharia Agrícola e Ambiental**, v. 22, n. 1, p. 32-37, 2018b. https://doi.org/10.1590/1807-1929/agriambi.v22n1p32-37

BONACINA, C.; CRUZ, R. M. S. DA; NASCIMENTO, A. B.; BARBOSA, L. N.; GONÇALVES, J. E.; GAZIM, Z. C. *et al.* Salinity modulates growth, oxidative metabolism, and essential oil profile in *Curcuma lona* L. (Zingiberaceae) rhizomes. **South African Journal of Botany**, v. 146, n. 1, p. 1-11, 2022. https://doi.org/10.1016/j.sajb.2021.09.023

DANTAS, M. V.; LIMA, G. S. DE; GHEYI, H. R.; SILVA, A. A. R. DA; MELO, A. S. DE; MEDEIROS, L. C. de. Gas exchange and photosynthetic pigments of West Indian cherry under salinity stress and salicylic acid. **Comunicata Scientiae**, v. 12, e3664, 2021. https://doi.org/10.14295/cs.v12.3664

DIAS, A. S.; LIMA, G. S. DE; GHEYI, H. R.; SOARES, L. A. DOS A.; FERNANDES, P. D. Growth and gas exchanges of cotton under water salinity and nitrogen-potassium combination. **Revista Caatinga**, v. 33, n. 2, p. 470-479, 2020. https://doi.org/10.1590/1983-21252020v33n219rc

DIAS, A. S.; LIMA, G. S. de; PINHEIRO, F. W. A.; GHEYI, H. R.; SOARES, L. A. dos A. Gas exchanges, quantum yield and photosynthetic pigments of West Indian cherry under salt stress and potassium fertilization. **Revista Caatinga**, v. 32, n. 2, p. 429-439, 2019. https://doi.org/10.1590/1983-21252019v32n216rc

DIAS, M. J. T.; SOUZA, H. A.; NATALE, W.; MODESTO, V. C.; ROZANE, D. E. Adubação com nitrogênio e potássio em mudas de goiabeira em viveiro comercial. **Semina: Ciências Agrárias**, v. 33, Suplemento 1, p. 2837-2848, 2012. https://dx.doi.org/10.5433/1679-0359.2012v33Supl1p2837

DICKSON, A.; LEAF, A. L.; HOSNER, J. F. Quality appraisal of white spruce and white pine seedling stock in nurseries. **The Forestry Chronicle**, v. 36, n. 1, p. 10-13, 1960. https://doi.org/10.5558/tfc36010-1

EL-ESAWI, M. A.; ELANSARY, H. O.; EL-SHANHOREY, N. A.; ABDEL-HAMID, A. M. E., ALI, H. M.; ELSHIKH, M. S. Salicylic acid-regulated antioxidant mechanisms and gene expression enhance Rosemary performance under saline conditions. **Frontiers in Physiology**, v. 8, p. 716, 2017. https://doi.org/10.3389/fphys.2017.00716

FERREIRA, D. F. SISVAR: A computer analysis system to fixed effects split-plot type designs. **Revista Brasileira de Biometria**, v. 37, n. 4, p. 529-535, 2019. https://doi.org/10.28951/rbb.v37i4.450

GHASSEMI-GOLEZANI, K.; FARHANGI-ABRIZ, S.; BANDEHAGH, A. Salicylic acid and jasmonic acid alter physiological performance, assimilate mobilization and seed filling of soybean under salt stress. **Acta Agriculturae Slovenica**, v. 111, n. 3, p. 597-607, 2018. http://dx.doi.org/10.14720/aas.2018.111.3.08

IBGE. **Produção agrícola municipal**. Rio de Janeiro: IBGE, 2019.

JINI, D.; JOSEPH, B. Physiological mechanism of salicylic acid for alleviation of salt stress in rice. **Rice Science**, v. 24, n. 2, p. 97-108, 2017. https://doi.org/10.1016/j.rsci.2016.07.007

LACERDA, C. N. de; LIMA, G. S. de; SOARES, L. A. dos A.; FÁTIMA, R. T. de; GHEYI, H. R.; AZEVEDO, C. A. V. de. Morphophysiology and production of guava as a function of water salinity and salicylic acid. **Revista Brasileira de Engenharia Agrícola e Ambiental**, v. 26, n. 6, p.451-458, 2022. https://doi.org/10.1590/1807-1929/agriambi.v26n6p451-458

LIMA, G. S. de; ANDRADE, J. N. F. de; MEDEIROS, M. N. V. de; SOARES, L. A. dos A.; GHEYI, H. R.; NOBRE, R. G. Gas exchange, growth, and quality of passion fruit seedlings cultivated with saline water. **Semina**: **Ciências Agrárias**, v. 42, n. 1, p. 137-154, 2021. http://dx.doi.org/10.5433/1679-0359.2021v42n1p137

LIMA, G. S. de; FERNANDES, C. G. J.; SOARES, L. A. dos A.; GHEYI, H. R.; FERNANDES, P. D. Gas exchange, chloroplast pigments and growth of passion fruit cultivated with saline water and potassium fertilization. **Revista Caatinga**, Mossoró, v. 33, n.1, p.184-194, 2020. https://doi.org/10.1590/1983-21252020v33n120rc

LIMA, L. G. S.; ANDRADE, A. C.; SILVA, R. T. L.; FRONZA, D.; NISHIJIMA, T. Modelos matemáticos para estimativa de área foliar de goiabeira (*Psidium guajava* L.). *In*: REUNIÃO ANUAL da SBPC, 64. **Anais[...]** São Luiz: UFMA. 2012.

LOPES, M. de F. de Q.; SILVA, T. I. da; NÓBREGA, J. S.; SILVA, R. T. da; FIGUEIREDO, F. R. A.; BRUNO, R. de L. A. Crescimento de *Erythrina velutina* willd. submetida a estresse salino e aplicação de ácido salicílico. **Colloquium Agrariae**, v. 15, n. 4, p. 31-38, 2019. https://revistas.unoeste.br/index.php/ca/article/view/2831

MANICA, I.; ICUMA, I. M.; JUNQUEIRA, N. T. V.; SALVADOR, J. O.; MOREIRA, A.; MALAVOLTA, E. **Goiaba**: do plantio ao consumidor: tecnologia de produção, pós-colheita e comercialização. Porto Alegre: Cinco Continentes, 124p, 2001.

MEDEIROS, J. F. de. **Qualidade de água de irrigação e evolução da salinidade nas propriedades assistidas pelo GAT nos Estados de RN, PB e CE**. 1992. 173p. Dissertação (Mestrado) - Universidade Federal da Paraíba, Campina Grande, 1992.

MOHAMMADI, H.; IMANI, A.; ABDOSI, V.; ASGHARI, M. R.; TALAEI, A. R. Exogenous salicylic acid mitigates adverse effects of salinity on some photosynthesis-related parameters of almond. **Journal of Agricultural Science and Technology**, v. 22, n. 2, p. 519-534, 2020.

MONTES, R. M.; PARENT, L. E.; AMORIM, D. A. de; ROZANE, D. E. ; PARENT, S. E.; NATALE, W. Nitrogen and potassium fertilization in a guava orchard evaluated for five cycles: soil cationic balance. **Revista Brasileira de Ciência do Solo**, v. 40, e0140533, 2016. https://doi.org/10.1590/18069657rbcs20140532

NAZAR, R.; UMAR, S.; KHAN, N. A.; SAREER, O. Salicylic acid supplementation improves photosynthesis and growth in mustard through changes in proline accumulation and ethylene formation under drought stress. **South African Journal of Botany**, v. 98, n. 1, p. 84-94, 2015. https://doi.org/10.1016/j.sajb.2015.02.005

NOVAIS, R. F.; NEVES, J. C. L.; BARROS, N. F. Ensaio em ambiente controlado. *In*: OLIVEIRA, A. J.; GARRIDO, W. E.; ARAÚJO, J. D.; LOURENÇO, S. **Métodos de pesquisa em fertilidade do solo**. Brasilia, DF: Embrapa Sea, 1991. Cap. 2. p.189-198.

RAJESHWARI, V.; BHUVANESHWARI, V. Salicylic acid induced salt stress tolerance in plants. **International Journal of Plant Biology and Research**, v. 5, n. 3, p.1067-1073, 2017.

RICHARDS, L. A. **Diagnosis and improvement of saline and alkaline soils**. Washington: USDA, 1954. 160p. (USDA Handbook, 60).

SEMIDA, W. M.; ABD El-MAGEED, T. A.; MOHAMED, S. E.; El-SAWAH, N. A. Combined effect of deficit irrigation and foliar-applied salicylic acid on physiological responses, yield, and water-use efficiency of onion plants in saline calcareous soil. **Archives of Agronomy and Soil Science**, v. 63, n. 9, p. 1227-1239, 2017. https://doi.org/10.1080/03650340.2016.1264579

SILVA, A. A. R da; LIMA, G. S. de; AZEVEDO, C. A. V. de; GHEYI, H. R.; SOUZA, A. R. de; FERNANDES, P. D. Salicylic acid relieves the effect of saline stress on soursop morphysiology. **Ciência e Agrotecnologia**, v. 45, e007021, 2021a. https://doi.org/10.1590/1413-7054202145007021

SILVA, A. A. R. da; LIMA, G. S. de; AZEVEDO, C. A. V. de; VELOSO, L. L de S. A.; GHEYI, H. R. Salicylic acid as an attenuator of salt stress in soursop. **Revista Caatinga**, v. 33, n. 4, p. 1092-1101, 2020. https://doi.org/10.1590/1983-21252020v33n424rc

SILVA, A. A. R. da; VELOSO, L. L. de S. A.; LIMA, G. S. de; SOARES, L. A. dos A.; CHAVES, L. H. G.; SILVA, F. de A. da *et al.* Induction of salt stress tolerance in cherry tomatoes under different salicylic acid application methods. **Semina: Ciências Agrárias**, v. 43, n. 3, p. 1145-1166, 2022. http://dx.doi.org/10.5433/1679-0359.2022v43n3p1145

SILVA, S. S. da; LIMA, G. S. de; LIMA, V. L. A. de; SOARES, L. A. dos A.; GHEYI, H. R. *et al.* Quantum yield, photosynthetic pigments and biomass of mini-watermelon under irrigation strategies and potassium. **Revista Caatinga**, v. 34, n. 3, p. 659-669, 2021b. https://doi.org/10.1590/1983-21252021v34n318rc

SILVA, T. I.; NÓBREGA, J. S.; FIGUEIREDO, F. R. A.; SOUSA, L. V.; RIBEIRO, J. E. S.; BRUNO, R. L. A. *Ocimum basilicum* L. seeds quality as submitted to saline stress and salicylic acid. **Journal of Agricultural Science**, v. 10, n. 5, p. 159-166, 2018. https://doi.org/10.5539/jas.v10n5p159

SOARES, L. A. dos A.; OLIVEIRA, S. G. de; LIMA, G. S. de; FERNANDES, P. D.; ARAÚJO, R. H. C. R.; FERNANDES, E. A. Physiological changes of pomegranate seedlings under salt stress and nitrogen fertilization. **Revista Brasileira de Engenharia Agrícola e Ambiental**, v. 25, n. 7, p. 453-459, 2021. https://doi.org/10.1590/1807-1929/agriambi.v25n7p453-459

SOUANA, K.; TAÏBI, K.; ABDERRAHIM, L. A.; AMIRAT, M.; ACHIR, M.; BOUSSAID, M. *et al.* Salt-tolerance in *Vicia faba* L. is mitigated by the capacity of salicylic acid to improve photosynthesis and antioxidant response. **Scientia Horticulturae**, v. 273, n. 1, e109641, 2020. https://doi.org/10.1016/j.scienta.2020.109641

SOUZA, L. de P.; SENA, G. S. A. de; NOBRE, R. G.; BARBOSA, J. L.; SOUZA, C. M. A. de; ELIAS, J. J. Formação de porta-enxerto de goiabeira submetidas a diferentes salinidades da água e adubação nitrogenada. **Revista Brasileira de Agricultura Irrigada**, v. 11, n. 4, p. 1578-1587, 2017. https://dx.doi.org/10.7127/rbai.v11n400618

Ambiente & Água - An Interdisciplinary Journal of Applied Science
ISSN 1980-993X – doi:10.4136/1980-993X
www.ambi-agua.net
E-mail: ambi.agua@gmail.com

Sanitary quality of reused water for irrigation in agriculture in Brazil

ARTICLES doi:10.4136/ambi-agua.2809

Received: 08 Nov. 2021; Accepted: 16 Feb. 2022

Natasha Berendonk Handam[1*]; Ana Beatriz Loureiro Gonçalves da Silva[2]; Rodrigo Bezerra da Silva[3]; Priscila Gonçalves Moura[1]; Elvira Carvajal[4]; Adriana Sotero-Martins[5]; José Augusto Albuquerque dos Santos[6]

[1]Programa de Doutorado em Saúde Pública e Meio Ambiente. Escola Nacional de Saúde Pública Sérgio Arouca. Fundação Oswaldo Cruz (FIOCRUZ), Rua Leopoldo Bulhões, n° 1480, CEP: 21031-210, Rio de Janeiro, RJ, Brazil. E-mail: priscila.moura.gema@gmail.com
[2]Graduação em Engenharia Química. Centro de Tecnologia da Indústria Química e Têxtil (SENAI CETIQT), Rua Leopoldo Bulhões, n° 1480, CEP: 21041-210, Rio de Janeiro, RJ, Brazil. E-mail: beatrizloreiro@hotmail.com
[3]Graduação em Biologia. Universidade do Estado do Rio de Janeiro (UERJ), Rua Leopoldo Bulhões, n° 1480, CEP: 21041-210, Rio de Janeiro, RJ, Brazil. E-mail: rodrigobezera2@gmail.com
[4]Instituto de Biologia Roberto Alcantara Gomes. Departamento de Biologia Celular. Universidade do Estado do Rio de Janeiro (UERJ), Rua São Francisco Xavier, n° 524, CEP: 20550-900, Rio de Janeiro, RJ, Brazil. E-mail: elvira.dbiocel@gmail.com
[5]Departamento de Saneamento e Saúde Ambiental. Escola Nacional de Saúde Pública Sérgio Arouca. Fundação Oswaldo Cruz (FIOCRUZ), Rua Leopoldo Bulhões, n° 1480, CEP: 21041-210, Rio de Janeiro, RJ, Brazil. E-mail: adrianasotero@ensp.fiocruz.br
[6]Laboratório de Avaliação e Promoção da Saúde Ambiental. Instituto Oswaldo Cruz. Fundação Oswaldo Cruz (FIOCRUZ), Avenida Brasil, n° 4365, CEP: 21040-360, Rio de Janeiro, RJ, Brazil. E-mail: santosjaa@gmail.com
[*]Corresponding author. E-mail: natashabhandam@gmail.com

ABSTRACT

Reused water is produced from treated effluents, and can be an alternative source of water for agriculture. However, its quality must be assessed to avoid causing damage to human and environmental health. This study evaluated the sanitary quality (bacteriological and physicochemical) of reused water samples for agricultural irrigation, compared with those described in Brazilian and international regulations. Bacteriological analyses were performed, and the results were compared with the norm of the Brazilian Association of Technical Norms (ABNT) NBR nº 13.969/1997. Physical and chemical analyses of the reused water samples were carried out, and the results were compared with the standards described by regulations: Resolution of the State Council for the Environment of Ceará No. 2 of 2017; Resolution of the Bahia State Water Resources Council No. 75 of 2010; and "Guidelines for Water Reuse" from the U.S. Environmental Protection Agency - EPA. According to Brazilian regulations, bacteriological analyses showed that the "chlorinated" and "polished" samples were suitable for agriculture. However, the "biological" sample was unsuitable for use, and showed a high level of thermotolerant coliforms (25.800 CFU / mL). According to bacteriological and physical-chemical analyses, the "polished" sample was only proper for agriculture irrigation. Therefore, the work suggests the creation of federal law regarding agricultural reuse to control the sanitary quality of water for human and environmental health.

Keywords: agricultural reuse, agriculture, bacteriological and physicochemical evaluation, norms for reuse in agriculture.

This is an Open Access article distributed under the terms of the Creative Commons Attribution License, which permits unrestricted use, distribution, and reproduction in any medium, provided the original work is properly cited.

Qualidade sanitária de águas de reúso para irrigação na agricultura no Brasil

RESUMO

A água de reúso é um recurso proveniente de efluentes tratados e pode ser uma fonte alternativa de água para agricultura. No entanto, é importante a avaliação da sua qualidade para não causar agravos a saúde ambiental e humana. O objetivo foi avaliar a qualidade sanitária (bacteriológica, físicas e químicas) de amostras de água de reúso para irrigação da agricultura, de acordo com padrões estabelecidos em normativas brasileiras e internacional. Foram realizadas análises bacteriológicas, sendo os resultados comparados com a norma da Associação Brasileira de Normas Técnicas NBR nº 13.969/1997. E foram feitas análises físicas e químicas das amostras de água de reúso, sendo os resultados comparados com os padrões das normativas: Resolução do Conselho Estadual de Meio Ambiente do Ceará nº 2 de 2017; Resolução do Conselho Estadual de Recursos Hídricos da Bahia nº 75 de 2010; e "*Guidelines for Water Reuse" from the U.S. Environmental Protection Agency - EPA.* As análises bacteriológicas mostraram que as amostras "clorada" e "polida" estavam próprias para agricultura, de acordo com as normativas brasileiras. No entanto a amostra "biológica" estava imprópria para uso, apresentando nível elevado de coliformes termotolerantes (25,800 CFU/mL). Segundo as análises bacteriológicas e físico-químicas apenas a amostra de reúso "polida" estava própria para reúso agrícola. O estudo mostrou a importância da forma de tratamento de água de reúso para qualidade sanitária da água, e isso é fundamental a criação de lei federal de reúso agrícola, a fim de evitar danos à saúde humana e ambiental.

Palavras-chave: agricultura, avaliação bacteriológica e físico-química, normativas de reúso na agricultura, reúso agrícola.

1. INTRODUCTION

There are currently several examples of reusing water in agriculture in Brazil and worldwide (Fito and Van Hulle, 2021; Mancuso and Santos, 2013). Reused water is defined as the reuse of water from treated effluents (Morais *et al.*, 2016). It can be classified according to Moura *et al.* (2020), who conceptualized the origin of reuse water as follows:

"(i) Local or internal reuse, the water reuse obtained from greywater treatment from residential reuse (house or building) and reuse of new commercial or non-commercial ventures; (ii) External reuse, the water reuse obtained from black water (raw sewage) and sewage treatment plant and which subsequently pass through wastewater treatment plants (STP+WWTP)."

Agriculture is the economic activity that most consumes freshwater, reaching around 70% (Peng *et al.*, 2019). However, the scarcity of water sources for this activity in several regions makes reused water an alternative to face this problem (FAO, 2017).

The use of reused water in agriculture can bring benefits such as nutrients and water, favoring the growth of plants and reducing the use of artificial fertilizers (USEPA, 2012). Irrigation with reused water is a form of natural fertigation derived from nutrients such as nitrogen, potassium and phosphorus, which is essential for cultivation in poor soils (Lahlou *et al.*, 2020; Otenio, 2015). Furthermore, it represents an alternative to reduce the demand pressure on water sources and reduce the amount of sewage discarded (Lima *et al.*, 2021; Mancuso and Santos, 2013).

However, reused water must be well managed, or it can offer negative impacts such as posing risks to human and environmental health (WHO, 2006). Depending on the origin and treatment used to produce reused water, it may not be safe for human and environmental health

(Moura *et al.*, 2020). Disease transmission is also controlled by agronomic factors such as irrigation practices used as drip, culture and harvesting practices (Orlofsky *et al.*, 2016).

Countries have sought to expand the regulation and monitoring of pollutants and contaminants that were not the object of attention by legal provisions for wastewater reuse (Cui and Liang, 2019; USEPA, 2012). The United States is more advanced in the quality of water bodies; many states adopt guidelines for reused water, encouraging new uses, such as irrigation in agriculture.

In Brazil, there is still no federal legislation showing criteria and parameters for assessing the water reuse quality for agriculture (Handam *et al.*, 2021). The Brazilian Association of Technical Standards (ABNT) has only a technical standard, nº 13,969/97 (ABNT, 1997), but it is not specific, bringing few reused water quality parameters. There are specific laws in some Brazilian states that have quality parameters for the use of reused water in agriculture: Resolution of the State Council for the Environment (COEMA) of Ceará nº. 2 of February 2017 (CEARÁ, 2017) and the State Resolution of the State Water Resources Council (CONERH) of Bahia nº 75 of 2010 (BAHIA, 2010). According to FUNASA (2007), "For the agricultural use of effluents, the recommendations of the World Health Organization...and the recommendations of the United States Environmental Protection Agency (EPA)".

The study suggests measuring the sanitary quality (bacteriological and physicochemical) of reused water samples for agricultural irrigation, according to standards described in Brazilian and international regulations.

2. MATERIAL AND METHODS

Three samples of reused water from different sources were collected: “chlorinated” reused water obtained from treated sewage in a sewage treatment plant (STP), after which the effluent was chlorinated; “polished” reused water from sewage treated in STP and subsequently submitted to three treatments in wastewater treatment plants (WWTP), which were filtration, ultrafiltration and reverse osmosis; and "biological" reused water, from gray water that has been treated by a physical and biological filter system. The physical and biological filter system was according to Poblete (2010) (Figure 1).

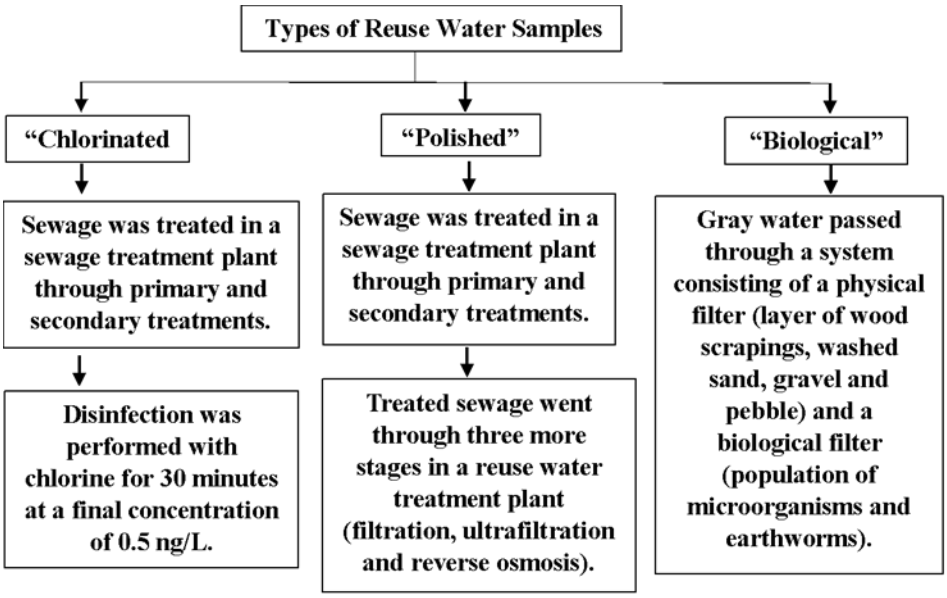

Figure 1. Flowchart on the treatment systems for the production of each reused water sample used in the research: "Chlorinated, Polished, Biological".

Bacteriological analyses (thermotolerant coliforms) were performed within 24 hours after

collections according to the Standard Methods for the Examination of Water and Wastewater (APHA *et al.*, 2017). Serial dilutions were carried out as described by Sotero-Martins (2017), using the membrane filter method with the chromogenic culture medium indicator Chromocult® Coliform Agar (Cat. No. 1,10426,0100/500 Merck) and quantified in Colonies Forming Units of water (CFU/mL) (Sotero-Martins *et al.*, 2017).

Physicochemical analyses of total hardness, turbidity, fluoride, chlorine residual, nitrate, nitrite, sulfate, alkalinity, conductivity, apparent color, pH and free chlorine were done according to the methods based on Standard Methods for the Examination of the Water and Wastewater (APHA *et al.*, 2017). The bacteriological results found in the reuse water samples were compared with the Class 4 standard for agriculture, established in the Norm of the Brazilian Association of Technical Norms (ABNT) NBR nº 13,969/1997 (ABNT, 1997).

Compared to international laws, the limit values recommended by ABNT regulations (5,000 NMP/100 mL) and Ceará Resolution 2/2017 (1,000 NMP/100 mL) were converted to values in CFU/mL, considering that the quantification in NMP is 2.167 times greater than in CFU (Sotero-Martins *et al.*, 2017), according to statistical data observed in the work of Gronewold and Wolpert (2008). Thus, the standard for thermotolerant coliforms converted from the ABNT 13,969/97 standard was 23 CFU/mL, and from the Ceará Resolution 2/2017, it was 4.6 CFU/mL. The standards of EPA (2012) and Resolution nº 75 of 2010 of Bahia were converted to CFU/mL, that is, in EPA (2012), the standard was 2 CFU/mL, and the standard of Resolution 75 of 2010 was 100 CFU/ mL.

For physical-chemical parameters, the Brazilian regulations for agricultural reuse do not set quality standards for all parameters analyzed in this study, with standards being established only for electrical conductivity, chlorine residual, pH and fluoride. Thus, the results were compared with the norms: Resolution of the State Council for the Environment (COEMA) of Ceará nº 2 (COEMA, 2017); and the State Resolution of the State Water Resources Council (CONERH) of Bahia nº 75 (CONERH, 2010). The results of the physicochemical parameters turbidity, chlorine, nitrate and apparent color were compared with the Maximum Allowable Values (VMP) defined by the international standard “Guidelines for Water Reuse” from the U.S. Environmental Protection Agency - EPA (USEPA, 2012). The regulation was considered because it has physical-chemical and microbiological quality parameters for reused water for agriculture based on scientific studies. The other parameters analyzed were total hardness, alkalinity, nitrite and sulfate were compared with the quality standards established in Consolidation Potability Ordinance nº 5 of 2017 (Brasil, 2017) because they do not have quality standards for agricultural reuse in Brazilian and international standards.

3. RESULTS AND DISCUSSION

Bacteriological analyses showed that the “chlorinated” reuse water sample had 20 CFU/mL of thermotolerant coliforms and the “polished” sample had no thermotolerant coliforms. The quality of both samples was in accordance with the quality standard for agricultural reuse established by NBR nº 13,969/97 (ABNT, 1997).

Research indicates that reused water produced by sewage treatment plants together with chlorination and/or ultrafiltration treatment reduces the level of coliforms in the water and the risks associated with the presence of other microorganisms (Bakopoulou *et al.*, 2011; Youn-Joo *et al.*, 2007), which corroborates the low level of coliforms found in the chlorinated reuse water and the absence of coliforms in the “polished” reuse water.

However, the "biological" reuse water sample showed a high level of thermotolerant coliforms (25.800 CFU/mL). It was inadequate and above the recommended limit for agricultural application according to Standard NBR nº. 13,969/97 (Figure 2).

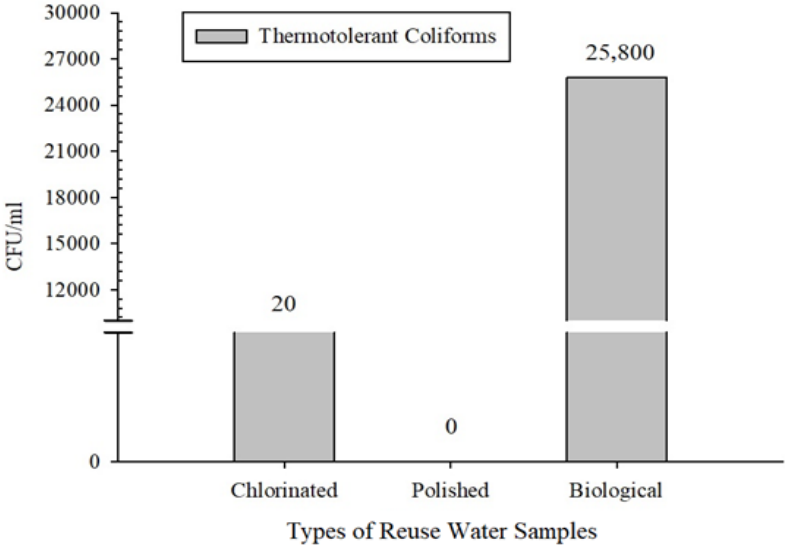

Figure 2. Thermotolerant coliform levels of contamination in water reuse samples from Brazil. Break interval: 5 – 10000. Water reuse samples from Brazil: "Chlorinated" - reused water from treated sewage (ETE) and then chlorinated; "Polished" from treated sewage (ETE) and reused water treatment (WWTP - filtration, ultrafiltration and reverse osmosis); "Biological" reused water from grey waters treated by the physical and biological filter.

The Resolution of the State Council for the Environment (COEMA) of Ceará nº 2/2017 (Ceará, 2017) determines parameters for water reuse for agricultural and forestry purposes. The "biological" sample showed a maximum of 4.6 CFU/mL of coliform thermotolerant. In addition, this law determines that there must be an absence of thermotolerant coliforms in cultures to be consumed raw whose consumed part has direct contact with the irrigation water. Bahia State Resolution nº 75/2010 (Bahia, 2010) has less restrictive bacteria levels than other regulations. The quality of the sample was also up to the established standard. This law determines a limit value for thermotolerant coliforms of 10 CFU/mL for Category A “Irrigation, including hydroponics, of any crop including food products consumed raw”, and of 100 CFU/mL for drip irrigation; and 100 CFU/mL of thermotolerant coliforms for Category B "Irrigation, including hydroponics, of uneaten raw food products, non-food products, forages, pastures, trees, crops used in revegetation and recovery of degraded areas" (Bahia, 2010).

The “biological” reuse water sample was characterized as unsuitable for irrigation of crops due to the level of bacteria, even with drip irrigation according to Resolution nº 75/2010 (Bahia, 2010). Drip irrigation is a strategy for watering water close to the ground, leaving the water available only to the plant's root system and reducing the risk of contamination (Mancuso and Santos, 2013).

Greywater is not effluent from toilets, so it does not have a direct faecal contribution, and it may have been contaminated with thermotolerant coliforms through hand washing, bathing, washing food and clothing and even diaper washing (Peters, 2006). In addition, there may have been a possible saturation of the biological filter due to a large amount of water, which may have caused the mortality of earthworms, which are part of the filtering system, impairing the treatment of gray water. The result may have been due to a specific improper condition;however, attention is recommended in the treatment of this effluent to ensure the quality of agricultural reuse, which may add another disinfection process. According to Bakopoulou *et al.* (2011), treatment with chlorination can contribute to eliminating coliforms, and it can be incorporated into the production of “biological” reuse water because it is not part of the system's treatment process. Another possible solution would be constructing another

physical and biological filter parallel to the existing one to divide the treatment of a large amount of gray water to produce higher-quality reused water (Dombroski *et al.*, 2013). Dombroski *et al.* (2013) also introduced a similar study of reused water samples from a greywater treatment system and identified 692.82 CFU/mL of thermotolerant coliforms, which is up to the level allowed for agricultural reuse.

It is worth mentioning that from an epidemiological and immunological point of view, the presence of pathogenic microorganisms in water does not mean that people will acquire diseases (Mancuso and Santos, 2013). However, signaling care in the face of risks concerning certain types of reuse water with potential contaminants, which can be added to the soil, which affect human and animal life, are fundamental data for health actions. Workers, especially those who continuously deal with agriculture, can be exposed to soil contaminated with elements that can be carried through reused water, a vehicle for transmitting diseases. However, the risk can be reduced through good practices, using personal protective equipment (PPE) in agriculture (WHO, 2006), so it is essential to know the contaminants and pollutants that may be in the reuse water. In addition, the transmission of diseases becomes less or even controlled through irrigation, culture and harvesting practices used, for example, application of drip irrigation (Morais *et al.*, 2016; Mancuso and Santos, 2013; WHO, 2006).

Gatta *et al.* (2016) found that despite identifying microorganisms such as E. coli and Salmonella spp. in sewage samples by secondary and tertiary treatment, the artichoke crops irrigated with these samples were not contaminated. Moreover, the reduction of these bioindicators in the soil may be due to the drip irrigation system, which avoids contact of water with the plant, and/or the death of bacteria in the soil and the barrier through the roots of the plants. In addition, the production of crops irrigated with reused water increased from 33 to 55% compared to crops irrigated with freshwater (Gatta *et al.*, 2016).

The physicochemical results showed that in all samples, only the parameters free residual chlorine, conductivity, pH, fluoride were in accordance with the Maximum Allowable Values (VMP) established by Brazilian and international regulations: Resolution of the State Environmental Council (COEMA) of Ceará nº 2 of February 2017 (Ceará, 2017), State Resolution of the State Water Resources Council (CONERH) of Bahia nº 75 of 2010 (Bahia, 2010) and Guidelines for Water Reuse - EPA (2012) (Table 1).

Table 1. Physicochemical results of reused water samples and quality standards according to Brazilian regulations: State Resolution of the State Water Resources Council of Bahia nº 75 of 2010; Resolution of the State Environmental Council of Ceará nº 2 of February 2, 2017; Guidelines for water reuse 2012 - EPA - U.S. Environmental Protection Agency.

Parameters	Chlorinated	Polished	Biological	EPA (2012)	Ceará (2017)	Bahia (2010)
Chlorine mg/L	0.15	0.05	0	1	ND	ND
Total hardness mg/L	68.5	14	645	ND	ND	ND
Alkalinity $CaCO_3$ mg/L	31.8	715	698	ND	ND	ND
Conductivity µS/cm	554	284	1017	3.0	3000	3.0
pH	7.0	7.0	7.0	6.5 – 8.4	6.0 – 8.5	ND
Turbidity NTU	2.55	0.3	44	2	ND	ND
Apparent color Pt-Co units	44.2	19	340	150	ND	ND
Fluoride mg/L	0.61	0.42	0.77	1.0	ND	1.0
Chlorine residual mg/L	97.68	16.6	146.24	10	ND	100 – 350
Nitrate mg/L	60.20	1.35	14.34	30	ND	ND
Nitrite mg/L	0.71	0.06	0	ND	ND	ND
Sulfate mg/L	38.93	22.37	15.56	ND	ND	ND

ND: Maximum permitted values of the parameter are not described in the regulations on agricultural reuse.

The "biological" reused water sample presented non-standard physical-chemical parameters, such as turbidity apparent color, as it presented values up to the permitted level according to EPA (2012) regulations. Turbidity indicates the presence of suspended solids in the water, it hinders the disinfection process, and pathogenic microorganisms may also be present (APHA *et al.*, 2017). The apparent color parameter is indicative of particles dissolved in water (Von Sperling, 1996), and its non-compliance does not necessarily imply a health risk. However, it needs to be observed as a warning.

The conductivity parameter analyzed in the "biological" sample, despite being within the VMP according to the Ceará regulations (2017), establishes a limit of up to 3,000 µS/cm; the sample presented a high conductivity value with 1017 µS/cm. Bahia (2010) and EPA (2012) regulations show the limit standard for conductivity around 1,000 times slower than the Ceará standard (2017), with a limit of up to 3 µS/cm being established. According to Ayres and Westcot (1991), reused water with electrical conductivity ranges from 700 to 3,000 µS/cm are classified as having moderate salinity and requires a moderate restriction of use for irrigation. The moderate salinity classification indicates that there may be a moderate reduction in the rate of water infiltration into the soil. Therefore, these waters become more suitable for irrigation of soils with salt-tolerant crops. Conductivity is an important parameter for agriculture as an indirect measure of salinity. The greater the electrical conductivity, the greater the degree of salinity, which affects the water availability for crops (USEPA, 2012). The result found for electrical conductivity was similar to the value identified in a study by Rolim *et al.* (2016), who found 1,200 µS/cm. They also used conductivity as an indicator of salinity. The "chlorinated" reuse water sample was unsuitable for the nitrate-nitrogen parameter with a level of 60.2 mg/L. It is up to the standard value recommended by the normative Guidelines for Water Reuse (USEPA, 2012), which establishes a limit of up to 30 mg/L of nitrate.

The parameters nitrate and nitrite are essential macronutrients for soil fertility and crop productivity (Rolim *et al.*, 2016), but it can be a public health risk in large quantities, up to 30 mg/L, making it harmful to plant development. Above this level, plants can absorb nitrogen, which is very dangerous for some cultures, as it causes excessive vegetative growth (Ayres and Westcot, 1991). In the environment, especially in sandy soils, nitrogen can reach the water table more efficiently and is considered highly soluble in water (Mancuso and Santos, 2013). The result demonstrates that the treatment by ETE and chlorination did not show good efficiency in removing nutrients.

The “chlorinated” and “biological” reuse water samples were unsuitable in terms of turbidity level for agricultural purposes according to EPA (2012), as the quality standard is 2 NTU, the standard established in the Food Crops category "The use of reclaimed water for surface irrigation or a sprinkling of food crops intended for human consumption, consumed raw" presented in the EPA (2012). The “chlorinated” sample was 1.3 times larger than the standard recommended by the regulations. The "biological" sample was 22 times higher than allowed; it showed a high turbidity level. Results of reuse water analysis by Rolim *et al.* (2016) also showed unacceptable levels for the turbidity parameter with an average value of 32.4 NTU. They did not recommend unrestricted irrigation in agriculture, as they are not suitable for use in drip or sprinkler irrigation systems.

According to Bakopoulou *et al.* (2011), sand filtration treatment is recommended to reduce turbidity in reuse water, as it is considered an effective and essential method before the effluent disinfection process. With filtration, the treatment can better remove coliforms in the disinfection stage (Bakopoulou *et al.*, 2011). In view of this, the treatment for "biological" reuse water production needs to be improved because of the high turbidity level. The filter sand layers could be increased, thus favouring more significant coliform removal in the reused water.

The results of the physical-chemical parameters of the “polished” reused water sample showed that it is within the VMP according to EPA (2012) and Ceará (2017) regulations. Only

the chlorine residual parameter presented a value of 16.6 mg/L, being below the range of 100 to 350 mg/L, standard established by Bahia Resolution nº 75/10. Furthermore, it was slightly above the limit recommended by EPA (2012), 10 mg/L. According to Ayres and Westcot (1991), chlorine residual at a level above 10 mg/L, as presented by the "polished" reused water sample, can be slightly toxic to the plants. Compared to other reuse water samples, "polished" was the lowest level of chlorine residual, which can be explained by the treatment method with ultrafiltration technology, which according to Rolim *et al.* (2016), is considered effective in further removing salts.

There is no standard for agricultural reuse of parameters such as total hardness, total alkalinity, nitrite and sulfate, but other norms and studies can indicate the level of quality of these parameters. In the reuse water samples, the nitrite and sulfate parameters were in accordance with the potability standard, Ministry of Health Consolidation Ordinance nº 5 of 2017 (Brasil, 2017). However, the “biological” sample was unsuitable for total hardness, with a value above the standard for potability, which establishes a maximum value of 500 mg/L (Brasil, 2017). Total hardness is defined as the sum of the concentrations of calcium and magnesium ions in water, expressed as calcium carbonate (FUNASA, 2013). Indirect contact with water levels above the potability standard can cause a laxative effect on humans (Von Sperling, 1996). According to Almeida (2010), it can also cause encrustations in the pipes. Thus, for drip irrigation systems, it can be detrimental. According to Almeida (2010), to reduce the hardness of the water, aeration can be done, as it induces calcium precipitation. However, it is recommended to use water with a higher degree of hardness in soils with high sodium. As for total alkalinity, the "polished" and "organic" reused water samples had high and similar levels compared to the "chlorinated" sample, with levels of 715 mg/L, 698 mg/L, 31.8 mg /L, respectively. This parameter is of great importance because it shows the capacity of water to neutralize acids present, which is measured by the total concentration of hydroxides, carbonates and bicarbonates. The presence of these substances neutralizes the effects of acidic substances, for example, due to acid rain (FUNASA, 2013). Moreover, in the soil, it is essential to check alkalinity, because when the soil is acidic, substances previously present in the mineral form are transformed into ions, some of which are toxic to plants, such as aluminium and cadmium ions (Carmo *et al.*, 2016; Silva, 2012).

4. CONCLUSIONS

According to the analysis carried out in the study, only "polished” reused water is suitable according to Brazilian and international regulations, and it can be considered for agricultural reuse. According to current regulations that determine standards for agricultural reuse, the other samples of reused water, "biological and chlorinated", were unsuitable.

The results showed that the production of reused water by physical and biological filters studied in this article cannot remove microorganisms effectively. This suggests a reassessment of the proposed treatment or the inclusion of a new treatment phase. Reused water with similar treatments should be used in agriculture if it undergoes a complementary treatment to reduce impacts on the soil and ensure a supply of nutrients to crops, reducing costs with artificial fertilizers, and not offering risks to public health and the environment.

Therefore, the study of the sanitary quality of three samples from different sources shows the importance of treating and producing reused water with good quality for safe use that does not adversely impact public and environmental health. For an assessment of quality that can guarantee the safety of reused water for use in agricultural irrigation, it is essential to create legislation at the national level for agricultural reuse, which codifies the origin of this water, sanitary quality standards and forms of treatment for production. Every state must comply with the law in order to avoid human and environmental health damage at the national level.

5. ACKNOWLEDGEMENTS

Support from the Vice-Direction of Research and Innovation, VDPI/ENSP/Fiocruz

6. REFERENCES

ABNT. **NBR 13.969 de 30 de outubro de 1997**. Unidades de tratamento complementar e disposição final dos efluentes líquidos. Rio de Janeiro, 1997. 60p.

ALMEIDA, O. A. de. **Qualidade da água de irrigação.** Cruz das Almas: Embrapa Mandioca e Fruticultura, 2010.

APHA; AWWA; WEF. **Standard Methods for the examination of water and wastewater**. 23 ed. Washington, 2017. 1496 p.

AYRES, R. S.; WESTCOT, D. W. **A qualidade da água na agricultura**. Campina Grande: UFPB, 1991. 218p.

BAHIA (Estado). Resolução CONERH nº 75 de 29 de julho de 2010. Estabelece modalidades, diretrizes e critérios gerais para prática de reúso direto não potável de água. **Diário oficial [do] Estado - BA**, Salvador, 01 ago. 2010.

BAKOPOULOU, S.; EMMANOUIL, C.; KUNGOLOS, A. Assessment of wastewater effluent quality in Thessaly region, Greece, for determining its irrigation reuse potential. **Ecotoxicology and Environment**, v. 74, p. 188-194, 2011. https://doi.org/10.1016/j.ecoenv.2010.06.022

BRASIL. Ministério da Saúde. Portaria n. 05, de 28 de setembro de 2017. Consolidação das normas sobre as ações e os serviços de saúde do Sistema Único de Saúde. **Diário Oficial [da] União**: seção 1, Brasília, DF, n. 190, supl. p. 516-531, 03 de out. de 2017.

CARMO, A. H. D. *et al.* Os efeitos da chuva ácida na fertilidade do solo e em cultivares agrícolas. **Revista da META**, v. 1, n. 1, p. 393 – 399, 2016.

CEARÁ (Estado). Resolução do Conselho Estadual do Meio Ambiente (COEMA) nº 2, de 02 de fevereiro de 2017. Dispõe sobre padrões e condições para lançamento de efluentes líquidos gerados por fontes poluidoras. **Diário oficial [do] Estado - CE**, Fortaleza, 21 fev. 2017.

CUI, B.; LIANG, S. Monitoring Opportunistic Pathogens in Domestic Wastewater from a Pilot-Scale Anaerobic Biofilm Reactor to Reuse in Agricultural Irrigation. **Water**, v. 11, n. 6, p. 1283, 2019. https://doi.org/10.3390/w11061283

DOMBROSKI, S. A. G.; SANTIAGO, F. dos S.; JALFIM, F. T.; DIAS, I. C. G. M. Eficiência de tratamento de água cinza pelo bioágua familiar. *In:* ENCONTRO INTERNACIONAL DAS ÁGUAS, 7., 15 a 17 de maio 2013, Recife. **Gestão de água: água, meio ambiente e saúde**. Recife: Unicap, 2013.

FAO. **Water for Sustainable Food and Agriculture**. A report was produced for the G20 Presidency of Germany. Rome, 2017.

FITO, J.; VAN HULLE, S. W. H. Wastewater reclamation and reuse potentials in agriculture: towards environmental sustainability. **Environment, Development and Sustainability**, v. 23, p. 2949–2972, 2021. https://doi.org/10.1007/s10668-020-00732-y

FUNASA (Brasil). **Manual Prático de Análise de Água**. 4. ed. rev. Brasília, 2013.

FUNASA (Brasil). **Aplicação controlada de água residuária e lodo de esgoto no solo, para melhorar e incrementar a agricultura do semi-árido nordestino**. Brasília, 2007. 120p.

GATTA, G. *et al.* Reuse of treated municipal wastewater for globe artichoke irrigation: Assessment of effects on morpho-quantitative parameters and microbial safety of yield. **Scientia Horticulturae**, v. 213, p. 55–65, 2016. https://doi.org/10.1016/j.scienta.2016.10.011

GRONEWOLD, A. D.; WOLPERT, R. L. Modeling the relationship between most probable number (MNP) and colony-forming unit (CFU) estimates of fecal coliform concentration. **Water Research**, v. 42, p. 3327-3334, 2008. https://doi.org/10.1016/j.watres.2008.04.011

HANDAM, N. B.; SILVA, A. B. L. G.; SOTERO-MARTINS, A.; SANTOS, J. A. A. Agricultural reuse: comparison between Brazilian and international quality standards. **International Journal of Hydrology**, v. 5, n. 1, p. 28-31, 2021. https://doi.org/10.15406/ijh.2021.05.00262

LAHLOU, F.; NAMANY, S.; MACKEY, H. R.; AL-ANSARI, T. Treated Industrial Wastewater as a Water and Nutrients Source for Tomatoes Cultivation: an Optimization Approach. **Computer-Aided Process Engineering**, v. 48, p. 1819–1824, 2020. https://doi.org/10.1016/B978-0-12-823377-1.50304-9

LIMA, M.; ARAUJO, B. M.; SOARES, S. R. A.; SANTOS, A. S. P.; VIEIRA, J. M. P. Water reuse potential for irrigation in Brazilian hydrographic regions. **Water Supply**, v. 21, n. 6, p. 2799–2810, 2021. https://doi.org/10.2166/ws.2020.280

MANCUSO, P. C. S.; SANTOS H. F. **Reúso de Água**. São Paulo: Manole, 2013.

MORAIS, M. A.; FERREIRA NETO. M.; SILVA, G. DE F.; DE LIRA, R. B., DE BRITO, R. F.; MIGUEL, L. C. V. Contaminação microbiológica no perfil do solo por águas residuárias. **HOLOS**, v. 3, p. 76-83, 2016. https://dx.doi.org/10.15628/holos.2016.2782

MOURA, P. G. *et al.* Água de reúso: uma alternativa sustentável para o Brasil. **Engenharia Sanitária e Ambiental**, v. 25, n. 6, p. 791–808, 2020. https://doi.org/10.1590/S1413-4152202020180201

ORLOFSKY, E.; BERNSTEIN, N.; SACKS, M.; VONSHAK, A.; BENAMI, M.; KUNDU, A. *et al.* Comparable levels of microbial contamination in soil and tomato crops after drip irrigation with treated wastewater or drinking water. **Agriculture, Ecosystems & Environment**, v. 215, p. 140-150, 2016. https://doi.org/10.1016/j.agee.2015.08.008

OTENIO, M. H. Reaproveitamento de água residuária em sistemas de produção de leite. *In*: MARTINS, P. do C.; PICCININI, G. A.; KRUG, E. E. B.; MARTINS, C. E.; LOPES, F. C. F. **Sustentabilidade ambiental, social e econômica da cadeia produtiva do leite**: desafios e perspectivas. Brasíia: Embrapa Gado de Leite, 2015. Cap. 7.

PENG, Yaoqi *et al.* Precision irrigation perspectives on the sustainable water-saving of field crop production in China: Water demand prediction and irrigation scheme optimization. **Journal of cleaner production**, v. 230, p. 365-377, 2019. https://doi.org/10.1016/j.jclepro.2019.04.347

PETERS, M. R. **Potencialidade de uso de fontes alternativas de água para fins não potáveis em uma unidade residencial**. 2006. Dissertação (mestrado em Engenharia Ambiental) - Universidade Federal de Santa Catarina, Centro Tecnológico, Florianópolis, 2006.

POBLETE, C. P. C. **Estudio del Comportamiento de una Mezcla de Aserrín y Grasa Láctea de Desecho**. Valdivia: Universidad Austral de Chile, 2010.

ROLIM, H. de O.; CHAVES, J. R.; NUNES, A. B. de A. *et al.* Qualidade dos Efluentes de Sistemas de Tratamento Biológico UASB e UCT para Reúso Agrícola. **Revista em Agronegócio e Meio Ambiente**, v. 9, n. 2, 2016.

SILVA, S. Aluminium Toxicity Targets in Plants. **Journal of Botany**, v. 2012, p. 1–8, 2012. http://doi.org/10.1155/2012/219462

SOTERO-MARTINS, A.; HANDAM, N. B.; MOURA, P. G.; AMARAL, L. S.; CALDAS, L. V. L.; CARVAJAL, E. Methods for Sanitary Inspection of Microbiological and Parasitary Quality of Water and Sand of Recreation Areas. **American Journal of Engineering Research (AJER),** v. 6, p. 56–2, 2017.

USEPA. **Guidelines for water reuse**. Washington D.C., 2012.

VON SPERLING, M. V. **Introdução à qualidade das águas e ao tratamento de esgotos**. Belo Horizonte: Departamento de Engenharia Sanitária e Ambiental, Un. Federal de Minas Gerais, 1996. 243p.

WHO. **Guidelines for the safe use of wastewater, excreta and greywater**. Geneva, 2006. V. 2.

YOUN-JOO, A.; YOON, C. G.; JUNG, K. W.; HAM, J. H. Estimating the Microbial risk of E. Coli Reclaimed Wastewater Irrigation on Paddy Field. **Enronmental Monitoring and Assessment**, v. 129. p. 53-60, 2007. https://doi.org/10.1007/s10661-006-9425-0

Ambiente & Água - An Interdisciplinary Journal of Applied Science
ISSN 1980-993X – doi:10.4136/1980-993X
www.ambi-agua.net
E-mail: ambi.agua@gmail.com

O_3/UV-type POAs integrated with catalytic material based on scrap iron and mineral clay to degrade 2,4 and 2,6-dinitrotoluene in Red Water

ARTICLES doi:10.4136/ambi-agua.2813

Received: 09 Nov. 2021; Accepted: 18 Apr. 2022

Jilvana Bárbara Walter*; Francisnara Tonholi; Marcio Barreto Rodrigues

Universidade Tecnológica Federal do Paraná (UTFPR), Câmpus Pato Branco, Via do conhecimento, s/n, Km 01, CEP: 85503-390, Pato branco, PR, Brazil. E-mail: fran.tonholi@hotmail.com, marcioutfpr@gmail.com
*Corresponding author. E-mail: jilvanawalter@live.com

ABSTRACT

Nitroaromatic compounds have significant economic and industrial relevance in various inputs such as dyes, inks, agrochemicals, and explosives. In the manufacture of the explosive 2,4,6 trinitrotoluene (TNT), there is the formation of contaminated wastewater that is difficult to treat because it contains, among other compounds, high concentrations of 2,4 and 2,6-trinitrotoluene (DNT). In this work, the application of advanced oxidation processes of the O_3/UV type was studied in sequential integration with catalytic material based on metallic iron slag (SZVI) and mineral matrix to treat an industrial effluent from the explosives industry contaminated with compounds nitroaromatics. Two types of mineral matrix composition were studied, kaolinite (Kau) and pumice powder (Pum), having been observed in the conditions of best efficiency (O_3/UV-SZVI/Kau) 100% removal of both nitroaromatic compounds and residual ozone. On the other hand, photo-ozonation alone could only partially remove these components, with 38% DNT removal and 3.2 mg/L residual O_3 observed, proving the importance of integration with the catalytic matrix for more effective treatment of the studied effluent.

Keywords: DNT degradation, explosives industry effluent, Scrap zero-valent iron.

Aplicação de POAs do tipo O_3/UV em integração com material catalítico a base de escória de ferro e argilo minerais, para a degradação de 2,4 e 2,6-dinitrotolueno em Red Water

RESUMO

Os compostos nitroaromáticos possuem importante relevância econômica e industrial fazendo parte de diversos insumos como corantes, tintas, agroquímicos e explosivos. Na fabricação do explosivo 2,4,6 trinitrotoluneo (TNT), há a formação de águas residuárias contaminadas de difícil tratamento por conter, dentre outros compostos, elevadas concentrações de 2,4 e 2,6-trinitrotolueno (DNT). Neste trabalho foi estudada a aplicação de Processos oxidativos avançados do tipo O_3/UV em integração sequencial com material catalítico a base de escória de ferro metálico (SZVI) e matriz mineral, para o tratamento de um efluente industrial oriundo da indústria de explosivos contaminado com compostos nitroaromáticos. Foram estudados dois tipos de composição de matriz mineral, caulinita (Kau) e pedra pomes

This is an Open Access article distributed under the terms of the Creative Commons Attribution License, which permits unrestricted use, distribution, and reproduction in any medium, provided the original work is properly cited.

em pó (Pum), tendo sido observado, nas condições de melhor eficiência (O_3/UV-SZVI/Kau), 100% de remoção tanto dos compostos dinitroaomáticos quanto de ozônio residual. Por outro lado, a foto-ozonização isoladamente, foi capaz de remover apenas parcialmente estes componentes, tendo sido observados 38% de remoção de DNT e 3,2 mg/L de O_3 residual, comprovando a importância da integração com a matriz catalítica para um tratamento mais efetivo do efluente em estudo.

Palavras-chave: degradação de DNT, efluentes da indústria de explosivos, escória de ferro.

1. INTRODUCTION

The contamination of water by emerging pollutants has been identified as one of today's most relevant challenges, mainly due to its possible effects on the endocrine, hormonal and genetic systems. These contaminants can also be converted into chiral metabolites (chiral pollution), which can cause enantioselective carcinogenesis and diverse impacts on soil and water ecosystems (Basheer, 2018b; Basheer and Ali, 2018; Khan *et al.*, 2020). This class includes pesticides, phenols, polycyclic aromatic hydrocarbons and nitroaromatic compounds, such as dinitrotoluene (DNT), and conventional processes for the treatment of contaminated effluents (typically physicochemical and biological processes) have limited efficiency, mainly due to the persistent toxic effects that these compounds impart to the effluent (Bilal *et al.*, 2021; Barreto-Rodrigues *et al.*, 2009). As an alternative, several processes have been studied to remove emerging pollutants, including UV photodegradation, reverse osmosis, removal by nano-adsorbents, and photocatalysis (Basheer, 2018a; Ali *et al.*, 2018; Khan *et al.*, 2020).

In this context, advanced oxidative processes mediated by ozone and ultraviolet radiation have been presented as a promising alternative for the treatment of various contaminants, including nitroaromatic compounds, which can be used as a pre-treatment of biological processes due to their ability to increase biodegradability and dissolved oxygen concentration (Equation 1). The effect caused by the joint action of O_3 and UV makes possible the simultaneous occurrence of degradation mechanisms of direct photolysis, direct ozonation, and oxidation by hydroxyl radicals. The process starts with the photolysis of ozone-producing hydrogen peroxide, followed by the ion reaction hydroperoxide (HO2 -) with O_3 to produce O_3^- and hydroxyl radicals, the latter of which can lead to effective oxidation and eventual mineralization of typically refractory organic compounds (Chen *et al.*,2007). However, when applied to residues of greater complexity, such as industrial effluents with a high organic load and diversity of refractory compounds, such systems may have some limitations, mainly associated with the need to complement the treatments carried out to ensure the elimination of any intermediates (e.g., phenolic compounds) and remaining oxidants from the process, such as O_3 and H_2O_2 (Bui and Minh, 2021).

$$3\,O_2 + H_2O + h\upsilon \rightarrow 2\,HO\bullet + 4\,O_2 \qquad (1)$$

To overcome these limitations, alternatives such as the sequential association with ferrous catalysts can eliminate the remaining oxidants by converting them into additional doses of HO• through Fenton-type reactions or catalytic ozonation emerge (Bhanot *et al.*, 2020). It is essential to point out that various forms of chemical synthesis can obtain ferrous catalytic materials, but also by using metallurgical/steel industrial waste, which can be used in combination with inert matrices such as calcium alginate, chitosan, bentonite, cellulose, zeolite, stone-pumice, carboxymethylcellulose, kaolinite, among others, to control the hydraulic conductivity and reduce the self-aggregation of particles which reduces the reactivity (Limper *et al.*, 2018; Abukhadra *et al.*, 2021; Sewwandi and Nitisoravut, 2020; Pereira *et al.*, 2021; Ali *et al.*, 2018). Among the matrices reported in the literature, kaolinite is a widely applied clay

mineral used in several processes, mainly in the paper industry, with a load function and surface material. In this same sense, pumice has also stood out, as it is a porous material with a large surface area; it can be an efficient and low-cost adsorbent (Calabrò *et al.*, 2012). It is interesting to note that the application of materials of this nature, whether in the form of filters or reactive barriers, tends to improve the efficiency and cost of the process (Ali *et al.*, 2018).

In this context, this work describes a study of the potential of catalytic ozonation mediated by mixtures of ZVSI and clay mineral materials (kaolinite and pumice) in an effluent composed of 2,4 and 2,6-Dinitrotoluene. The main innovative element of the research is the operation of two advanced oxidative processes (O_3/UV + Fe/O_3) in a single reaction system.

2. MATERIAL AND METHODS

2.1. Chemicals and supplies

All chemicals used were of analytical grade and were obtained from Merck, Reagen, or Sigma. The effluent samples were collected from an explosives-manufacturing industry in the State of São Paulo, Brazil. The wastewater resulted from the purification stage of the trinitrotoluene manufacturing process. After being collected at room temperature, it was stored under refrigeration (4ºC), and the concentration of nitroaromatic compounds present were estimated in the form of 2,4 and 2,6-dinitrotoluene 316 ± 10 mg.L^{-1}. Kaolinite and pumice were dried in an oven at 110°C for approximately three h, then ground and processed through a 0.135 mm sieve. The scrap zero-valent iron (SZVI) used was donated by a company in the Grinding area, located in Pato Branco and Francisco Beltrão, Paraná. After collection, the material was sampled using the splitting method, processed in a 0.150mm sieve. The splitting of the samples was performed according to the technical standard (ABNT, 2001).

2.2. Analytical control

The following parameters were used to determine the pollution potential of the effluent and ensure analytic control of the system:

UV-visible spectroscopy (UV–Vis): Spectroscopic analyses were performed on a spectrophotometer Thermal Scientific Evolution 60S Model-UV-visible, using quartz cuvettes with an optical path of 1 cm. Absorbance measurements at ʎmax = 275nm were performed to quantify the degradation rate of nitroaromatic compounds in the effluent.

Gas chromatography/mass spectrometer analysis: One hundred millimeters (100 mL) of effluent were dried under reduced pressure, and the residue was solubilized with methanol chromatographic grade. After treatment with anhydrous sodium sulfate for moisture extraction and filtering on 0.45µm cellulose membrane, it was transferred to a sample vial. The proportional sample amount (0.4µL) was injected into a gas chromatograph/mass spectrometer (Varian 431-GC/210MS) equipped with a capillary column (DB5, 30 m×0.25mm, film thickness 0.25µm), operated from 313 to 573K at a programming rate of 20 K.min^{-1}. Compared to authentic standard compounds, the obtained mass spectra were used to identify 2,4 and 2,6-dinitrotoluene in the wastewater.

Red Water Contaminant Toxicity: The level of oral toxicity was determined based on the chemical structure of the substance through the classification method, which uses a decision tree model, developed by Cramer in 1978, using the ToXtree software for data analysis.

For the characterization of the catalytic material and mineral matrices, the following analytical techniques were used:

X-Ray Diffractometry: The diffractograms were obtained in a Rigaku diffractometer (model Mini Flex 600), with copper radiation (CuKα λ=1.5418 Å), power of 40 kV, and current of 15 mA. The acquisition will occur in Bragg angle interval from 3 to 90º, step scan mode, 0.02º step, and 2 seconds per step.

Energy Dispersive Spectroscopy (EDS): Elementary chemical analyses (mapping) were

performed by EDS ("Energy Dispersive Spectroscopy") using Oxford equipment, with the voltage of 15 kV and electron backscattered detector.

2.3. Effluent treatment

Experimental Design: To select and evaluate the effect of the nature of the mineral clay matrix as well as the SZVI concentration on the removal efficiency and permeability coefficient, a complete 2^2 factorial design with three genuine replicas was carried out preliminarily in the absence of ozone and ultraviolet radiation. This study evaluated the effects of X_1: matrix type (pumice and kaolinite) and X_2: % SZVI (10 and 50% w/w) on the removal of nitroaromatic compounds measured by the percentage reduction in absorbance at ʎmax = 275 nm. For statistical calculations, the values of the independent variables were coded into two levels (- and +), as shown in Table 1.

Table 1. Factorial planning matrix, DNT removal efficiencies, and permeability coefficients.

Test	Codified levels		Real conditions		DNT Removal (%)		k
	X_1	X_2	tipo de matriz	% SZVI			cm/s
1	-1	-1	*pumice*	10	25	26.8	$1.47\ 10^{-3}$
2	+1	-1	*kaolinite*	10	15.4	12.6	$6.79\ 10^{-4}$
3	-1	+1	*pumice*	50	16.3	15.46	$1.76\ 10^{-3}$
4	**+1**	**+1**	***kaolinite***	**50**	32.2	**36.7**	$1.56\ 10^{-3}$
5	--	--	--	100	19.0	17.9	$7.86\ 10^{-3}$

X_1: matrix type; X_2: % SZVI; k= permeability coefficient (20°C).

Red water effluent treatment: A modified Hellma model HP UV 50F W 500V photochemical reactor was used, with 1000 mL capacity, water cooling, homogenization promoted by a magnetic stirrer, air/O_3 feed through the base with a flow of 1LMP (liter per minute) and passage inflow by catalytic mixture based on SZVI (preliminarily selected) supported on a sidearm, as illustrated in Figure 1. For characterization of the proposed treatment system (O_3/UV-SZVI/Kau/Pum), tests were also conducted without the assistance of UV radiation (O_3/SZVI/Kau/Pum) and the use of catalytic matrix (O_3/UV).

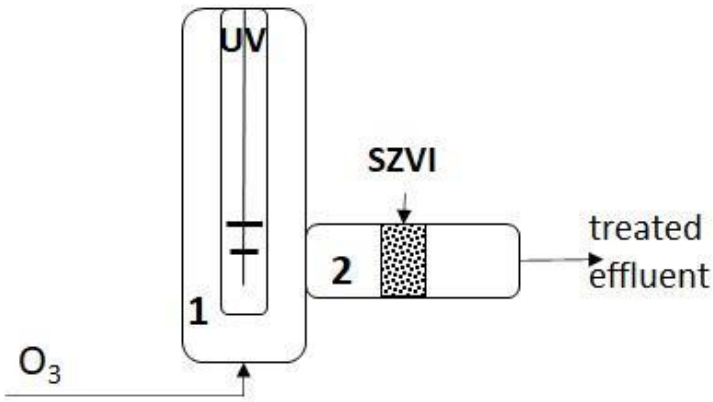

Figure 1. The photochemical reactor used in the research; (1): advanced oxidation zone UV/O_3 and (2): secondary oxidation zone and depletion of O_3/H_2O_2.

3. RESULTS AND DISCUSSION

3.1. Characterization of catalytic materials, mineral matrices, and effluent

The X-ray diffractograms of the SZVI showed peaks at 27, 45, 55, 65, and 83° of 2Θ, while

those at 27 and 45° were narrow and intense, evidencing the crystalline character of the material. According to the Crystallographic Identification Chart 31829 of the Inorganic Crystal Structure Database (ICSD) database, the peaks at 27 and 55° are characteristic of carbon graphite, while the peaks located at 45, 65 and 83° refer to metallic iron (iron zero), based on ICSD identification letter 64999.

The results of the elemental quantitative chemical analysis of kaolinite, based on the intense peaks obtained from detected atoms, confirm the presence of oxygen (58.91%), silicon (14.14%), aluminum (13.49%), carbon (11.96%), and iron (1.50%). Regarding pumice, the presence of oxygen (58.60%), silicon (31.24%), carbon (8.15%), iron (1.61%), and aluminum (0.40%), was confirmed on the analyzed surface. Finally, in the SZVI samples, elements such as Iron (Fe), Carbon (C), Oxygen (O), Silicon (Si), Chromium (Cr), Manganese (Mn), and Calcium (Ca) were identified, with Carbon and Iron have the highest percentages, which were 48.5 and 43.6%, respectively.

The toxicity of 2,4,6-trinitrotoluene (TNT) and its respective degradation products was investigated using the Toxtree program. According to Cramer's rules, it was concluded that both TNT and its two degradation products identified in the studied effluent (2,4 and 2,6-DNT) have high toxicity (Class III) and biodegradability classified as persistent.

3.2. Multivariate study for the composition of the catalytic matrix

Table 1 shows the codes, real tests, and the results obtained in each experiment carried out with the same experimental errors. The data (responses) received based upon the statistical design was assessed by analysis of variance (ANOVA). Levene's test checked the homogeneity of variance, and the normal distribution of results was studied using the Shapiro-Wilk test with a 5% significance level. In general, degradation rates of nitroaromatic compounds ranged from 12.6 to 36.7%, obtained in Tests 4 and 7, which used *kaolinite* with 10% and 50% of SZVI, respectively. The permeability coefficients obtained indicated that the hydraulic flow through the catalytic material is favored with the increase in the concentration of SZVI, with the lowest and highest permeability being observed for the matrices of kaolinite with 10% of SZVI and of pumice with 50% of SZVI.

It is also interesting to note that the hydraulic permeability of the matrix with the best efficiency (Test 4) was five times lower than the matrix composed only of SZVI, suggesting that a longer hydraulic retention time increases the effectiveness of the interactions that lead to DNT degradation in the matrix.

For better interpretation, a statistical analysis carried out with Statgraphics Plus 5.1 software estimated the effects of the variables of interest on the removal rate of nitroaromatic compounds; the results are shown in Table 2, in which it's possible to observe estimated effect values, regression coefficients, interactions with significant and non-significant parameters, in addition to associated errors and level of significance attributed to each parameter. Factors in bold and marked with an asterisk were considered adequate for the 95% confidence interval (X_2: SZVI and interactions $X_1.X_2$).

Table 2. Effects, regression coefficients, and interaction to DNT removal efficiencies.

Factors	Effect	Effect error	t calc	p-Value	Coefficient	Coefficient error
Average	22.55	± 0.707	31.89		22.55	± 0.353
X_1: Matrix	3.33	± 1.415	2.35	0.0779	1.667	± 0.707
X_2: SZVI*	**5.21**	**± 1.415**	**3.68**	**0.0211***	**2.607**	**± 0.707**
X_1. X_2*	**15.23**	**± 1.415**	**10.76**	**0.0004***	**7.617**	**± 0.707**

*Statistically significant factors ($p<0.05$). t_{tab} 0.05; 4 = 2.776.

Equation 2 was generated considering only the significant coefficients listed in Table 2, and it explains mathematically how each variable affects the nitroaromatic compound's removal during the treatment of red water effluent.

$$\text{DNT removal (\%)} = 22{,}5575 + 2{,}6075 * X_2 + 7{,}6175 * X_1.X_2 \quad (2)$$

As it would be interesting to use Equation 1 as a model for predictive and interpretive purposes, the fit of the equation was evaluated with analysis of variance (ANOVA) (Barros Neto *et al.*, 2002). The results are shown in Table 3 and show that the model explains 97% of the variability in the DNT removal rate. Additionally, the F_{calc} ratio value was higher than the Ftab value, suggesting that a regression involving the study variables can be considered significant and suitable to be used for predictive purposes (Box *et al.*, 1978). Thus, Equation 2 was used to construct response surfaces "Matrix versus SZVI" (X1.X2) illustrated in Figure 2. It is used to interpret the interaction of significant effects on the removal rate of dinitrotoluenes from the red water effluent.

Table 3. Variance analysis to DNT removal efficiencies.

Variance source	GL	SQ	QM	F_{calc}
Model	3	540.847	180.282	45.02
Pure error	4	16.0178	4.00445	
Total	7	556.8648		

R^2 = 97.12; F_{tab} 0.05; 3; 4 = 6.59

The main effects and the response surface profile in Figure 2 show that an increase in the concentration of SZVI in the catalytic matrix promotes an increase in the DNT removal rate. This effect is more pronounced when the base of the catalytic matrix is based on kaolinite. The selected proportion (50:50) corroborates the studies by Moraci and Calabrò (2010). They evaluated the potential of a mixture between ZVI and pumice for the removal of heavy metals in reactive permeable barriers.

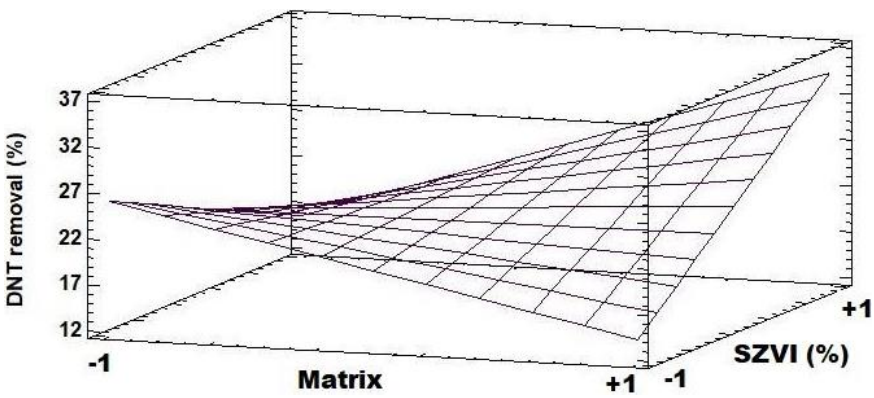

Figure 2. Response surface for the effects on DNT removal.

3.3. Red Water treatment through the O_3/UV-SZVI/Kao process

The composition of the catalytic matrix identified through factorial design (SZVI / kaolinite 50:50) was reproduced in a photochemical reactor (Figure 1), generating the results illustrated in Figure 3.

The chromatograms obtained for the samples submitted to the O_3/UV-SZVI/Kau treatment (Figure 3d) indicated, about the untreated effluent (Figure 3a), total degradation of the nitroaromatic compounds in the red water effluent, and it was not possible to detect 2,4 and 2,6-DNTs after 120 minutes of treatment. On the other hand, for this same reaction time, treatments that were not integrated with the catalytic matrix (b) or that used a matrix composed only of SZVI (c) showed lower efficiency, being possible in these cases, the detection of both 2,4 and 2,6-DNT after both types of treatment. These results are also illustrated in Table 4.

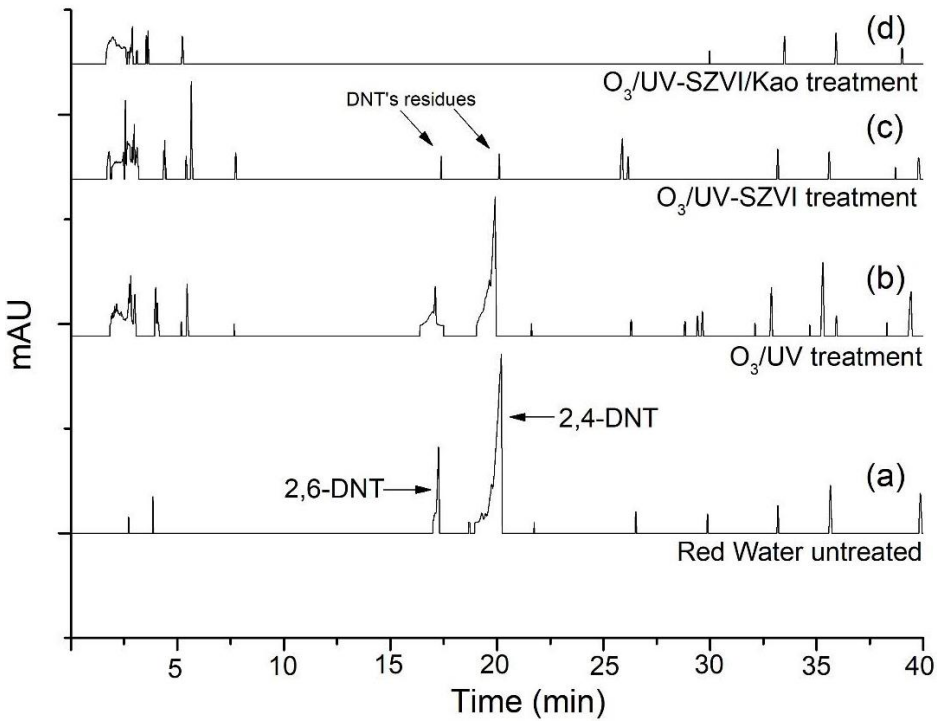

Figure 3. Chromatograms of samples of untreated and subjected to different treatments: (a) Untreated red water; (b) Red water treated by O_3/SZVI/Kao; (c) Red water treated by O_3/UV e (c) Red water treated by O_3/UV-SZVI/Kao. Experimental conditions: initial pH of 2.0; 10g/L of SZVI/Kao, and 120 minutes of treatment.

Table 4. Variance analysis to DNT removal efficiencies.

Parameter	Untreated Red Water	after 120 min of treatment			*Reduction (%)
		O_3/UV	O_3/UV-SZVI	O_3/UV-SZVI/Kao	
total DNT, $mg.L^{-1}$	316	196	47	not detected	100.0
pH	2-3	3.0	3.0	3.0	--
residual O_3 $mg.L^{-1}$	0.0	3.2	0.4	not detected	100.0

*Calculated based on the data for the process O_3/UV-SZVI/Kao.

The results also reveal that, compared to other processes, the treatment via photo-ozonation (O_3/UV) presented a higher residual ozone concentration, revealing the importance of the integrated use of the catalytic matrix. Additionally, a comparison between the results obtained by the O_3/UV-SZVI and O_3/UV-SZVI/Kau processes about the degradation of DNTs reveals the effect of the mineral matrix, suggesting that the addition of kaolinite in the matrix could be

promoting a reduction in the hydraulic permeability and self-aggregation of SZVI particles, increasing the effectiveness of advanced oxidation reactions on the matrix surface.

4. CONCLUSIONS

The results obtained in this work indicated that although advanced oxidative processes such as O_3/UV (photo-ozonation) and O_3/UV-SZVI (catalytic photo-ozonation) have shown significant efficiency for the degradation of nitroaromatic compounds present in red water, the addition of kaolinite to the catalytic matrix promotes an effect capable not only of fully degrading the 2,4 and 2,6-dinitrotoluene compounds but also removing residual concentrations of dissolved ozone, suggesting that the photo-ozonation process operating in coupling with a unit composed of a catalytic matrix based on SZVI and kaolinite, has significant potential for the treatment of effluents contaminated with nitroaromatic compounds. However, it is recommended to carry out additional tests to optimize the process and evaluate the effect of the treatment on other parameters of environmental relevance characteristic of the effluent.

5. ACKNOWLEDGMENTS

To CAPES, Araucária Fundation, UTFPR and to the Multiuser Central Analysis Laboratory.

6. REFERENCES

ABNT. **NBR NM 27, A.** Agregados - Redução da amostra de campo para ensaios de laboratório Rio de Janeiro, 2001.

ABUKHADRA, M. R.; ALHAMMADI, A.; EL-SHERBEENY, A. M.; SALAM, M. A.; EL-MELIGY, M. A.; AWWAD, E. M.; LUQMAN, M. Enhancing the removal of organic and inorganic selenium ions using an exfoliated kaolinite/cellulose fibers nanocomposite. **Carbohydrate Polymers**, v. 252, n. 117163, 2021. https://doi.org/10.1016/j.carbpol.2020.117163.

ALI, I. *et al*. Kinetics, thermodynamics, and modeling of amido black dye photodegradation in water using Co/TiO2 nanoparticles. **Photochemistry and Photobiology**, v. 94, n. 5, p. 935-941, 2018. https://doi.org/10.1111/php.12937

BARRETO-RODRIGUES, M.; SILVA, F. T.; PAIVA, T. C. B. Characterization of wastewater from the Brazilian TNT industry, **Journal of Hazardous Materials**, v. 164, n. 1, p. 385-388, 2009. https://doi.org/10.1016/j.jhazmat.2008.07.152

BARROS NETO, B.; SCARMÍNIO, S.; BRUNS, R. E. **Como fazer experimentos**: pesquisa e desenvolvimento na ciência e na indústria. 2. ed. Campinas: Editora UNICAMP, 2002. 401 p.

BASHEER, Al A. Chemical chiral pollution: impact on the society and science and need of the regulations in the 21st century. **Chirality**, v. 30, n. 4, p. 402-406, 2018a. https://doi.org/10.1002/chir.22808

BASHEER, Al A. New generation nano-adsorbents for the removal of emerging contaminants in water. **Journal of Molecular Liquids**, v. 261, p. 583-593, 2018b. https://doi.org/10.1016/j.molliq.2018.04.021

BASHEER, Al A.; ALI, I. Stereoselective uptake and degradation of (±)-o, p-DDD pesticide stereomers in water-sediment system. **Chirality**, v. 30, n. 9, p. 1088-1095, 2018. https://doi.org/10.1002/chir.22989

BILAL, M.; BAGHERI, A. M.; BHATT, P.; CHEN, S. Environmental occurrence, toxicity concerns, and remediation of recalcitrant nitroaromatic compounds. **Journal of Environmental Management**, v. 291, p. 112, 2021. https://doi.org/10.1016/j.jenvman.2021.112685

BHANOT, P.; CELIN, S. M.; SREEKRISHNAN, T.R.; KALSI, A.; SAHAI, S.K.; SHARMA, P. Application of integrated treatment strategies for explosive industry wastewater—A critical review. **Journal of Water Process Engineering**, v. 35, n. 101232, 2020. https://doi.org/10.1016/j.jwpe.2020.101232.

BOX, G. E. P.; HUNTER, W. G.; HUNTER, J. S. **Statistics for experimenters**. An introduction to design, data analysis and model building. Nova York: Wiley, 1978.

BUI, D. N.; MINH, T. T. Investigation of TNT red wastewater treatment technology using the combination of advanced oxidation processes. **Science of The Total Environment**, v. 756, n. 143852, 2021. https://doi.org/10.1016/j.scitotenv.2020.143852.

CALABRÒ, P. S.; MORACI, N.; SURACI, P. Estimate of the optimum weight ratio in zero-valent Iron/Pumice granular mixtures used in permeable reactive barriers for the remediation of nickel contaminated groundwater. **Journal of Hazardous Materials**, v. 207–208, p. 111-116, 2012. https://doi.org/10.1016/j.jhazmat.2011.06.094.

CHEN, W.; JUAN, C.; WEI, K. Decomposition of dinitrotoluene isomers and 2,4,6-trinitrotoluene in spent acid from toluene nitration process by ozonation and photo-ozonation. **Journal of Hazardous Materials**, v. 147, n. 1–2, p. 97-104, 2007. https://doi.org/10.1016/j.jhazmat.2006.12.052

KHAN, N. A. *et al*. Occurrence, sources and conventional treatment techniques for various antibiotics present in hospital wastewaters: a critical review. **TrAC Trends in Analytical Chemistry**, v. 129, p. 115921, 2020. https://doi.org/10.1016/j.trac.2020.115921

LIMPER, D.; FELLINGER, G. P.; EKOLU, S. O. Evaluation and microanalytical study of ZVI/scoria zeolite mixtures for treating acid mine drainage using reactive barriers – Removal mechanisms. **Journal of Environmental Chemical Engineering**, v. 6, n. 5, p. 6184-6193, 2018. https://doi.org/10.1016/j.jece.2018.08.064

MORACI, N.; CALABRÒ, P. S. Heavy metals removal and hydraulic performance in zero-valent iron/pumice permeable reactive barriers. **Journal of Environmental Management**, v. 91, p. 2336-2341, 2010. https://doi.org/10.1016/j.jenvman.2010.06.019

PEREIRA, C. A. A.; NAVA, M. R.; WALTER, J. B.; SCHERER, C. E.; DALFOVO, A. D. K.; BARRETO-RODRIGUES, M. Application of zero valent iron (ZVI) immobilized in Ca-Alginate beads for C.I. Reactive Red 195 catalytic degradation in an air lift reactor operated with ozone. **Journal of Hazardous Materials**, v. 401, 2021. https://doi.org/10.1016/j.jhazmat.2020.123275

SEWWANDI, K. A. H. S.; NITISORAVUT, R. Nano zero-valent iron embedded on chitosan for enhancement of biohydrogen production in dark fermentation. **Energy Reports**, v. 6, p. 392-396, 2020. https://doi.org/10.1016/j.egyr.2020.11.225

Ambiente & Água - An Interdisciplinary Journal of Applied Science
ISSN 1980-993X – doi:10.4136/1980-993X
www.ambi-agua.net
E-mail: ambi.agua@gmail.com

Spatio-temporal variability of water quality in Billings Reservoir Central Body - São Paulo, Brazil[1]

ARTICLES doi:10.4136/ambi-agua.2823

Received: 22 Dec. 2021; Accepted: 18 Apr. 2022

Beatriz Milz[1*]; Patricia Oliveira de Aquino[2]; Jean Carlo Gonçalves Ortega[3]; Ana Luisa Vietti Bitencourt[2]; Cristina Souza Freire Nordi[2]

[1]Instituto de Energia e Ambiente. Divisão Científica de Gestão, Ciência e Tecnologia Ambiental. Universidade de São Paulo (USP), Avenida Professor Luciano Gualberto, n° 1289, CEP: 05508-010, Butantã, SP, Brazil.
[2]Instituto de Ciências Ambientais, Químicas e Farmacêuticas. Laboratório de Paleoecologia e Ecologia da Paisagem. Universidade Federal de São Paulo (UNIFESP), Campus Diadema, Rua Professor Arthur Riedel, n° 275, CEP: 09972-270, Diadema, SP, Brazil. E-mail: patricia.oaquino@outlook.com, ana.bitencourt@unifesp.br, cristina.freire@unifesp.br
[3]Instituto de Ciências Biológicas. Universidade Federal do Pará (UFPA), Rua Augusto Correa, n° 1, CEP: 66075-110, Belém, PA, Brazil. E-mail: ortegajean@gmail.com
[*]Corresponding author. E-mail: milz.bea@gmail.com

ABSTRACT

The Billings Reservoir is an important water body for public supply of the Metropolitan Region of São Paulo, Brazil, and water captation for public supply is located in the Rio Grande environmental compartment. This article evaluates the water quality of the environmental compartment Central Body I of the Billings Reservoir, which receives the reversed waters from the polluted Pinheiros River, at four sampling points with different contributions from the surroundings, seeking to verify the influence of seasonality on water quality and whether there was a difference in water quality between the sampling points. Water sampling was carried out on the surface at four points, in a longitudinal profile, covering two periods (dry and rainy) distributed in six samplings between 2016 and 2019. Analyzed variables included temperature, dissolved oxygen, pH, electrical conductivity, chlorophyll-a and nutrients (phosphorus and nitrogen). Space-Time Interaction tests revealed that physicochemical variables did not vary due to the interaction between sampling periods and points, but several variables varied significantly during the sampling period. The results of the Trophic State Index show that waters of Central Body I are classified as Hypereutrophic, highlighting the degradation of water quality in this compartment. This research will better inform public managers and assist their

[1]The raw dataset and the code for the data and statistical analysis present in this paper are available in the repository: https://github.com/beatrizmilz/ambi-agua-2823

This is an Open Access article distributed under the terms of the Creative Commons Attribution License, which permits unrestricted use, distribution, and reproduction in any medium, provided the original work is properly cited.

efforts to minimize and mitigate the effects of progressive water quality degradation in this reservoir.

Keywords: eutrophication, Pinheiros river, urban reservoir.

Variabilidade espaço-temporal da qualidade da água superficial do Corpo Central I da represa Billings - São Paulo, Brasil

RESUMO

A represa Billings é um reservatório importante para o abastecimento público da região metropolitana de São Paulo, no Brasil, e a captação de água para abastecimento público está localizada no compartimento ambiental Rio Grande. Este artigo tem como objetivo avaliar a qualidade das águas do compartimento ambiental Corpo Central I da represa Billings, que recebe as águas revertidas do poluído rio Pinheiros, em quatro pontos de coleta com contribuição do entorno diferenciada, buscando verificar a influência da sazonalidade nos resultados obtidos e se houve diferença da qualidade da água entre os pontos de coleta. As coletas de água foram realizadas na superfície em quatro pontos, em um perfil longitudinal, contemplando dois períodos (estiagem e chuvoso) distribuídos em seis coletas, entre os anos de 2016 e 2019. As variáveis analisadas foram temperatura, oxigênio dissolvido, pH, condutividade elétrica, clorofila-a e nutrientes (fósforo e nitrogênio). Os testes de Interação Espaço-Tempo revelaram que as variáveis físico-químicas não variaram devido à interação entre os pontos e períodos de amostragem, mas diversas variáveis variaram significativamente em função do período de amostragem. O resultado do Índice de Estado Trófico evidenciou que as águas do Corpo Central I foram classificadas como Hipereutróficas, destacando a degradação da qualidade das águas neste compartimento. Os resultados desta pesquisa podem subsidiar os gestores públicos na tentativa de minimizar os efeitos da degradação progressiva da qualidade da água deste reservatório.

Palavras-chave: eutrofização, reservatório urbano, Rio Pinheiros.

1. INTRODUCTION

Eutrophication is the enrichment by nutrients (mainly nitrogen and phosphorus) in aquatic ecosystems and is a growing global problem (Sinha *et al.*, 2017). Eutrophication causes a decrease in water quality and prevents its use for human consumption in many cases (Nogueira *et al.*, 2015; Andrade *et al.*, 2020; Nobre *et al.*, 2020). For example, eutrophication increases turbidity and algae biomass, particularly toxin-producing groups (e.g., *Microcystis aeruginosa*).

The Metropolitan Region of São Paulo (MRSP) is located in the Southeast region of Brazil, with a population of more than 21.1 million inhabitants, which represents around 50% of the population of the State of São Paulo. The Billings Reservoir is the largest reservoir of water in the Metropolitan Region of São Paulo, and has multiple uses, including supply of water to the population (Risso *et al.*, 2018); unfortunately, the low quality of its waters has been compromising its use for public supply.

The Billings Reservoir was constructed in 1927 in order to supply water to the Henry Borden Complex, a hydroelectric power plant. To supply the amount of water needed by the Henry Borden Complex, the Billings Reservoir received reversed waters from the Tietê and Pinheiros Rivers by the Pedreira Pumping Plant.

The Billings Reservoir has been impacted by eutrophication, which has been detected by several studies (Cardoso-Silva *et al.*, 2014; Pompêo *et al.*, 2015; Gargiulo *et al.*, 2016; CETESB, 2020; Alcantara *et al.*, 2021). Eutrophication in this reservoir results from two main

sources: reversal of waters from the polluted Pinheiros and Tietê Rivers, and occupation of its watershed (Wengrat and Bicudo, 2011; Cardoso-Silva *et al.*, 2014; CETESB, 2020). The increasing pollution of waters from the Tietê and Pinheiros Rivers, the consequent degradation of the Billings Reservoir waters, and the increasing need to use its waters as a source for public supply led to restrictions regarding the reversal of water from the Tietê and Pinheiros Rivers (Collaço *et al.*, 2020). Since 1992, pumping of water from the Pinheiros River into the Billings Reservoir has been allowed mainly for flood management purposes, which occurs most frequently in the rainy season. Nowadays, reversion of waters from Pinheiros and Tiete Rivers is still allowed by legislation (Joint Resolution SMA/SSE-002/2010) in certain conditions, such as: flood control; formation of surfactant foams in the Tietê River that may form atop the water surface; drop in water intake by the Henry Borden Plant to levels insufficient to ensure the supply of electricity in emergencies; and formation of algal blooms in water bodies of the Metropolitan Region of São Paulo and Médio Tietê, compromising their quality for purposes of public supply (Sao Paulo, 2010).

This study evaluated spatial and temporal variability of water quality of the Billings Reservoir in its central body. The following research questions drove this study: I) Is there a difference in water quality regarding sampling seasons?; II) Does water quality vary spatially within the reservoir?; and, III) Which variables have the largest influence on water quality at different sampling points and seasons?

2. MATERIAL AND METHODS

2.1. Characterization of study area

The Billings Reservoir is located in the Metropolitan Region of São Paulo (State of São Paulo - Brazil) (Figure 1), and is part of six municipalities: Santo André, São Bernardo do Campo, Diadema, Ribeirão Pires, Rio Grande da Serra and São Paulo. This reservoir is part of the Upper Tietê Hydrographic Basin, a basin with low water availability per inhabitant.

The “Area of Protection and Recovery of Water Sources - Billings Reservoir” (APRWS - Billings) was created by the government of São Paulo (State law #13.579/2009), and separated the reservoir area into environmental compartments for land use and occupation planning purposes, namely as: Central Body I, Central Body II, Taquacetuba-Bororé, Rio Grande and Rio Pequeno, and Capivari-Pedra Branca. Water captation for public supply in the Billings reservoir is located in the Rio Grande environmental compartment, and in the 1980s a dam was constructed with the purpose of separating its waters from other environmental compartments, which were already impacted by water pollution.

2.2. Analysis

The analysis and visualization of data and statistical analysis were performed using the R software (*https://www.r-project.org/*) (R Core Team, 2021). R Packages used in this research are available on the Comprehensive R Archive Network (CRAN).

2.3. Quality evaluation of surface waters

Water was sampled on the surface covering four sampling points (P1 to P4) (Figure 1) and in two samplings periods: three in the dry season (August/2016, August/2017, August/2018) and three in the rainy season (January/2017, February/2018, February/2019), in order to analyze the influence of seasonality. The first sampling point (P1) is located close to the Pedreira Pumping Plant, and the fourth sampling point (P4) is located farthest from it.

Water temperature (WT), dissolved oxygen (DO), pH and electrical conductivity (EC) of water were measured *in situ* using a HACH sensor (model HQ40D). Water samples were collected and analyzed for concentration of parameters: Total nitrogen (TN) (Valderrama, 1981), Nitrate (NO3) (Mackereth *et al.*, 1989), Nitrite (NO2) (Mackereth *et al.*, 1989),

Ammonium (NH4) (Koroleff, 1976), total phosphorus (TP) (Valderrama, 1981), total dissolved phosphorus (TDP) (Strickland and Parsons, 1960), Soluble reactive phosphorus (SRP) (Strickland and Parsons, 1960), and Chlorophyll-a (CHLA) (CETESB, 2014). The Trophic State Index for tropical/subtropical reservoirs (TSI-tsr) was calculated according to Cunha *et al.* (2013). The analysis and visualization of data was performed using the packages adespatial (Dray, 2020), SciViews (Grosjean, 2019), and tidyverse (Wickham *et al.*, 2019).

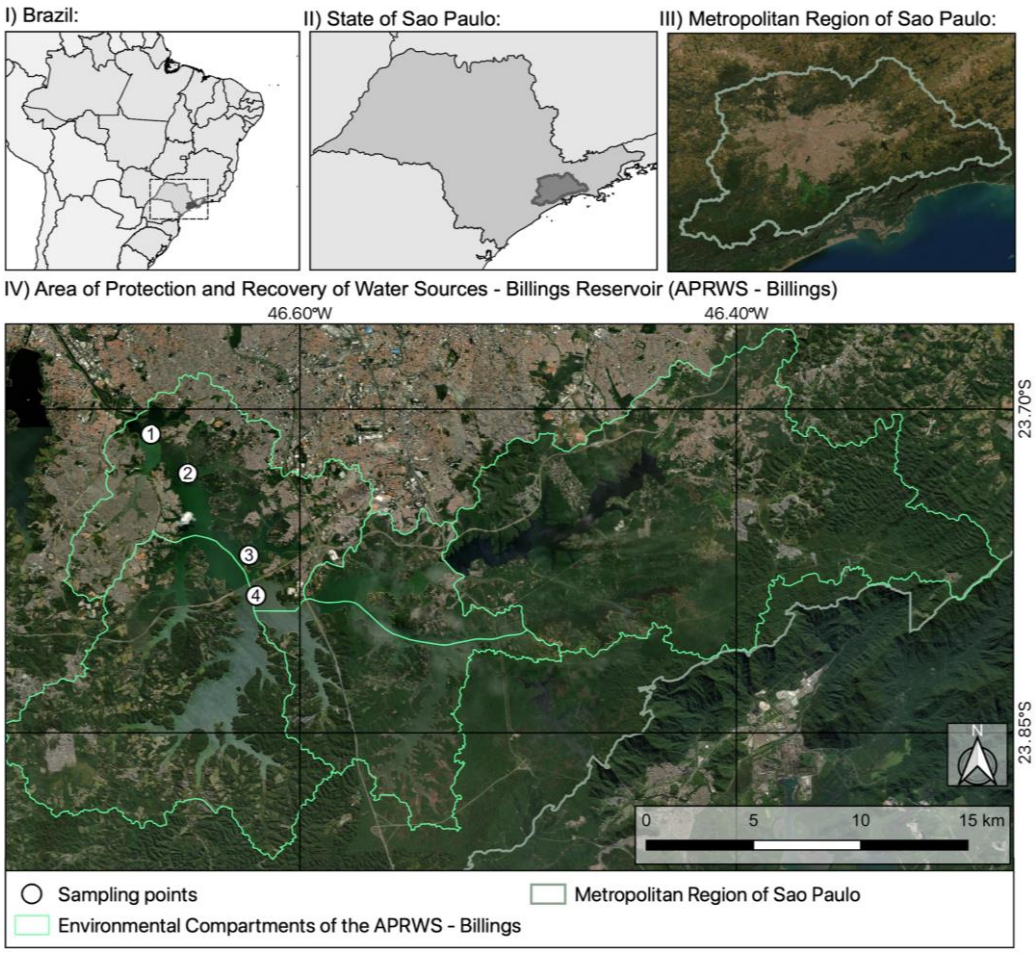

Figure 1. Map of the location of the Billings Reservoir and sampling points.
Source: Elaborated by the first author. Shapefiles from DataGEO (http://datageo.ambiente.sp.gov.br/).

2.4. Principal Component Analysis

A principal component analysis (PCA) was performed to summarize the variation of nutrients (TN, NO2, NO3, NH4, TP, TDP, SRP), chlorophyll-a, and the following measures from water surface: water temperature, pH, dissolved oxygen and electrical conductivity. PCA was conducted with normalized variables and with a correlation matrix (Legendre and Legendre, 2012). Axes were retained for interpretation following the Broken-Stick criterion (Jackson, 1993). Variables with loadings higher than |0.6| were considered as relevant for PCA axes ordination. PCA was performed using R software (R Core Team, 2021) with stats and vegan packages (Oksanen et al., 2020), and visualization of PCA ordinations were made with ggplot2 (Wickham *et al.*, 2019) and patchwork packages.

2.5. Space-time interaction analysis

Space-time interaction analysis (STI; Legendre *et al.*, 2010) was used to assess whether

there was an interaction between sampling points (space) and sampling periods (time) in the variation of physical, chemical, and biological parameters. This analysis is necessary because sampling in each period was carried out at four sampling points. In this case, testing the interaction between periods and sampling points by a traditional analysis of variance (ANOVA) is not possible due to the absence of replicates to estimate the sum of squares of residuals (Legendre *et al.*, 2010). In STI, a factorial ANOVA model was used with sub-adjusted interaction (Model 5 in Legendre *et al.*, 2010). This model allows testing the interaction in the absence of replication, has correct Type I error rates and allows the use of univariate or multivariate response variables (Legendre *et al.*, 2010). Therefore, as a response matrix in STI, we used a matrix with all 15 physicochemical variables transformed by log10 (x + 1) (except pH) and standardized.

To explore which parameters varied according to sampling points and sampling periods, univariate STIs were performed with each physicochemical variable transformed by log10 (x + 1) (except pH) as response variable. Significance in STI was assessed using 999 permutations. A significance level of 5% was adopted and all analyses were performed in the R software (R Core Team, 2021) with adespatial (Dray, 2020) package.

2.6. Water quality standards in Brazil

The National Council for the Environment (CONAMA) created Resolution No. 357 (CONAMA, 2005), which classifies water resources and regulates their predominant uses with water quality standards. The classification of water bodies proposed by this resolution presents classes as a set of conditions and standards of water quality necessary to meet the prevailing uses, current or future, and that must be considered as goals to be achieved by public managers.

The Billings Reservoir was classified by the State Government of São Paulo as a Class II water body (Sao Paulo, 1977). According to the aforementioned resolution, Class II waters can be used for human consumption (after conventional treatment), for protection of aquatic communities, for primary contact recreation, for irrigation of vegetables, fruit plants and parks, gardens, sports fields and leisure, with which the public may have direct contact, aquaculture, and fishing activities (CONAMA, 2005).

The results of this study will be compared with the standards established in the Conama Resolution No. 357 for Class II water bodies, in order to know if the quality standards of the water in the reservoir are in accordance with those established in the Brazilian legislation.

3. RESULTS AND DISCUSSION

3.1. Space-time interaction (STI)

Physicochemical variables did not vary due to the interaction between sampling periods and points ($F_{2,13}$ = 1.41, p = 0.20). Together, physicochemical variables varied between sampling periods (Sampling period: $F_{5,13}$ = 4.48, p < 0.01, R^2adj = 0.25) and between sampling points (Sampling point: $F_{3,13}$ = 5.46, p < 0.01, R^2adj = 0.2), and these factors explained about 25% and 20% of this physicochemical variability, respectively.

The interaction between sampling point and period was only significant when physicochemical variables were modeled separately for NO2 and WT, with low predictive power in these cases (Table 1). TN, NO3, NH4, TDP, SRP, CHLA, DO, EC, and pH varied significantly in function of time (Table 1). For variation in time, explanatory power varied from a weak relationship (R^2adj = 0.17) to a strong predictive power (R^2adj = 0.79; Table 1). NH4, TP, TDP, SRP, DO, EC, and pH varied significantly in function of space, among sampling points (Table 1). For differences in space, explanatory power varied from a very weak relationship (R^2adj ≈ 0.00) to a moderate predictive power (R^2adj = 0.37; Table 1).

Table 1. Effect of space (sampling point) and time (sampling period) on the variation of physicochemical variables. S: space; T: time; S*T: interaction between space and time. F values in bold were significant.

Variable	Parameters	F	p	R²adj
Total Nitrogen (TN)	Space × Time	1.77	0.23	0.00
	Space	2.45	0.1	0.00
	Time	**24.42**	< 0.01	0.79
Nitrite (NO2)	Space × Time	**5.4**	0.02	0.04
	Space	**17.7**	< 0.01	0.56
	Time	1.82	0.18	0.00
Nitrate (NO3)	Space × Time	2.01	0.15	0.02
	Space	1.62	0.07	0.00
	Time	**3.4**	0.02	0.28
Ammonium (NH4)	Space × Time	0.03	0.97	0.00
	Space	**4.99**	< 0.01	0.21
	Time	**3.82**	0.03	0.24
Total Phosphorus (TP)	Space × Time	1.61	0.23	0.01
	Space	**3.74**	0.04	0.22
	Time	1.51	0.25	0.00
Total Dissolved Phosphorus (TDP)	Space × Time	0.62	0.55	0.00
	Space	**7.77**	< 0.01	0.20
	Time	**7.81**	0.01	0.37
Soluble Reactive Phosphorus (SRP)	Space × Time	2.47	0.1	0.00
	Space	**3.24**	0.04	0.00
	Time	**10.02**	< 0.01	0.55
Chlorophyll-a (CHLA)	Space × Time	0.46	0.65	0.00
	Space	2.4	0.13	0.06
	Time	**3.68**	0.04	0.32
Water Temperature (WT)	Space × Time	**4.86**	0.03	0.00
	Space	**5.22**	0.02	0.00
	Time	**731.07**	< 0.01	0.99
Dissolved Oxygen (DO)	Space × Time	1.73	0.22	0.00
	Space	**12.93**	< 0.01	0.37
	Time	**6.03**	< 0.01	0.17
Electrical Conductivity (EC)	Space × Time	0.2	0.85	0.00
	Space	**10.79**	< 0.01	0.12
	Time	**18.37**	< 0.01	0.58
pH (pH)	Space × Time	1.83	0.19	0.00
	Space	**8.28**	< 0.01	0.27
	Time	**5.14**	0.02	0.21

3.2. Principal Component Analysis (PCA)

The first three components from the Principal Component Analysis (PCA) were retained for interpretation following the Broken-Stick criterion. These three PCA axes explained 71.75% of the total variance of limnological data (Table 2). The PC1 explained 37.54% of the total

variance of data, representing a gradient of individual contribution of nutrients (NO2, NO3, TDP and SRP) and electrical conductivity on the positive side, and dissolved oxygen and pH on the negative side (Table 2). All these parameters are related to anthropogenic activities and high levels of eutrophication in the Billings Central Body I. PC2 explained 19.49% of the total variance, with NO2, WT and CHLA presenting the highest negative loadings. These results suggest the influence of higher temperature on phytoplankton growth indicated by high levels of CHLA that influence the change of pH due to the high consumption of CO2. Finally, PC3 explained 14.72% of the total variance, represented by a gradient of total nutrients (TN and TP) with higher values on the negative side of this axis.

Table 2. Loadings, Eigenvalues and Proportion of explained variance of a Principal Component Analysis (PCA) ordination summarizing limnological variables sampled in Billings reservoir from August, 2016 to February, 2019. Only the axes with eigenvalues higher than those expected by a Broken-Stick distribution are presented.

Group	Variables	PCA1	PCA2	PCA3
Proportion of variance explained		37.544	19.494	14.717
Eigenvalues		4.505	2.339	1.766
Eigenvectors	Total Nitrogen (TN)	-0.061	0.507	-0.809
	Nitrite (NO2)	0.618	-0.617	-0.185
	Nitrate (NO3)	0.739	0.462	0.355
	Ammonium (NH4)	0.253	0.339	-0.537
	Total Phosphorus (TP)	0.549	0.014	-0.656
	Total Dissolved Phosphorus (TDP)	0.632	-0.185	0.219
	Soluble Reactive Phosphorus (SRP)	0.835	0.202	0.228
	Chlorophyll-a (CHLA)	0.267	-0.793	-0.335
	Water Temperature (WT)	-0.527	-0.762	-0.088
	Dissolved Oxygen (DO)	-0.775	0.154	-0.093
	Electrical Conductivity (EC)	0.817	-0.244	-0.019
	pH (pH)	-0.703	-0.078	0.064

Samples are more clearly grouped by season than by spatial differences in limnological variables following a combination of PC1 and PC2 (Figure 2a), and PC2 and PC3 (Figure 2c). Samples from the dry period tended to present higher NO3, SRP, and lower WT (Figure 2a). This tendency can be related to lower phytoplankton biomass in this season. Within the rainy season, spatial differences were more evident mainly due to a tendency of increasing values of WT from Site 1 to Site 4. Furthermore, sampling Point P1 also presented a higher variability in limnological variables considering both PC1 and PC2 scores, particularly in the rainy season (Figure 2a). Seasonal differences were less clear considering PC1 and PC3, but it is possible to infer that in the dry season, samples tended to present higher EC, lower DO and pH (Figure 2b). Finally, considering both PC2 and PC3, samples also tended to group by sampling season, with samples from the rainy season presenting higher WT and chlorophyll-a than those from the dry season (Figure 2c). These results probably indicate the influence of temperature and rainfall effects from reservoir adjacent areas favoring the growth of phytoplankton and elevating CHLA levels.

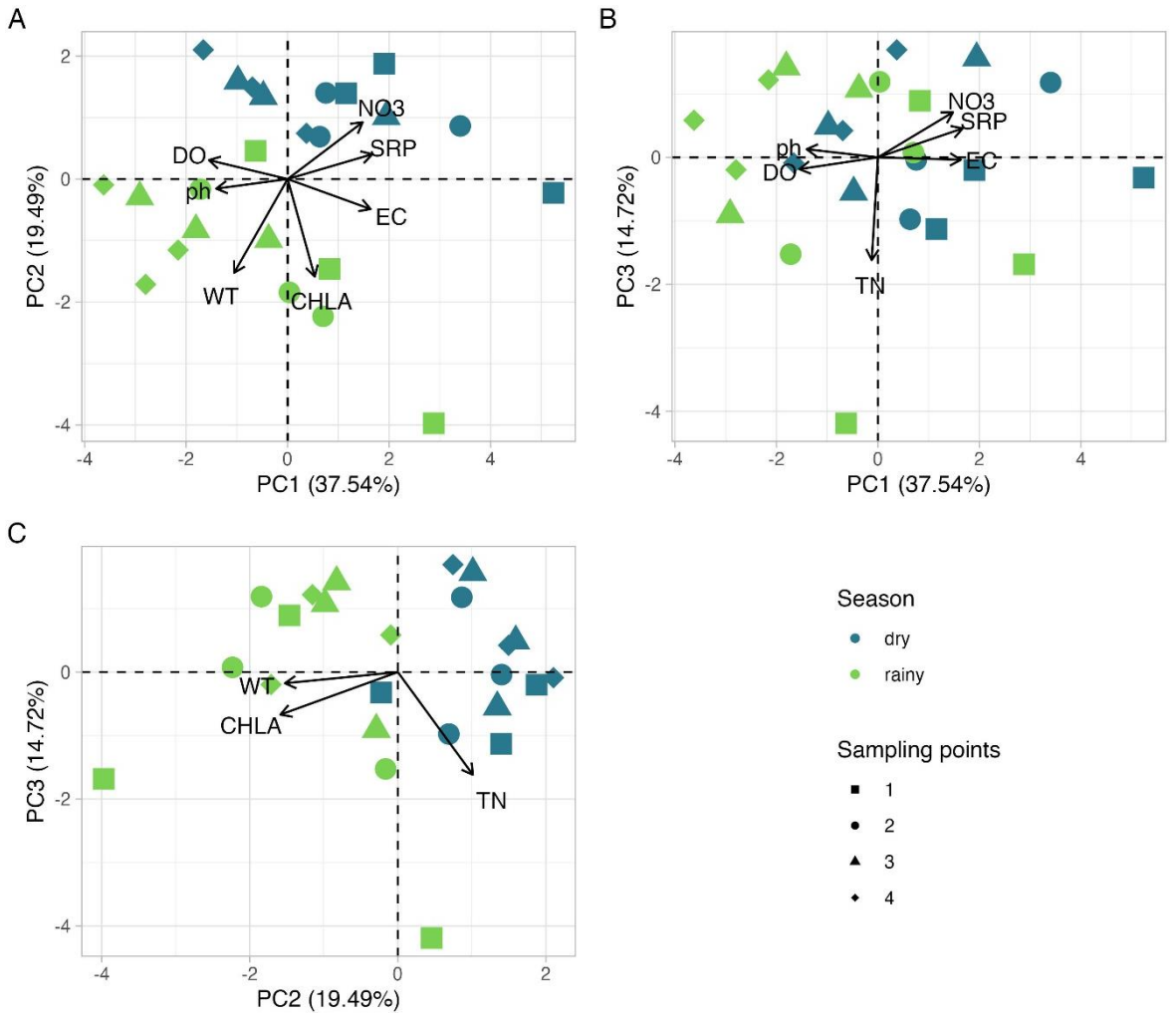

Figure 2. Principal Component Analysis ordination summarizing limnological variables sampled in Billings reservoir from August, 2016 to February, 2019.

3.3. Physicochemical parameters

Water temperature (WT) tended to be higher in the rainy season than in the dry one for all sampling points (Figure 3). WT is an important parameter that influences the DO and also affects aquatic communities (Saha *et al.*, 2021). That happens because with increasing temperature, oxygen solubility decreases (Matear and Hirst, 2003), which further hampers its consumption by organisms and may cause physiological stress when oxygen consumed does not supply metabolic demands (Nebeker *et al.*, 1996; Roman *et al.*, 2019). Mean values for the dry and rainy seasons were 18.58°C and 26.09°C, respectively. Results for water temperature were similar to other tropical reservoirs and this difference is related to air temperature. Similar results about seasonality influence on WT were obtained by Saha *et al.* (2021) in the tropical Metther Reservoir, in India.

Dissolved oxygen (DO) ranged from 4.39 to 9.14 mg/L during the dry season. Variation in the rainy season was from 2.37 to 13.86 mg/L. DO tended to be more variable in each sample site in the rainy season. For site four, DO tended to be higher in the rainy season than in the dry season. All sampling points showed the highest values during the rainy season. The standard for DO for Class II water bodies is > 5.0 mg/L (CONAMA, 2005), and 25% of water samples in both seasons were not in accordance with this standard. The high concentration of CHLA in the same period (Figure 3) indicates the possible contribution produced by phytoplankton photosynthesis. Furthermore, the diffusion by turbulent mixing by rain and/or water reversal

from the Pinheiros and Tietê Rivers to the Billings Reservoir may also contribute to higher O_2 in the rainy period.

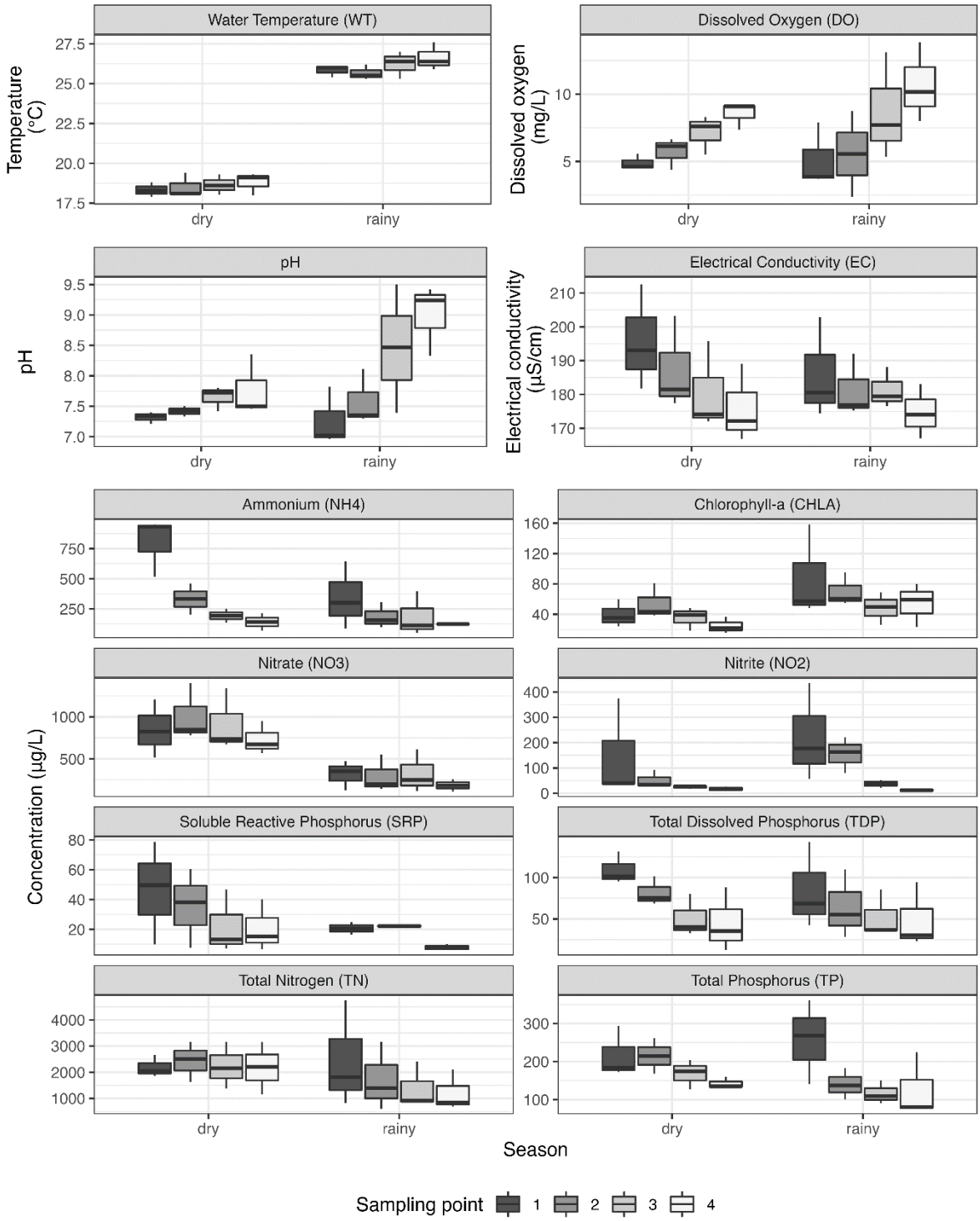

Figure 3. Variation of Water temperature, Dissolved oxygen, pH, Electrical conductivity, nutrients, and Chlorophyll-a according to season and sampling point. Each box represents interquartile range, horizontal thick line represents median and whiskers represent minimum and maximum values.

The variation of pH values was from 7.21 to 8.35 in the dry season and from 6.96 to 9.5 in the rainy season. pH tended to be more variable in each sample site in the rainy season. For sites three and four, pH tended to be higher in the rainy season than in the dry one (Figure 3).

The standard for pH for Class II water bodies is between 6.0 and 9.0 (CONAMA, 2005), and 25% of water samples in the rainy season were not in accordance with this standard. pH results indicated the tendency from neutral (P1) to alkalinity (P4) conditions in both seasons along the sampling points.

The activities of aquatic microorganisms are influenced by pH and drive pH variation. Higher values of CHLA verified during the rainy season can indicate phytoplankton growth. With a higher phytoplankton growth, a higher photosynthesis would be fixing more C and releasing H (both often available as HCO3- in the observed pH range) to the water column, collaborating to the change toward alkaline conditions (Horne and Goldman, 1994; Maberly, 1996; Nazneen *et al.*, 2019). The highest values for pH were observed in the rainy season; the same tendency was observed for DO. In the report from CETESB (2020), pH followed the behavior observed for DO, with values that exceed those considered a quality standard in 44% of the samples during 2019, and high oxygen concentrations are due to algal bloom events, confirming the state of eutrophication of the reservoir (CETESB, 2020).

Electrical conductivity (EC) is the ability of a solution to conduct a given electrical current; it means that the higher ion concentration in the water, the greater its electrical conductivity. EC ranged from 166.8 to 212.5 µS/cm in the dry season and from 167 to 202.9 µS/cm in the rainy season. EC tended to be lower in the rainy season than in the dry one, especially in sampling sites one and two (Figure 3). Comparing EC between sampling points, the highest value was obtained for P1 for both seasons. EC results showed higher values during the dry season, and it showed the opposite tendency compared to DO and pH tendencies. Wengrat and Bicudo (2011) also obtained higher values in the dry season. Saha *et al.* (2021) also observed higher values of EC (183.6 - 428.8 µS/cm) in an Indian tropical reservoir and attributed it to pollution accumulation. In this work, we also attribute this highest concentration to pollution accumulation, because in the dry season there is less rainwater to dilute pollutants. Also, mean values in this study were around 182.91 µS/cm and similar in both seasons.

Total nitrogen (TN; Figure 3) presented higher values during the dry season compared to the rainy season, except for P1. TN mean value was 1977.48 µg/L, which shows an increase in TN compared to values obtained by Cardoso-Silva *et al.* (2014), who carried out sampling at some points in the Billings Reservoir in 2014, obtaining a mean of 1230 µg/L for TN. Values obtained for Nitrite-N (NO2) were lower when compared to NO3 and NH4. This result is explained because among nitrogenous forms, nitrite is considered the most unstable one in aquatic ecosystems, as it is quickly converted to nitrate (Saha *et al.*, 2021). The standard for NO2 and NO3 for Class II water were met in all water samples, in the dry and rainy seasons.

Nitrate (NO3) and NH4 have an important role in water quality, being the main sources of nitrogen for aquatic primary producers. Nitrate (Figure 3) showed higher values during the dry season (517.16 - 1400.94 µg/L) compared to the rainy season (112.09 - 614.24 µg/L). The highest value of NO3 and TN during dry season may be due to the entry of more concentrated sewage because there is little rain contribution, and it may also be related to lower phytoplankton biomass. Cardoso-Silva *et al.* (2014) obtained results in the Billings reservoir for NO3 that ranged from 290.52 µg/L to 464.1 µg/L. The highest value of 1400.94 obtained in this study was much higher than the one found in 2014 by Cardoso-Silva *et al.* (2014), revealing an increasing of nitrate levels in the Central Body I. Higher NH4 values were obtained in P1 for both seasons, with mean values of 799.56 µg/L (dry season) and 343.46 µg/L (rainy season) in P1. The highest value obtained for NH4 concentration by Cardoso-Silva *et al.* (2014) was 233.00 µg/L. The highest values for NH4 at P1 in this study can be a consequence of reversal waters from the Pinheiros River, since this sampling point is located close to the Pedreira Pumping Plant. Around 42% of water samples in the rainy season were not in accordance with the standard for Class II water bodies (CONAMA, 2005), while around 50% of water samples were not in accordance with this standard in the dry one.

Phosphorus is an important nutrient to primary producers and it is also used to indicate trophy of aquatic ecosystems. Total Phosphorus (TP) varied from 126.54 to 293.63 µg/L in the dry season and from 76 to 360.89 µg/L in the rainy season. The mean value for TP in both seasons was 172.76 µg/L, and it was higher in the rainy season than in the dry season only for sampling site one, while the remaining sites tended to show lower values in the rainy season than in the dry season (Figure 3). The same tendency was observed by Wengrat and Bicudo (2011), who also determined higher results for TP during the rainy season. The trend of increasing TP concentrations in rainy months, in the Central Body of the Billings Reservoir, may be associated with the increase in surface runoff due to the rainy season carrying nutrients to waters; and to the Pinheiros River reverse pumping to the Billings Reservoir, which increases the affluent polluting loads into the water CETESB (2020). According to CETESB (2020), in 2019, a greater volume of waters from the Pinheiros River was pumped into the Billings Reservoir in the rainy season, especially in February and March, resulting in a greater input of Phosphorus and other pollutants into the Central Body I of the reservoir (CETESB, 2020). The standard for TP for Class II water bodies is < 100 µg/L (CONAMA, 2005), and all water samples in the rainy season were not in accordance with this standard, while 75% of water samples were not in accordance with this standard in dry one.

Results for Total dissolved phosphorus (TDP) ranged from 12.43 to 131.35 µg/L during the dry season and from 23.33 to 143.24 µg/L during the rainy season. The soluble reactive phosphorus (SRP) fraction or Orthophosphate comprises all types of inorganic phosphorus in solution (Markad *et al.*, 2019). SRP varied seasonally, being higher and more variable in the dry season than the rainy season for all sampling points. SRP results in the dry season ranged from 6.77 to 78.77 µg/L, and from 6.09 to 24.94 µg/L during the rainy season. As SRP is the main form of phosphorus assimilated by phytoplankton, the lower values obtained in the rainy season can be associated with greater phytoplankton biomass (Chlorophyll-a) obtained in that season.

Chlorophyll-a (CHLA) is a parameter used as an indicator of algal biomass and also considered the main indicator of the trophic state of aquatic environments (CETESB, 2020). CHLA concentration in the dry season ranged from 15.59 to 81.08 µg/L and from 23.17 to 158.3 µg/L in the rainy season. Higher values of CHLA were observed during the rainy season. The highest CHLA value was verified in P1 during the rainy season and may be associated with the reversing of waters from Pinheiros River waters into the Billings Reservoir, to prevent flooding in the floodplain of the Pinheiros River during the rain period in the city of São Paulo (Cardoso-Silva *et al.*, 2014). The standard for CHLA for Class II water bodies is < 30 µg/L (CONAMA, 2005), and around 85% of water samples in the rainy season were not in accordance with this standard, while around 67% of water samples were not in accordance with this standard in the dry one.

Nitrogen and phosphorus forms had the highest values in the dry season. Comparison with CHLA variation indicated an inverse trend, presenting higher values in the rainy season. These results indicate that the highest phytoplankton density contributed with the decay of nitrogen and phosphorus since they are essential to phytoplankton development and reproduction (Jeppesen *et al.*, 2005; Marcarelli and Wurtsbaugh, 2007; Filstrup and Downing, 2017). Nutrient availability and increased concentrations of CHLA in the water surface from the water ascending operational phase appear to be linked to the rainy season, bringing organic matter and dissolved nutrients from surrounding areas to the reservoir.

Results indicate P1 in the rainy season as a nutrient-rich environment, and may indicate the presence of cyanobacteria (Rocha *et al.*, 2014) (Figure 3). Ribeiro *et al.* (2020) observed highest cyanobacteria concentration in the same period confirming the tendency of eutrophic environments favoring the presence of these groups of microorganisms. Furthermore, lower CHLA concentrations in the falling water compared with the low water operational phase also

seem to be explained by water residence time.

The application of Trophic State Index for tropical/subtropical reservoirs (Cunha *et al.*, 2013) resulted in around 91.7% of the samples being classified as Hypereutrophic, and 8.3% as Supereutrophic. These results show that, in all four sampling points, and in the rainy and dry seasons, waters of the Billings Reservoir are impacted by eutrophication. In a study by Alcantara *et al.* (2021) in the Billings Reservoir, waters of the Central Body I were classified as Hypereutrophic both in 2019 and 2020.

Other examples of tropical reservoir that are impacted by eutrophication are: Guarapiranga reservoir, in the State of São Paulo - Brazil (Alcantara *et al.*, 2021) and Barra Bonita reservoir, also in the State of São Paulo - Brazil (Watanabe *et al.*, 2015). Also, Boëchat *et al.* (2019) studied six shallow lakes and two reservoirs at the Atlantic forest in Southeastern Brazil and determined hypereutrophic state to lake Rasa and Pampulha Reservoir.

4. CONCLUSIONS

The results of this study show that waters of the Central Body I in Billings Reservoir are impacted by eutrophication in both seasons (dry and rainy) and all sampling points. It is important to monitor the water quality of this reservoir, especially for TP, CHLA and NH4, for which several samples showed that the results were not in accordance with the standards of the Brazilian Legislation, set by the CONAMA (2005).

Statistical analysis showed that seasonality presents a greater influence on water quality in the reservoir, compared to the difference between sampling points. Response variables that have the largest influence on the analysis of water quality, at the different sampling points and seasons, were TN, EC, and SRP, since they varied significantly and presented the highest predictive power in the STI tests. WT is a variable closely related to sampling season, and other variables are more related to the input of pollution on the reservoir.

P1 is the sampling point that is closer to the Pedreira Pumping Plant, and results indicate that waters in this sampling point are the most polluted. These results showed the influence of dumping reversed waters from the polluted Pinheiros and Tiete Rivers on the Billings Reservoir. It is important that the quality of waters of the Pinheiros and Tiete Rivers are improved, in order to minimize the degradation of the Central Body I of the Billings Reservoir. Another important effort that is needed is to improve the collection and treatment of wastewater on the households that are on the Billings watershed. One important step towards these goals is the “New Pinheiros River Program” (https://novoriopinheiros.sp.gov.br/), which is a program led by the State Government. This program aims at the depollution of the Pinheiros River, based on basic sanitation, cleaning, dredging and environmental education. The effects of this program will be seen in future research, and the results obtained in this research will serve as comparative parameters, in order to evaluate the effects of the future Pinheiros River depollution on the water quality of the Central Body I of the Billings Reservoir.

This study presents recent data about a water body that is important to the public water supply in the Metropolitan Region of São Paulo, a region with more than 21 million inhabitants. Therefore, these results can assist public managers in minimizing the effects of progressive water quality degradation of this reservoir.

5. ACKNOWLEDGMENTS

The first author thanks the São Paulo Research Foundation (FAPESP) - Grant number 18/23771-6. The third author thanks the Coordination for the Improvement of Higher Level Personnel (CAPES) for a postdoctoral scholarship - Grant Number 88887.374969/2019-00. The last author thanks the São Paulo Research Foundation (FAPESP) and Basic Sanitation Utility

Company of the State of São Paulo (SABESP) - Grant number PITE-SABESP 2010/50738-8.

6. REFERENCES

ALCANTARA, E. *et al.* A Satellite-Based Investigation into the Algae Bloom Variability in Large Water Supply Urban Reservoirs During COVID-19 Lockdown. **Remote Sensing Applications: Society and Environment**, v. 23, p. 100555, 2021. https://doi.org/10.1016/j.rsase.2021.100555

ANDRADE, E. M. de *et al.* Balanço de nitrogênio e fósforo em um reservatório na região semi-árida tropical. **Revista Ciência Agronômica**, v. 51, n. 1, 2020. https://doi.org/10.5935/1806-6690.20200020

BOËCHAT, I. G. *et al.* Dissolved Organic N in Shallow Tropical Lakes and Reservoirs: Contribution to Total Dissolved N and Relationships with Eutrophication. **International Review of Hydrobiology**, v. 104, n. 5-6, p. 106–115, 2019. https://doi.org/10.1002/iroh.201801958

CARDOSO-SILVA, S. *et al.* Compartimentalização e qualidade da água: o caso da Represa Billings. **Bioikos**, v. 28, n. 1, 2014.

CETESB. **Determination of chlorophyll-a and pheophytin-a: spectrophotometric method**. São Paulo, 2014.

CETESB. **Qualidade das águas interiores no estado de São Paulo 2019**. São Paulo, 2020.

COLLAÇO, F. M. de A. *et al.* Understanding the Energy System of the Paulista Macrometropolis: First Step in Local Action toward Climate Change. **Ambiente & Sociedade**, v. 23, 2020. https://doi.org/10.1590/1809-4422asoc0176r1vu2020l6td

CONAMA (Brasil). Resolução nº 357 de 17 de março de 2005. Dispõe sobre a classificação dos corpos de água e diretrizes ambientais para o seu enquadramento, bem como estabelece as condições e padrões de lançamento de efluentes, e dá outras providências. **Diário Oficial [da] União**: seção 1, Brasília, DF, n. 053, p. 58-63, 18 mar. 2005.

CUNHA, D. G. F.; CALIJURI, M. do C.; LAMPARELLI, M. C. A Trophic State Index for Tropical/Subtropical Reservoirs (TSItsr). **Ecological Engineering**, v. 60, p. 126–134, 2013. https://doi.org/10.1016/j.ecoleng.2013.07.058

DRAY, S. et al. adespatial: Multivariate Multiscale Spatial Analysis. R package version 0.3-8. 2020. https://CRAN.R-project.org/package=adespatial.

FILSTRUP, C. T.; DOWNING, J. A. Relationship of Chlorophyll to Phosphorus and Nitrogen in Nutrient-Rich Lakes. **Inland Waters**, v. 7, n. 4, p. 385–400, 2017. https://doi.org/10.1080/20442041.2017.1375176

GARGIULO, J. R. B. C. *et al.* Benthic Macroinvertebrates as Bioindicators of Water Quality in Billings Reservoir Fishing Sites (SP, Brazil). **Acta Limnologica Brasiliensia**, v. 28, 2016. https://doi.org/10.1590/S2179-975X2315

GROSJEAN, P. SciViews-R. UMONS, MONS, Belgium. R package version 0.9-13.1. 2019. http://www.sciviews.org/SciViews-R

HORNE, A. J.; GOLDMAN, C. R. **Limnology**. New York: McGraw-Hill, 1994.

JACKSON, D. A. Stopping Rules in Principal Components Analysis: A Comparison of Heuristical and Statistical Approaches. **Ecology**, v. 74, n. 8, p. 2204–2214, 1993. https://doi.org/10.2307/1939574

JEPPESEN, E. *et al.* Lake Responses to Reduced Nutrient Loading an Analysis of Contemporary Long-Term Data from 35 Case Studies. **Freshwater Biology**, v. 50, n. 10, p. 1747–1771, 2005. https://doi.org/10.1111/j.1365-2427.2005.01415.x

KOROLEFF, F. Determination of Nutrients. *In*: GRASSHOFF, K. (ed.). **Methods of Seawater Analysis**. New York: Verlag Chemie, 1976. p. 117–181.

LEGENDRE, P.; CÁCERES, M. D.; BORCARD, D. Community Surveys through Space and Time: Testing the SpaceTime Interaction in the Absence of Replication. **Ecology**, v. 91, n. 1, p. 262–272, 2010. https://doi.org/10.1890/09-0199.1

LEGENDRE, P.; LEGENDRE, L. **Numerical Ecology**. 3. ed. Amsterdam: Elsevier, 2012. v. 24

MABERLY, S. C. Diel, Episodic and Seasonal Changes in pH and Concentrations of Inorganic Carbon in a Productive Lake. **Freshwater Biology**, v. 35, n. 3, p. 579–598, 1996. https://doi.org/10.1111/j.1365-2427.1996.tb01770.x

MACKERETH, F. J. H.; HERON, J.; TALLING, J. F. **Water Analysis: Some Revised Methods for Limnologists**. United Kingdom: Freshwater Biological Association, 1989.

MARCARELLI, A. M.; WURTSBAUGH, W. A. Effects of Upstream Lakes and Nutrient Limitation on Periphytic Biomass and Nitrogen Fixation in Oligotrophic, Subalpine Streams. **Freshwater Biology**, v. 52, n. 11, p. 2211–2225, 2007. https://doi.org/10.1111/j.1365-2427.2007.01851.x

MARKAD, A. T. *et al.* Trophic State Modeling for Shallow Freshwater Reservoir: A New Approach. **Environmental Monitoring and Assessment**, v. 191, n. 9, p. 586, 2019. https://doi.org/10.1007/s10661-019-7740-5

MATEAR, R. J.; HIRST, A. C. Long-Term Changes in Dissolved Oxygen Concentrations in the Ocean Caused by Protracted Global Warming. **Global Biogeochemical Cycles**, v. 17, n. 4, 2003. https://doi.org/10.1029/2002GB001997

NAZNEEN, S. *et al.* Spatial and Temporal Dynamics of Dissolved Nutrients and Factors Affecting Water Quality of Chilika Lagoon. **Arabian Journal of Geosciences**, v. 12, n. 7, p. 243, 2019. https://doi.org/10.1007/s12517-019-4417-x

NEBEKER, A. V. *et al.* Effect of Low Dissolved Oxygen on Aquatic Life Stages of the Caddisfly Clistoronia Magnifica (Limnephilidae). **Archives of Environmental Contamination and Toxicology**, v. 31, n. 4, p. 453–458, 1996. https://doi.org/10.1007/BF00212427

NOBRE, R. L. G. *et al.* Precipitation, Landscape Properties and Land Use Interactively Affect Water Quality of Tropical Freshwaters. **Science of The Total Environment**, v. 716, p. 137044, 2020. https://doi.org/10.1016/j.scitotenv.2020.137044

NOGUEIRA, P. F. *et al.* Eutrofização no reservatório da UHE Foz do Rio Claro (GO). **Revista do Departamento de Geografia**, v. 30, p. 19–33, 2015. https://doi.org/10.11606/rdg.v30i0.90090

OKSANEN, J. *et al*. vegan: Community Ecology Package. R package version 2.5-7. 2020. Available: https://CRAN.R-project.org/package=vegan

POMPÊO, M. *et al.* Heterogeneidade Espacial Horizontal Da Qualidade Da Água No Reservatório Rio Grande, Complexo Billings, São Paulo, Brasil. *In*: POMPÊO, M. *et al.* (ed.). **Ecologia de Reservatórios e Interfaces**. São Paulo: Universidade de São Paulo. Instituto de Biociências, 2015. p. 82–95.

R CORE TEAM. R: A Language and Environment for Statistical Computing. Vienna, Austria: R Foundation for Statistical Computing, 2021. https://www.R-project.org/.

RIBEIRO, M. S. F. *et al.* Detection of Cyanotoxin-Producing Genes in a Eutrophic Reservoir (Billings Reservoir, São Paulo, Brazil). **Water**, v. 12, n. 3, p. 903, 2020. https://doi.org/10.3390/w12030903

RISSO, S. S. O. *et al.* Análise do desempenho de reservatório de uso múltiplo: estudo de caso na sub-bacia Billings. **Desenvolvimento e Meio Ambiente**, v. 46, 2018. https://doi.org/10.5380/dma.v46i0.54521

ROCHA, F. C.; ANDRADE, E. M.; LOPES, F. B. Water Quality Index Calculated from Biological, Physical and Chemical Attributes. **Environmental Monitoring and Assessment**, v. 187, n. 1, p. 4163, 2014. https://doi.org/10.1007/s10661-014-4163-1

ROMAN, M. R. *et al.* Interactive Effects of Hypoxia and Temperature on Coastal Pelagic Zooplankton and Fish. **Frontiers in Marine Science**, v. 6, p. 139, 2019. https://doi.org/10.3389/fmars.2019.00139

SAHA, A. *et al.* Evaluation of Spatio-Temporal Changes in Surface Water Quality and Their Suitability for Designated Uses, Mettur Reservoir, India. **Natural Resources Research**, v. 30, n. 2, p. 1367–1394, 2021. https://doi.org/10.1007/s11053-020-09790-5

SÃO PAULO (Estado). Assembleia Legislativa. Decreto n 10.755, de 22 de novembro de 1977. Dispõe sobre o enquadramento dos corpos de água receptores na classificação prevista no Decreto nº 8.468, de 8 de setembro de 1976 e dá providências correlatas. **Diário Oficial** - Executivo, p. 1, 23 nov. 1977.

SÃO PAULO (Estado). Secretaria do Meio Ambiente; Secretaria de Saneamento e Energia. Resolução Conjunta SMA/SSE-002 de 19 de fevereiro de 2010. Trata de procedimentos a serem adotados em casos de emergência na operação do sistema hídrico da bacia do Alto Tietê e bacias a ela interligadas. **Diário Oficial** – Executivo, p. 112, 19 fev. 2010.

SINHA, E.; MICHALAK, A. M.; BALAJI, V. Eutrophication Will Increase during the 21st Century as a Result of Precipitation Changes. **Science**, v. 357, n. 6349, p. 405–408, 2017. https://doi.org/10.1126/science.aan2409

STRICKLAND, J. D.; PARSONS, T. R. **A Manual of Seawater Analysis**. Ottawa: Fisheries Research Board of Canada, 1960.

VALDERRAMA, J. C. The Simultaneous Analysis of Total Nitrogen and Total Phosphorus in Natural Waters. **Marine Chemistry**, v. 10, n. 2, p. 109–122, 1981. https://doi.org/10.1016/0304-4203(81)90027-X

WATANABE, F. S. Y. *et al.* Estimation of Chlorophyll-a Concentration and the Trophic State of the Barra Bonita Hydroelectric Reservoir Using OLI/Landsat-8 Images. **International Journal of Environmental Research and Public Health**, v. 12, n. 9, p. 10391–10417, 2015. https://doi.org/10.3390/ijerph120910391

WENGRAT, S.; BICUDO, D. de C. Spatial Evaluation of Water Quality in an Urban Reservoir (Billings Complex, Southeastern Brazil). **Acta Limnologica Brasiliensia**, v. 23, p. 200–216, 2011. https://doi.org/10.1590/S2179-975X2011000200010

WICKHAM, H. *et al.* Welcome to the tidyverse. **Journal of Open Source Software**, v. 4, n. 43, p. 1686, 2019. https://doi.org/10.21105/joss.01686

Ambiente & Água - An Interdisciplinary Journal of Applied Science
ISSN 1980-993X – doi:10.4136/1980-993X
www.ambi-agua.net
E-mail: ambi.agua@gmail.com

Physiographic analysis of the Atibaia River Basin and flood susceptibility mapping in the municipality of Campinas-SP, Brazil

ARTICLES doi:10.4136/ambi-agua.2832

Received: 27 Jan. 2022; Accepted: 18 Apr. 2022

Bruno de Souza Garcia[1*]; Camila da Silva Dourado[1,2]; Ana Maria Heuminski de Avila[2]

[1]Departamento de Engenharia Agronômica. Centro Universitário Adventista de São Paulo (UNASP), Estrada Municipal Pastor Walter Boger, s/n, CEP: 13448-900, Engenheiro Coelho, SP, Brazil.
E-mail: camila.dourado@edu.unasp.br
[2]Centro de Pesquisas Meteorológicas e Climáticas Aplicadas à Agricultura. Universidade Estadual de Campinas (UNICAMP), Avenida André Tosello, n° 209, CEP: 13083-886, Campinas, SP, Brazil.
E-mail: camila.dourado@edu.unasp.br, avila@cpa.unicamp.br
[*]Corresponding author. E-mail: bruno_garcia@educadventista.org

ABSTRACT

This study characterized and analyzed the physiographic factors of the Atibaia River Basin and their influence on flooding processes and evaluated the susceptibility to flooding in the municipality of Campinas during the years 1985 and 2019. At first, geoprocessing techniques and indices defined in the literature were used to provide a comprehensive understanding of the Atibaia River Basin regarding its geometric, relief, and drainage attributes and its influence on flooding processes, to provide decision-making support regarding preventive and mitigating actions for the socioeconomic and environmental impacts in the region. The pedogeomorphological characteristics and land use and occupation of Campinas were applied to the Analytic Hierarchy Process using geoprocessing techniques to generate the specific mapping of the municipality's susceptibility to flooding. The mapping allowed us to identify the critical sites of the municipality of Campinas, choosing priority areas for government action and programs regarding urban and environmental management. It can also guide new studies on the detail scale aiming to prevent and mitigate flooding events.

Keywords: hydrographic basin, spatial multi-criteria analysis, water risk.

Análise fisiográfica da bacia do rio Atibaia e mapeamento de suscetibilidade à inundação no município de Campinas-SP, Brasil

RESUMO

Este trabalho teve por objetivo a caracterização e análise dos fatores fisiográficos da bacia do rio Atibaia e sua influência nos processos de enchentes e inundações, além de avaliar a suscetibilidade a eventos de inundação para o município de Campinas, nos anos de 1985 e 2019. Em um primeiro momento, foram utilizadas técnicas de geoprocessamento e índices definidos na literatura a fim de proporcionar uma compreensão abrangente da bacia do rio Atibaia quanto a seus atributos geométricos, de relevo e drenagem e sua influência aos processos de inundação, com o intuito de fornecer suporte à tomada de decisão referente às ações preventivas e mitigadoras dos impactos socioeconômicos e ambientais na região. Em um segundo momento,

This is an Open Access article distributed under the terms of the Creative Commons Attribution License, which permits unrestricted use, distribution, and reproduction in any medium, provided the original work is properly cited.

as características pedogeomorfológicas e de uso e ocupação da terra do município de Campinas foram processadas por meio de técnicas de geoprocessamento e aplicadas ao Processo Analítico Hierárquico com a finalidade de gerar o mapeamento específico do município quanto a sua suscetibilidade a inundações. O mapeamento permitiu conhecer os locais críticos do município de Campinas, elegendo áreas prioritárias às ações e programas governamentais no tocante à gestão urbana e ambiental, podendo orientar ainda a geração de novos estudos na escala de detalhe, com vistas à prevenção e contingência de possíveis impactos decorrentes dos processos de inundação.

Palavras-chave: análise espacial multicritério, bacia hidrográfica, risco hídrico.

1. INTRODUCTION

Floods are geoenvironmental problems arising from natural phenomena of a hydrometeorological or hydrological nature, which can be atmospheric, hydrological, or even oceanographic (UN-ISDR, 2009). Floods cause devastating impacts on society, being classified among the most dangerous disasters in the world (Bathrellos *et al.*, 2016).

Identifying and evaluating the potential and restrictions of basins, especially urban basins, contributes to the management of water resources, such as prediction of vulnerability to flooding, inundations, and erodibility (Villela and Mattos, 1975). Several indices were developed to determine these properties, considering as physiographic characteristics those which can be obtained from maps, aerial photographs, or satellite images (Souza *et al.*, 2018).

The municipality of Campinas has been characterized by significant urban and demographic growth since the 1970s (Caiado and Pires, 2006). It is a region that concentrates a high density of headwaters of rivers that are crucial for the hydrological balance of the state of São Paulo, including the Atibaia River Basin, with an extension of 2,814.59 km^2. Thus, mapping and analyzing susceptibility to flooding in this municipality play important roles in guiding strategies to prevent and mitigate future water risks since they identify the most vulnerable areas based on the physical conditions that determine the propensity to flooding (Vojtek and Vojteková, 2019).

Since floods result from multidimensional phenomena with spatial and temporal aspects, the delimitation of risk areas to these hydrological processes can be analyzed based on a multicriteria methodology. Among the methods developed in the Multicriteria Decision Analysis (MCDA) environment, the Analytic Hierarchy Process (AHP) stands out (Saaty, 1990). This method is based on the creation of an importance scale by assigning weights between the evaluated parameters to determine the proportion of influence of each factor in the possible flooding of the analyzed area (Saaty, 1987; 1990).

The determination and analysis of physiographic factors, also applied to the AHP method, has been used by several authors at municipal or hydrographic basin scales (Lorenzon *et al.*, 2015; Souza and Sobreira, 2017; Caldas *et al.*, 2018; Souza *et al.*, 2018; Cezar *et al.*, 2019; Vajtek and Vojteková, 2019; Silva *et al.*, 2020), especially combined with geoprocessing techniques, for assessing the impacts of continuous territorial changes and the zoning of areas susceptible to possible natural disasters.

Given the above, the assessment of flooding risk plays an important role in territorial planning, especially as an indication of limitations and potential in future projections of urban occupation. In this context, this study aimed to characterize and analyze the physiographic factors of the Atibaia River Basin and its influence on the inundation and flooding processes, and evaluate the susceptibility to flooding events for the municipality of Campinas, in the years 1985 and 2019, using the AHP method and geoprocessing techniques, to provide support for decision-making regarding preventive and mitigating actions of socioeconomic and

environmental impacts in the region.

2. MATERIAL AND METHODS

The physiographic factors were first characterized and the concentration times in the entire Basin of the Atibaia River were determined to provide a comprehensive understanding of the basin regarding its geometric attributes, relief, and drainage and its relationship to flooding processes. Subsequently, the study was limited to the municipality of Campinas, specifying its pedogeomorphological characteristics, land use and occupation to analyze in more detail the influence between the natural and anthropic aspects in attributing risk to flooding processes in the municipality.

2.1. Characterization of the study area

The Atibaia River Basin, located between coordinates 22°40’ and 23°20’ south and 47°20’ and 46°00’ west, covers, total or partially, 16 municipalities in the state of São Paulo and one in the state of Minas Gerais, in the Southeast region of Brazil (Figure 1). Due to its location, the Atibaia River Basin shows a contrast between relatively preserved natural environments and extremely urbanized areas. Its basin is directly related to the Campinas metropolitan area with an extension of 2,814.59 km^2. Among the many peculiarities of this basin, its insertion in a region with wide urban expansion and a vast and diversified industrial park, besides an important technological center in the national scenario, stands out (Demanboro *et al.*, 2013a; 2013b).

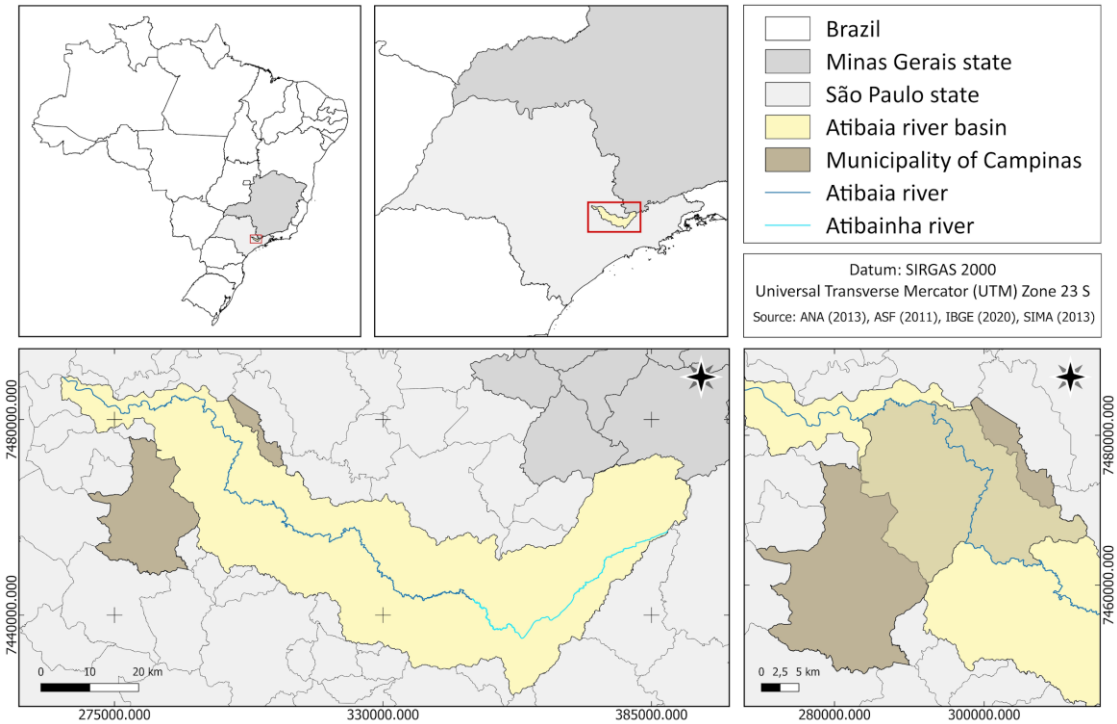

Figure 1. Location of the study area.

Recent studies conducted by Young and Papini (2020) indicate a scenario of more than 5,000 people exposed to the risks of flooding disasters associated with a part of the Atibaia River Basin covering the municipality of Campinas in response to urban sprawl that has already reached flood-prone areas, as well as intense agricultural activities and degraded pastures in the locality. A portrait of use and occupation was identified throughout the territorial extension of the municipality of Campinas.

The municipality of Campinas, partially inserted into the Atibaia River Basin, is in the east-central part of the state of São Paulo, between the coordinates 22°53’20” south and 47°04’40” west. Its territory covers an area of approximately 794.6 km^2 and has a population of 1,223,137 inhabitants (IBGE, 2021), being the third most populous city in the state of São Paulo and the fourteenth in Brazil. Its climate is humid tropical (Cwa, according to the Köppen-Geiger classification), expressed as mild winters and hot, wetter summers (Beck *et al.*, 2018).

2.2. Physiographic characterization of the Atibaia River Basin

For the characterization of the physiographic aspects and determination of the time of concentration of the Atibaia River Basin, the factors and indexes referring to the geometry of the basin, the relief characteristics, and its drainage network were evaluated. The analyses were performed using geographic, vector, and matrix information referring to the drainage sections of the Ottocodified Hydrographic Database of the Tietê River Basin (ANA, 2013) and to the sub-basins of the state of São Paulo (São Paulo, 2013), both in a 1:50,000 scale, in addition to the information from images from the ALOS PALSAR radar sensor satellite with 12.5 meters of spatial resolution, provided by Alaska Satellite Facility (ASF DAAC, 2020) Figure 1.

In the analysis of the basin’s geometric variables, the area, perimeter, and axial length of the basin were evaluated. According to the equations described by Cezar *et al.* (2019), the shape factor (Sf), the compactness coefficient (Cc), and the circularity index (Ci) of the basin were also calculated since they determine the shape of the basin from geometric shapes. These indices allow estimating the tendency of flooding in a basin, as Table 1 indicates, since the shape of the basin directly influences surface runoff (Collischonn and Dornelles, 2013).

Table 1. Values and interpretation of shape factor (Sf), circularity index (Ci) and compactness coefficient (Cc).

Sf	Ci	Cc	Basin shape	Basin characteristics
1.00 – 0.75	1.00 – 0.8	1.00 – 1.24	Circular	Great tendency to flooding
0.75 – 0.50	0.8 – 0.6	1.25 – 1.50	Oval	Average tendency to flooding
0.50 – 0.30	0.6 – 0.4	1.50 – 1.70	Oblong	Low tendency to flooding
< 0.30	< 0.4	> 1.70	Elongated	Tendency of conservation

Source: Nardini *et al.* (2013, adapted by the authors, 2022).

The characterization of the relief of the basin was performed by remote sensing techniques applied to the Digital Elevation Model provided by the Alaska Satellite Facility, previously mentioned, enabling the preparation of the hypsometric and slope maps of the basin (Figure 2), from which altitude and maximum, medium, and minimum slope information were extracted, as well as the altimetric amplitude (Hm). The relief ratio (Rr) was also determined, indicated by the ratio between the altimetric range and the extension of the main channel (Cezar *et al.*, 2019). According to Nardini *et al.* (2013), Rr allows comparing altimetry between different regions, demonstrating that the higher its values, the more uneven is the predominant relief in the analyzed region, classified into three classes: low (0 to 0.1), medium (0.11 to 0.30), and high (0.31 to 0.60). The slope of the main river was defined from the longitudinal profile of the thalweg and the area of the curve was calculated, obtaining a right triangle of equivalent area, with a base equal to the length of the watercourse, as equated by Lorenzon *et al.* (2015). The creation of the longitudinal profile also made defining the maximum, average, and minimum height of the main river possible, as well as its altimetric range.

To evaluate the basin drainage network, the order of the channels, the total number and length of the drainage, and the real and vector length of the main river were analyzed. The drainage network was organized according to the methodology proposed by Strahler (1957).

Drainage density (Dd) and sinuosity index (Si) were determined using the method of Cezar *et al.* (2019). Drainage density represents a parameter indicative of the drainage efficiency of a basin: as its numerical value increases, the capacity of the basin to perform rapid drainage at the outlet also increases (Villela and Mattos, 1975). Thus, Dd values above 2.5 mean good drainage of the basin, whereas values between 1.5 and 2.5 represent average drainage, and subsequently, values below 1.5 mean low drainage of the basin (Nardini *et al.*, 2013). In turn, the sinuosity index describes the flow velocity of the main channel; the smaller the sinuosity, the less difficulty the water courses encounter in reaching the outlet (Cezar *et al.*, 2019).

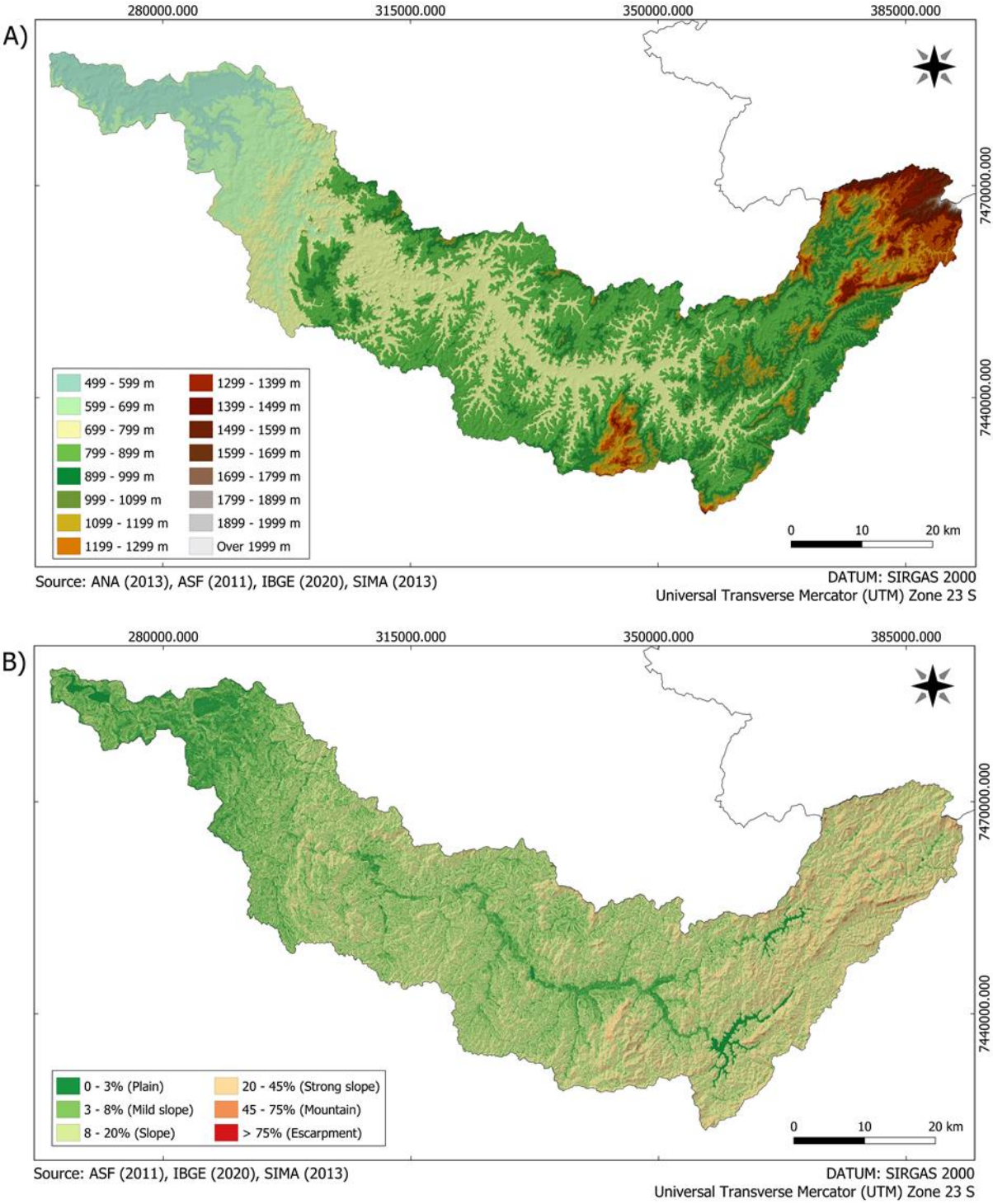

Figure 2. Characterization of the relief of the Atibaia River Basin by its A) hypsometric map and B) slope map.

In addition to the physical aspects of the basin, the knowledge of its concentration time plays a decisive role in estimating the maximum flows since it defines the time the water takes to travel the entire length of the basin until contributing to the flow in its outlet (Collischonn and Dornelles, 2013). Thus, to estimate the time of concentration, the methods of Giandotti, Johnstone-Cross, Temez, and the Corps of Engineers, developed for basins with similar physical characteristics to the Atibaia Basin, were used as described by Zahraei *et al.* (2021).

2.3. Flood susceptibility mapping in the Municipality of Campinas

In this stage, the city of Campinas was emphasized, aiming at mapping the risks of flooding in the location for the years 1985 and 2019. Based on the literature review and vulnerability to water risks, four factors conditioning floods were selected: altitude, slope, pedology, and land use and cover. According to Tucci and Bertoni (2003), the main natural conditions for the occurrence of floods are relief, due to the accumulation of water in the lower regions due to the action of the force of gravity, and the drainage capacity, since sandy soils provide greater infiltration and percolation of water, whereas clay soils produce greater surface runoff. Likewise, the artificial characterization of the physical environment due to the increase in the density of occupation and urban infrastructure, directly impacts the increase of impermeable areas, promoting greater accumulation of water on the surface than in soils with vegetation cover, since they are less compacted.

The cartographic base used consisted of: vector and matrix products referring to the mesh of municipal units in the state of São Paulo (IBGE, 2020), from which the limit of the municipality of Campinas was extracted; image information from the ALOS PALSAR radar sensor satellite with 12.5 meters of spatial resolution (ASF DAAC, 2020), for the delimitation of altimetric and slope variables of the study area; the Semi-Detailed Pedological Map of the municipality of Campinas, on a scale of 1:50,000, prepared by Embrapa in 2008 (Campinas, 2021a), identifying the soil classes of the municipality; and the fifth collection of land use and occupation maps made available by the Mapbiomas Project (2021), with 30 meters of spatial resolution, for the years 1985 and 2019. The Datum Geocentric Reference System for the Americas 2000 (SIRGAS 2000) and the Universal Transverse Mercator plane projection in the 23 S zone were used. As validation of the final map, records of critical points of flooding and inundation in the municipality of Campinas were also used, prepared in 2018 and provided by the City Hall of Campinas (Campinas, 2021b; 2021c).

As indicated by the mapping of the conditioning factors for inundation (Figure 3), the city of Campinas presents an altimetric range of 537 m, with altitudes that vary between 545 to 1082 m. It has diversified reliefs, with an average slope of 11.4%, classified as wavy relief (Embrapa, 1979). Regarding pedology, eight orders of soils were identified in the municipality, highlighting the predominance of soils classified as Argisols and Latosols, characterized by high clay content and pedogenetic development (Santos *et al.*, 2018). Pedological portions are also directly associated with the marginal regions of water courses, classified as Gleysoils and Organosols, which have a strong propensity to hydromorphism and a restricted drainage rate (Santos *et al.*, 2018). Concerning land use and cover, of the five classes established, between the years 1985 and 2019, municipal urban infrastructure increased 96.51%, water bodies, 82.44%, forest areas, 52.07%, and rocky outcrops, 8.38%. In turn, areas of agricultural use decreased by 26.02%. In 2019, among the 794.57 km^2 of the municipality of Campinas, 446.98 km^2 represented areas of agricultural use, 251.79 km^2 of urban infrastructure, 91.2 km^2 of forests, 4.58 km^2 of bodies of water and 0.01 km^2 of rocky outcrop.

In this study, an analysis based on matrix data was used. In this sense, the conditioning factor referring to pedology was converted to raster format with a cell size of 12.5 m resolution. As a method of comparing the conditioning factors, the classes of the evaluated information levels received scores from one to five according to the level of susceptibility to flooding, with

Grade 1 (very low), Grade 2 (low), Grade 3 (moderate), Grade 4 (high), and Grade 5 (very high).

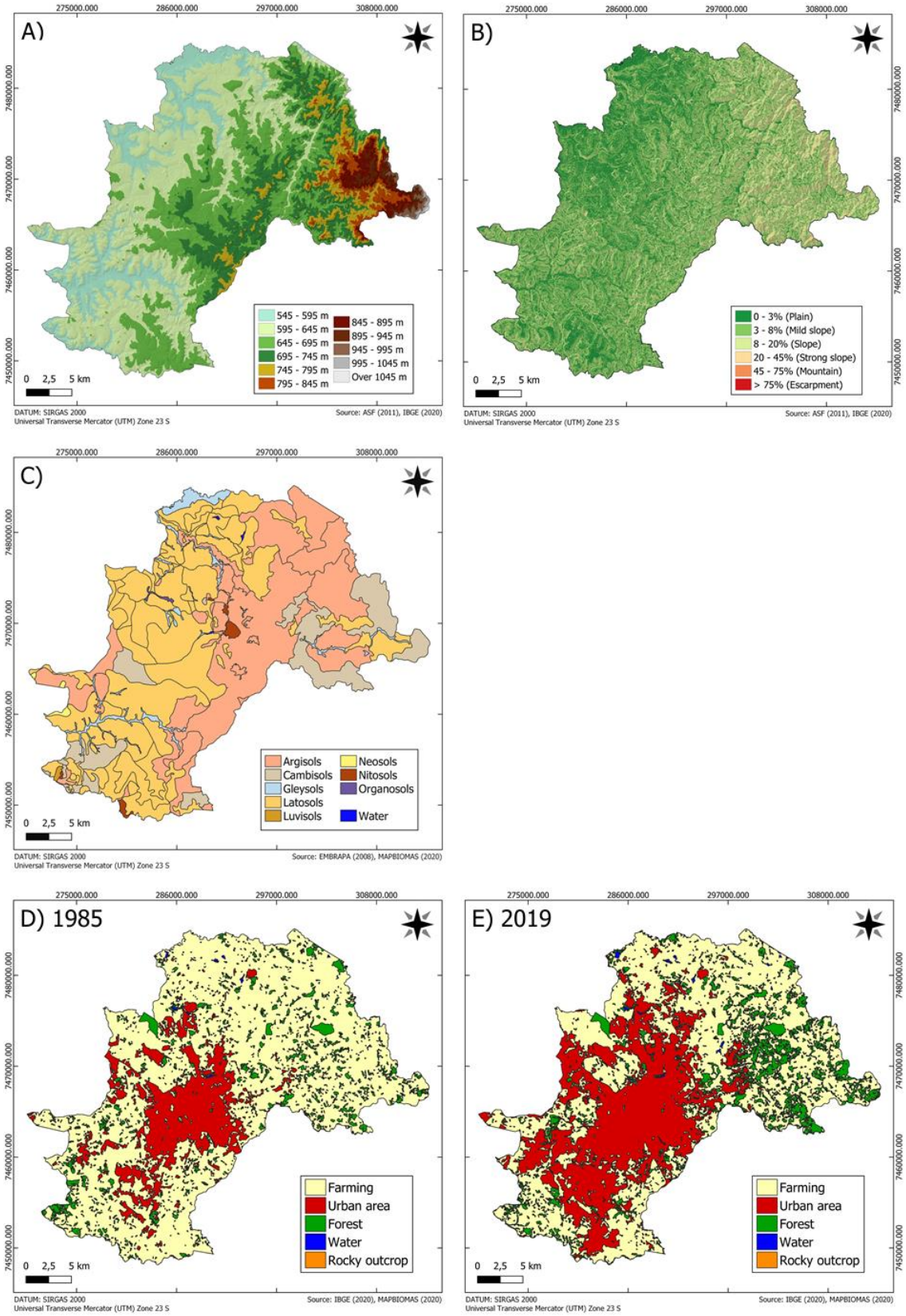

Figure 3. Information levels adopted in the analysis of susceptibility to flooding in Campinas, referring to A) hypsometric map, B) slope map, C) pedological map and maps of land use and land cover in the years D) 1985 and E) 2019.

The application of the AHP method was carried out from the comparative judgment between the conditioning factors by the Paired Comparison Matrix. To this end, the fundamental scale of weights defined by Saaty (1990) was used to measure the intensity of the relationship between the variables analyzed in terms of flooding processes, as Table 2 shows:

Table 2. Fundamental criteria judgment scale.

Importance Values	Reciprocal Importance Values	Importance
1	1	Equal importance
3	1/3	Weak importance of one over another
5	1/5	Essential or strong importance
7	1/7	Very strong importance
9	1/9	Absolute importance
2, 4, 6, 8	1/2, 1/4, 1/6, 1/8	Intermediate values between adjacent importance intensities

Source: Saaty (1990, adapted by the authors, 2022).

Since the greater the number of comparisons analyzed, the greater the tendency towards uncertain results, Equations 1, 2, and 3 were applied, referring to the calculation of the Consistency Index (CI) and the Consistency Ratio (CR), to validate the results obtained by the paired matrix.

$$CR = \frac{CI}{RI} \tag{1}$$

$$CI = \frac{(\lambda_{max} - n)}{n-1} \tag{2}$$

$$\lambda_{max} = \frac{1}{n}\sum_{j=1}^{n}\frac{[Aw]_i}{w_i} \tag{3}$$

Where:

CR = Consistency ratio

RI = Random index

CI = Consistency index

n = number of factors evaluated (number of columns or rows)

λ_{max} = Eigenvector

[AW]i = matrix resulting from the product of the comparison matrix *[AW]i* by the calculated weights (*wi*)

(*Wi*) = calculated weights

In turn, the zoning of areas susceptible to flooding was obtained from the joint sum of each criterion of the matrix data by the *raster calculator* tool of the QGIS 3.16 software. The resulting flood susceptibility map was divided into five classes according to their probability of flooding, namely: very low, low, moderate, high, and very high risk.

3. RESULTS AND DISCUSSION

3.1. Physiographic aspects of the Atibaia River Basin

Table 3 shows 26 physiographic parameters of the Atibaia River Basin established by the proposed methodology.

Table 3. Physiographic characteristics of the Atibaia River Basin – SP.

	Physical Characteristics	Units	Results
Geometric Characteristics	Drainage area	km^2	2,814.59
	Perimeter	km	579.71
	Axial length	km	131.27
	Shape factor (Sf)	Dimensionless	0.16
	Compactness coefficient (Cc)	Dimensionless	3.06
	Circularity index (Ci)	Dimensionless	0.11
Relief Characteristics	Minimum basin altitude	m	499
	Average basin altitude	m	850.3
	Maximum basin altitude	m	2,026
	Altimetric range	m	1,527
	Minimum basin slope	%	0
	Average basin slope	%	20.2
	Maximum basin slope	%	279.60
	Relief ratio (Rr)	Dimensionless	0.029
	Minimum altitude of the main river	m	504
	Average altitude of the main river	m	708.69
	Maximum altitude of the main river	m	802
	Altimetric range of the main river	m	1,306
	Slope of the main river	%	0.021
Drainage Network Characteristics	Basin order	-	7th
	Total number of channels	-	12,365
	Total length of drainage	km	6,599.48
	Length of the main river	km	257.48
	Vector length of the main river	km	127.56
	Drainage density (Dd)	km/km^2	2.34
	Sinuosity index (Si)	Dimensionless	2.02

The analysis of the physiographic factors made determining and understanding important variables to aid in the planning and environmental management of the region possible. Regarding the shape of the basin, the values obtained for the shape factor (Sf = 0.16), compactness coefficient (Cc = 3.06), and circularity index (Ci = 0.11) give the Atibaia Basin a more elongated shape (Nardini *et al.*, 2013; Villela and Mattos, 1975). This indicates a low tendency to flooding in the locality since rainfall over the basin is concentrated at different points, helping to mitigate the influence of rainfall intensity (Villela and Mattos, 1975).

Regarding relief, the low value of the relief ratio indicates a lower general slope of the Atibaia River Basin, confirmed by the average slope of the basin in the order of 20.2%, thus, classified as strong-wavy relief (Lepsch *et al.*, 2001). This relief class presents moderate fragility to erosion and environmental degradation and has limitations to agricultural mechanization, recommended in the use of semi-intensive agriculture (Lepsch *et al.*, 2001).

The shape and relief of the basin also affect the time of concentration (Collischonn and Dornelles, 2013). The results obtained for the time of concentration by the different formulas

show a variability of values for the Atibaia Basin, as indicated by Table 4. In this study, the mean value between the results was adopted as an indication of the time of concentration of the basin.

Table 4. Time of concentration of the Atibaia River Basin – SP.

Method	Time of concentration (hours)
Giandotti	52.29
Johnstone-Cross	61.9
Temez	102.27
Corps of Engineers	65.11
Mean	70.39

Thus, the high time of concentration calculated for the study area reflects the elongated shape of the basin and its mostly undulating relief.

The characteristics of the drainage network, in turn, reveal the drainage density of the basin and the sinuosity index of the main river. The calculated value of drainage density (Dd) indicates the Atibaia Basin shows medium drainage, allowing us to infer a moderate permeability and infiltration of water in the locality (Nardini *et al.*, 2013). In turn, the main river presented a sinuosity index (Si) of 2.02, classified as a winding watercourse (Cezar *et al.*, 2019).

3.2. Flood susceptibility mapping in the Municipality of Campinas

Based on Saaty's (1990) fundamental scale, the pairwise comparison matrix resulted in a square matrix of order four. The values assigned to the matrix represent the intensity of importance of the parameters evaluated between them for the susceptibility to flooding; the main diagonal represents the comparison between the same criteria, while whereas the elements arranged above and below the diagonal represent the judgment of importance between the different criteria (Table 5).

Table 5. Paired comparison matrix of the analyzed criteria.

	Pedology	Land use and cover	Altitude	Slope
Pedology	1	1/3	1/5	1/7
Land use and cover	3	1	1/3	1/5
Altitude	5	3	1	1/3
Slope	7	5	3	1

The values assigned to the matrix allowed the calculation of the statistical weights of each analyzed variable by the quotient between the sum of the n elements of each variable in the matrix and the total of the respective sums. Thus, the calculated weights (w_i) defined the importance between the conditioning factors, in a range from 0 to 1, where the predominance of one criterion over another is larger as w_i approaches 1, as shown in Table 6.

Table 6. Priority and consistency values of the resulting matrix.

Analyzed criteria	w_i	$[Aw]_i$	λmax	CI	CR
Slope	0.558	2.356	4.118	0.039	0.044
Altitude	0.263	1.099			
Land use and cover	0.122	0.492			
Pedology	0.057	0.229			

The information levels that most influenced the susceptibility map were slope and hypsometry, given the occurrence of low slope and general altimetric range in the municipality, followed by land use and occupation, and finally, acting to a lesser extent in the results, pedology.

According to the dimensions of the matrix, the tabulated value of 0.90 was adopted to express the Random Index, according to Saaty (1987). In turn, the judgment of the analyzed variables, by the validation of the assigned weights, as outlined in Equations 1, 2, and 3, presented satisfactory statistical conditions, whereas the calculation of the consistency ratio of the matrix elements did not exceed the indicated value of 0.10, which demonstrated coherence (CI) and reliability (CR) of the generated data (Saaty, 1987).

Digital image processing was used to prepare the flood susceptibility maps by weighted combination of established hierarchical data, allowing the estimation of the territorial susceptibility of Campinas to flooding processes, using the matrix data calculator expressed in the form of Equation 4:

$$SF = 0.057PE + 0.122LUC + 0.263AL + 0.558SL \quad (4)$$

Where:

SF = Susceptibility to flooding

PE = Pedology

LUC = Land use and cover

AL = Altitude

SL = Slope

Figure 4 shows that, in 1985, the municipality of Campinas presented mainly areas of moderate and high risk of flooding, equivalent to 393.70 km^2 and 324.42 km^2, or 49.96% and 41.17% of the total area, respectively. The very low risk, low risk, and very high risk areas covered, in this order, areas of 0.19 km^2 (0.02%), 41.53 km^2 (5.27%), and 28.18 km^2 (3.58%). Compared with the flood susceptibility mapping for the year 2019, very low risk, low risk, high risk, and very high risk areas increased, respectively, to 0.28 km^2 (0.03%), 44.9 km^2 (5.70%), 349 km^2 (44.29%), and 28.98 km^2 (3.68%), and moderate risk areas decreased to 364.84 km^2 (46.30%).

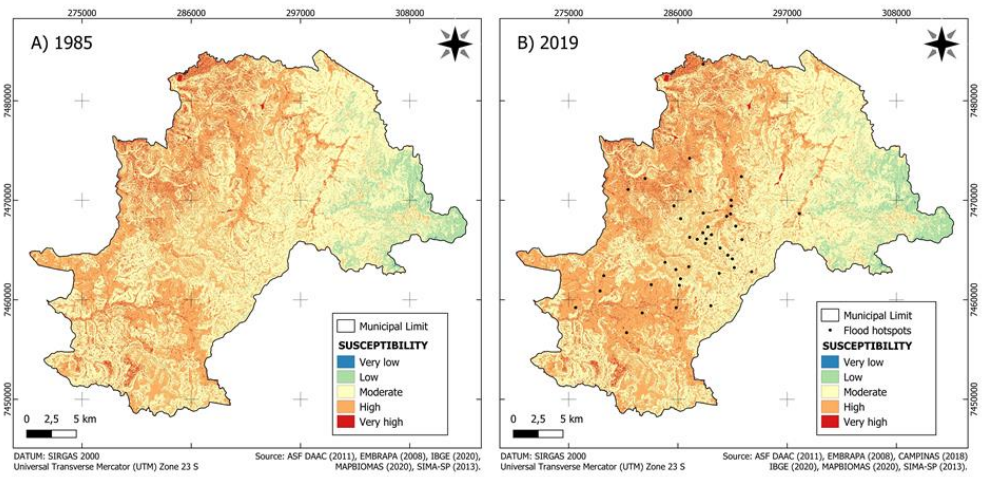

Figure 4. Flood susceptibility maps of Campinas – SP, for the years of A) 1985 and B) 2019.

The areas classified with the highest degree of susceptibility are directly related to the

marginal edges of rivers and streams since they present the smallest slope intervals and soils with a greater tendency to hydromorphism or low infiltration capacity. This risk is potentiated, as observed in the past 35 years, by urban expansion to areas close to water courses, resulting in potential areas vulnerable to problems arising from the reach of hydrological processes, especially in the event of critical rainfall. For 2019, among the 48 critical flood points established by the City Hall of Campinas, 37 points are in areas of high and very high susceptibility to flooding, whereas the remaining 11 points are in areas of moderate susceptibility.

4. CONCLUSIONS

The characterization of the Atibaia Hydrographic Basin regarding its physical aspects and concentration time is fundamental to a better understanding of the hydrogeomorphological processes occurring in the basin, besides adding auxiliary information to future studies regarding diagnosis, planning, and environmental management in the locality.

For the municipality of Campinas, based on this study, the mapping of areas susceptible to flooding identified critical zones of the territory, defining priority areas for government action and programs regarding urban and environmental management, which may guide new studies on a more detailed scale, aiming to prevent and mitigate possible impacts resulting from the flooding processes.

In addition, when comparing the flood susceptibility map for 2019 with the records of floods in 2018, we have found agreement between the zones of susceptibility and critical flooding points recorded, of which 77.1% coincided with areas of high and very high susceptibility levels, thus confirming the effectiveness of the adopted methodology.

Furthermore, due to being a qualitative method, the importance of correctly defining the grades and weights assigned to the analyzed variables, as well as the necessary rigor regarding the scales and quality of the data used is emphasized since they can result in over- or underestimated mappings. In this sense, despite possible variations in the result of the consistency index value, within the acceptable limit, it is valid to apply this methodology as a basis for preliminary studies and to guide decision-making in the management and prevention of flooding processes.

5. ACKNOWLEDGEMENTS

The authors thank Espaço da Escrita – Pró-Reitoria de Pesquisa – UNICAMP – for the language services provided.

6. REFERENCES

ANA (Brasil). **Base Hidrográfica Ottocodificada da Bacia do Rio Tietê**. 2013. Available in: https://metadados.snirh.gov.br/geonetwork/srv/por/catalog.search#/metadata/29c5995f-5bbd-4698-b301-694a3c1ca748. Access Aug. 2020.

ASF DAAC. Alaska Satellite Facility Distributed Active Archive Center. **ALOS PALSAR - Radiometric Terrain Correction**. 2020. Available in: https://asf.alaska.edu/data-sets/derived-data-sets/alos-palsar-rtc/alos-palsar-radiometric-terrain-correction/. Access Sep. 2020.

BATHRELLOS, G. C.; KARYMBALIS, E.; SKILODIMOU, H. D.; GAKI-PAPANASTASSIOU, K.; BALTAS, E. A. Urban flood hazard assessment in the basin of Athens Metropolitan city, Greece. **Environmental Earth Sciences**, v. 75, n. 319, 2016. https://doi.org/10.1007/s12665-015-5157-1

BECK, H. E.; ZIMMERMANN, N. E.; MCVICAR, T. R.; VERGOPOLAN, N.; BERG, A.; WOOD, E. F. Present and future köppen-geiger climate classification maps at 1-km resolution. **Scientific Data**, v. 5, p. 1-12, 2018.

CAIADO, M. C. S.; PIRES, M. C. Campinas Metropolitana: transformações na estrutura urbana atual e desafios futuros. *In*: CUNHA, J. M. da C. (org.). **Novas metrópoles paulistas: população, vulnerabilidade e segregação.** Campinas: Nepo/Unicamp, 2006, p. 275-304.

CALDAS, A. M. *et al.* Flood Vulnerability, Environmental Land Use Conflicts, and Conservation of Soil and Water: A Study in the Batatais SP Municipality, Brazil. **Water**, v. 10, n. 1357, 2018. https://doi.org/10.3390/w10101357

CAMPINAS. **Pedologia**. Available in: https://informacao-didc.campinas.sp.gov.br/metadados.php. Access May 2021a.

CAMPINAS. **Pontos críticos de alagamento**. Available in: https://informacao-didc.campinas.sp.gov.br/metadados.php. Access May 2021b.

CAMPINAS. **Pontos críticos de inundação**. Available in: https://informacao-didc.campinas.sp.gov.br/metadados.php. Access May 2021c.

CEZAR, V. R. S. *et al.* Morphometric analysis of an Aerial Watershed in Taubaté, SP, Brazil. **Revista Ambiente & Água**, v. 7, 2019. https://doi.org/10.4136/ambi-agua.2322

COLLISCHONN, W.; DORNELLES, F. **Hidrologia para Engenharia e Ciências Ambientais**. 1. ed. Porto Alegre: ABRH, 2013. 350 p.

DEMANBORO, A. C.; LAURENTIS, G. L.; BETTINE, S. C. Cenários ambientais na bacia do rio Atibaia. **Engenharia Sanitária Ambiental**, v. 18, n. 1, p. 27-37, 2013a. https://doi.org/10.1590/S1413-41522013000100004

DEMANBORO, A. C.; LAURENTIS, G. L.; BETTINE, S. C.; LONGO, R. M.; MEDIONDO, E. M. Watershed management of the Atibaia River Basin based on the elaboration of environmental scenarios. **WIT Transactions on Ecology and the Environment**, v. 175, p. 149-160, 2013b.

EMBRAPA. Serviço Nacional de Levantamento e Conservação de Solos. **Reunião Técnica de Levantamento de Solos**, 10. Rio de Janeiro, 1979. p. 83.

IBGE. **Estatísticas: cidades e estados**. Rio de Janeiro, 2021.

IBGE. **Malha Municipal**. 2020. Available in: https://www.ibge.gov.br/geociencias/organizacao-do-territorio/malhas-territoriais/15774-malhas.html?=&t=downloads. Access Aug. 2020.

LEPSCH, J. F. *et al.* **Manual para levantamento utilitário do meio físico e classificação de terras no sistema de capacidade de uso**. Campinas: SBCS, 2001. 175p.

LORENZON, A. S. *et al.* Influência das características morfométricas da bacia hidrográfica do rio Benevente nas enchentes no município de Alfredo Chaves-ES. **Revista Ambiente & Água**, v. 10, 2015. https://doi.org/10.4136/ambi-agua.2344

NARDINI, R. C.; POLLO, R. A.; CAMPOS, S.; DE BARROS, Z. X.; CARDOSO, L. G.; GOMES, L. N. Análise Morfométrica e Simulação de Áreas de Preservação Permanente de uma Microbacia Hidrográfica. **Irriga**, v. 18, n. 4, p. 687-699, 2013. https://doi.org/10.15809/irriga.2013v18n4p687

PROJETO MAPBIOMAS. **Coleção 5 da Série Anual de Mapas de Uso e Cobertura da Terra do Brasil.** Available in: https://mapbiomas.org/. Access Apr., 22 2021.

SAATY, R. W. The analytic hierarchy process - What it is and how it is used. **Mathematical Modelling**, v. 9, n. 3-5, p. 161-176, 1987. https://doi.org/10.1016/0270-0255(87)90473-8

SAATY, T. L. How to make a decision: The analytic hierarchy process. **European Journal of Operational Research**, v. 48, n. 1, p. 9-26, 1990. https://doi.org/10.1016/0377-2217(90)9005-I

SANTOS, H. G. *et al.* **Sistema brasileiro de classificação de solos**. 5. ed. Brasília, DF: Embrapa, 2018. 356 p.

SÃO PAULO (Estado). **Sub-bacias do Estado de São Paulo**. 2013. Available in: https://www.infraestruturameioambiente.sp.gov.br/cpla/sub-bacias-do-estado-de-sao-paulo/. Access Nov. 2020.

SILVA, L. G. *et al.* Analytic hierarchy process (AHP) applied to flood susceptibility in São José dos Campos, São Paulo, Brazil. **Revista Ambiente & Água**, v. 7, 2020. https://doi.org/10.4136/ambi-agua.2574

SOUZA, J. C. *et al.* Importance of adequate appropriation of physiographic information for concentration times determination. **Revista Ambiente & Água**, v. 13, 2018. https://doi.org/10.4136/ambi-agua.2184

SOUZA, L. A.; SOBREIRA, F. G. Bacia Hidrográfica do Ribeirão do Carmo: atributos morfométricos, equação de chuva intensa e tempo de concentração, e análise da suscetibilidade a inundação. **Revista Brasileira de Cartografia**, v. 69, n. 7, p. 1355-1370, 2017.

STRAHLER, A. N. Quantitative analysis of watershed geomorphology. **Transactions. American Geophysical Union**, v. 38, n. 6, p. 913-920, 1957.

TUCCI, C. E. M.; BERTONI, J. C. (Orgs) **Inundações Urbanas na América do Sul**. Porto Alegre: ABRH, 2003. 471 p.

UNISDR. **Terminology on Disaster Risk Reduction**. Geneva, 2009. Retrieved from: https://www.unisdr.org/files/7817_UNISDRTerminologyEnglish.pdf. Access: Nov. 2021.

VILLELA, S. M.; MATTOS, A. **Hidrologia aplicada**. São Paulo: McGraw-Hill, 1975. 245 p.

VOJTEK, M.; VOJKEKOVÁ, J. Flood Susceptibility Mapping on a National Scale in Slovakia Using the Analytical Hierarchy Process. **Water**, v. 11, n. 364, 2019. https://doi.org/10.3390/w11020364

YOUNG, A. F.; PAPINI, J. A. J. How can scenarios on flood disaster risk support urban response? A case study in Campinas Metropolitan Area (São Paulo, Brazil). **Sustainable Cities and Society**, v. 61, p. 102253, 2020. https://doi.org/10.1016/j.scs.2020.102253

ZAHRAEI, A.; BAGHBANI, R.; LINHOSS, A. Applying a Graphical Method in Evaluation of Empirical Methods for Estimating Time of Concentration in an Arid Region. **Water**, v. 13, n. 2624, 2021. https://doi.org/10.3390/w13192624

Ambiente & Água - An Interdisciplinary Journal of Applied Science
ISSN 1980-993X – doi:10.4136/1980-993X
www.ambi-agua.net
E-mail: ambi.agua@gmail.com

Spatial mapping of annual rainfall in the São Francisco River Basin

ARTICLES doi:10.4136/ambi-agua.2762

Received: 25 Jun. 2021; Accepted: 05 Jan. 2022

Willian dos Santos Oliveira[1]; Elias Silva de Medeiros[2*]; Alessandra Querino da Silva[2]; Luciano Antonio de Oliveira[2]

[1]Faculdade de Engenharia. Universidade Federal da Grande Dourados (UFGD), Rodovia Dourados/Itahum, Km 12, Unidade II, Caixa Postal: 364, Cep: 79804-970, Dourados, MS, Brazil.
E-mail: oliveira.wds@outlook.com
[2]Faculdade de Ciências Exatas e Tecnologia. Universidade Federal da Grande Dourados (UFGD), Rodovia Dourados/Itahum, Km 12, Unidade II, Caixa Postal: 364, Cep: 79804-970, Dourados, MS, Brazil.
E-mail: alessandrasilva@ufgd.edu.br, lucianoantonio@ufgd.edu.br
[*]Corresponding author. E-mail: eliasmedeiros@ufgd.edu.br

ABSTRACT

Precipitation is an important object of study and plays an important role in the dynamics of rainfall distribution in a region. This study investigated the spatial and temporal variation of precipitation in the São Francisco River Basin (SFRB). A historical series of data from 1989 to 2018 was analyzed, and a random function was decomposed into trend and residual components for analysis of precipitation. Interpolation techniques were used to analyze precipitation spatial behavior over time, using high-resolution precipitation maps. Our results showed that the exponential model prevailed in four periods. The findings also showed a high precipitation variability in the SFRB and enabled us to monitor precipitation behavior over the years, as well as in the different sub-regions in SFRB. Finally, important information was obtained, enabling, for instance, the identification of vulnerable areas suffering from lack of rainfall.

Keywords: kriging, R software, variogram.

Mapeamento espacial da precipitação pluviométrica anual na Bacia Hidrográfica do Rio São Francisco

RESUMO

A precipitação é um importante objeto de estudo e desempenha um papel importante na dinâmica da distribuição da chuva em uma região. Este estudo teve como objetivo investigar a variação espacial e temporal da precipitação na Bacia do Rio São Francisco (SFRB). Uma série histórica de dados de 1989 a 2018 foi analisada. Uma função aleatória foi decomposta em componentes de tendência e de resíduos para análise de precipitação. Técnicas de interpolação foram utilizadas para analisar o comportamento espacial da precipitação ao longo do tempo, usando mapas de precipitação de alta resolução. Nossos resultados mostraram que o modelo exponencial prevaleceu em quatro períodos. Os resultados também mostraram uma alta variabilidade da precipitação no SFRB e nos permitiu monitorar o comportamento da precipitação ao longo dos anos, bem como nas diferentes sub-regiões da SFRB. Por fim, foram obtidas informações importantes que permitiram, por exemplo, identificar áreas vulneráveis e que sofrem com a falta de chuvas.

This is an Open Access article distributed under the terms of the Creative Commons Attribution License, which permits unrestricted use, distribution, and reproduction in any medium, provided the original work is properly cited.

Palavras-chave: Krigagem, Software R, Variograma.

1. INTRODUCTION

Precipitation is a hydrological variable with high temporal and spatial variability; therefore, its study is central to understanding rainfall distribution dynamics within a given region. Such information is of great importance to manage water resources directly related to commercial activities and urban supply (Medeiros *et al.*, 2019b). Moreover, precipitation variability becomes more accentuated when considering large drainage basins, such as the São Francisco River Basin (SFRB) (Silva and Clarke, 2004). In this sense, to better understand precipitation dynamics, the use of statistical modeling to interpolate non-sampled sites has arisen; however, it is not an easy task due to equipment malfunction, operating errors, or lack of adequate coverage of instruments in the region under study (Araújo *et al.*, 2020).

SFRB covers several states and municipalities and is of paramount importance to urban and rural populations. In this drainage basin, water resources are used for consumption, irrigation, livestock, and energy generation. Many fishermen and boatmen make their living from this area, and underground minerals and vegetation drive the local economy. Furthermore, although power generation through hydroelectric plants is sustainable, water supply depends on streamflows which, in turn, depend on climatic conditions, especially a regular rainfall distribution (Pereira Filho *et al.*, 2020).

The construction of high-resolution maps of rainfall levels in a region is of fundamental importance for hydrological planning, helping to manage water resources and reducing the risks caused by natural disasters, such as floods, erosion and droughts (Parker *et al.*, 2019). Data on precipitation levels in a region is usually obtained from locations where irregularly distributed rainfall stations are installed. Although increasing the amount of rain gauges seems to be a more adequate solution, this implies an increase in the operating price (Pirani and Modarres, 2020). Given this, there is a need to use interpolation methods in order to provide a continuous map of precipitation, especially in regions with a low density of pluviometers.

There are several interpolation methods in the literature, especially deterministic methods, such as those based on inverse distance weighting (IDW) and geostatistical methods, such as ordinary and universal kriging. Chen and Liu (2012) used the IDW method to interpolate rainfall data in the middle Taiwan region based on information from 46 rainfall stations, verifying that this method produces more accurate estimates in the dry period than in the rainy ones. Geostatistics is one of the known statistical methodologies for obtaining estimated values in non-sampled locations, providing high-resolution maps of interpolated values for the entire study region. Wanderley *et al.* (2013) stated that geostatistical techniques, such as kriging, are useful to generate maps and show results matching the reality. Medeiros *et al.* (2019a) analyzed a data set consisting of 269 rain gauge stations in the state of Paraíba and modeled the spatiotemporal dynamics of precipitation using geostatistical techniques to obtain rainfall interpolation maps. Likewise, Barros *et al.* (2020) used geostatistical tools to investigate the variability of mean annual precipitation in the state of Pernambuco, building a rainfall distribution map.

Some scientific research has used interpolation techniques to model the spatial distribution of precipitation in the SFRB. Silva and Clarke (2004) built variograms, geostatistical method, to study the spatial correlation of heavy rainfall in the SFRB for 100 years of return time, featuring 100-year rainfall return maps, concluding that climate difference between the regions that make up the basin and the orographic justify the high spatial variability of rainfall. Santos *et al.* (2017b) performed a detailed evaluation of drought in the upper San Francisco Basin, and used the IDW interpolation technique for building maps of monthly and annual rainfall based on daily data from the TRMM satellite.

In this sense, high-resolution precipitation maps have become a useful tool for managing water resources. Thus, this study investigated the spatial variation and sought to understand the rainfall mechanism in the SFRB, identifying priority sectors for a more detailed investigation of areas with a shortage of rainfall.

2. MATERIAL AND METHODS

The São Francisco River Basin (SFRB) covers 8% of the Brazilian territory. It has an extension of 2,863 kilometers and a drainage area of more than 639,219 square kilometers. The São Francisco River extends from the Canastra Mountains in Minas Gerais state to the Atlantic Ocean on the border between Alagoas and Sergipe states. This vast basin integrates the Northeast, Southeast, and Midwest regions of Brazil, covering six states (Minas Gerais, Goiás, Bahia, Pernambuco, Alagoas, and Sergipe) and 508 municipalities, which hold a population of 20,330,051 inhabitants (CODEVASF, 2021). In short, the São Francisco River becomes a strategic link between the Southeast and Northeast regions of Brazil.

The main reservoirs in the SFRB for streamflow control and power generation are Três Marias in Minas Gerais, Sobradinho, Paulo Afonso, and Itaparica in Bahia, and Xingó between Alagoas and Sergipe states. The basin encompasses different biomes, namely, Cerrado, Atlantic Forest, coastal and island biomes, and Caatinga (CBHSF, 2021). Along the SFRB, socioeconomic differences can be observed, ranging from wealthy and highly-populated to extremely poor and sparsely-populated areas.

The dataset used in this study refers to rainfall in the SFRB region, divided into four hydrographic regions: Upper, Middle, Sub-Middle, and Lower São Francisco (Figure 1a). Figure 1b there is a map of the spatial distribution of altitude in the SFRB, obtained through ordinary kriging, and it is possible to observe that the Upper SF and Lower SF regions have the highest and lowest altitude values, respectively.

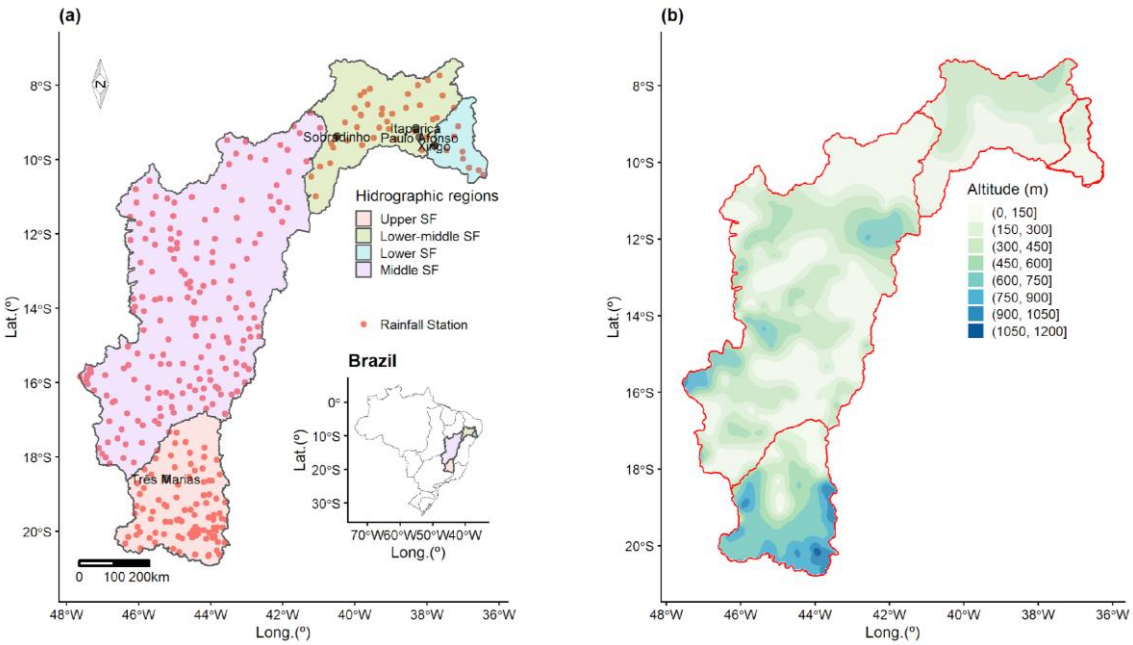

Figure 1. Maps of the hydrographic regions of the São Francisco River Basin (SFRB), highlighting its main reservoirs and 333 rain gauge stations (Figure 1a), and the spatial distribution of altitude (Figure 1b).

It is known that altitude influences the climatic conditions of a region. Cavalcanti and Côrrea (2015) report a linear relationship of 93% between altitude and rainfall in the Catimbau

National Park, Pernambuco. Petrungaro and Hora (2019) state that orographic configurations significantly influence the spatial distribution of precipitation in the basin that contributes to the Juturnaíba Dam, Rio de Janeiro.

It consisted of 333 rain gauge stations evaluated for 30 years (1989 to 2018), divided into five-year intervals to investigate the temporal behavior of precipitation. The data were gathered from the HidroWeb information system from the National Water Agency (ANA), which is available at the website http://hidroweb.ana.gov.br.

Descriptive measures of minimum, maximum, mean, median, standard deviation, and variation coefficient were used for data exploratory investigation every 5 years.

Geostatistical analysis of mean annual precipitation recorded in the 333 rain gauge stations considered the decomposition of random function $[Z(s)]$ into trend $[Y(s)]$ and stochastic residual $[\varepsilon(s)]$ components, as follows Equation 1:

$$Z(s) = Y(s) + \varepsilon(s) \tag{1}$$

In Equation (1), $Z(s)$ is the mean annual precipitation and s is the vector of geographical coordinates. A multiple linear regression fit was proposed for the analysis of trend component $Z(s)$, considering the linear effect of latitude, altitude and longitude, and quadratic effect of longitude. After the fitting, the coefficient of determination (R^2) was obtained to verify how much of the precipitation variability was explained by the trend.

The residuals obtained by the following regression $\hat{\varepsilon}(s) = Z(s) - \hat{Y}(s)$ were submitted to sample variogram (Webster and Oliver, 2007). Variogram theoretical models (spherical, exponential, and Gaussian) were fitted to sample variogram pseudo-data. Spatial dependence index (SDI), which is the ratio between nugget effect and sill, was also obtained (Cambardella *et al.*, 1994) and classified as follows: SDI ≤ 25% – strong spatial dependence, 25% < SDI < 75% – moderate spatial dependence, and SDI ≥75% – weak spatial dependence. Several works in the literature have used this index to measure the degree of spatial dependence in precipitation data in Brazil (Montebeller *et al.*, 2007; Gamero *et al.*, 2020).

A weighted least-squares method was used for model estimates, with weights being the ratio between the number of points and the square of their distances. In geostatistics there are different interpolation methods. In this research, the methods of Ordinary Kriging (OK) and Universal Kriging (UK) were proposed. After modeling the trend and obtaining estimates for theoretical variogram models, the next step was applying the OK and UK methods for interpolate annual rainfall values. Additionally, we use the IDW deterministic interpolation method in order to perform comparisons between these three methods. In this method, we insert a power value equal to 2, as recommended in the literature (Goovaerts 2000; Pirani and Modarres, 2020).

For selection of the interpolation method, we apply leave-one-out cross validation. This cross-validation consists of removing the value observed at a geographical coordinate s_i ($i = 1, 2, \ldots, 333$) and interpolating this value. To this end, root-mean-square error (RMSE), mean absolute error (MAE), and determination coefficient (R^2) were used to select the most suitable method for the interpolation. The lowest RMSE and MAE values and the highest R^2 values were sought for selection (Moriasi *et al.*, 2007).

After fitting and selecting the model, annual rainfall interpolation maps were built using a regular 50,000-point grid, with points equivalent to each interpolated value in an area of 12.82 square kilometers. All statistical analyses were conducted using the *R software* (R Core Team, 2018) and the *ggplot2* (Wickham, 2009) and *gstat* (Pebesma, 2004) libraries.

3. RESULTS AND DISCUSSION

Table 1 shows the descriptive measures for accumulated annual precipitation over 30 years

over a five-year interval. The analysis using information from the 333 rain-gauge stations in the SFRB showed that the highest annual mean (1143.7 mm) occurred from 1989 to 1993. A decrease in rainfall accumulation was also observed, except from 1999 to 2003. Such a decline continued over the periods and was reflected in the magnitude of the calculated means and medians. The coefficient of variation (CV) showed a variability higher than 30% for all periods, hence a high variability.

Table 1. Descriptive measures of accumulated annual precipitation in 333 rain-gauge stations in the São Francisco River Basin.

Period	Minimum	Maximum	Mean	Median	Standard deviation	CV (%)
1989–1993	367.8	2540.1	1143.7	1225.3	391.3	34.2%
1994–1998	390.8	2935.44	1124.3	1140.2	374.5	33.3%
1999–2003	86.4	1705.2	999.1	1026.3	332.9	33.3%
2004–2008	12.00	2087.4	1083.2	1092.5	374.2	34.5%
2009–2013	209.3	2031.8	1039.3	1086.7	387.5	37.3%
2014–2018	183.7	1457.3	797.3	805.3	294.4	36.9%

Climate changes in the SFRB are related to the transitioning from a humid and semi-humid climate in the Upper São Francisco to an arid and semi-arid climate in the Sub-Middle São Francisco. The climate in the SFRB area is strongly affected by rainfall indices, with mean annual precipitation between 400 and 1,500 mm, mean annual temperature from 18 to 27°C, and a low cloud cover, thus leading to a high solar radiation incidence (Pereira *et al.*, 2007; SINGREH, 2002). Dantas and Oliveira (2021) studied data from 39 rain-gauge stations in the SFRB, in the state of Minas Gerais, between 2014 and 2017 and found that precipitation ranged from 594 to 1730 mm, with a mean of 1,223 mm, a standard deviation of 310, maximum of 1,730 mm, and a minimum of 594 mm.

Figure 2 shows the behavior of precipitation as a function of longitude, latitude and altitude for each time interval. Note that latitude and altitude have a linear relationship and longitude a quadratic behavior in relation to total annual precipitation. Thus, in adjusting the trend we will use these effects on these components.

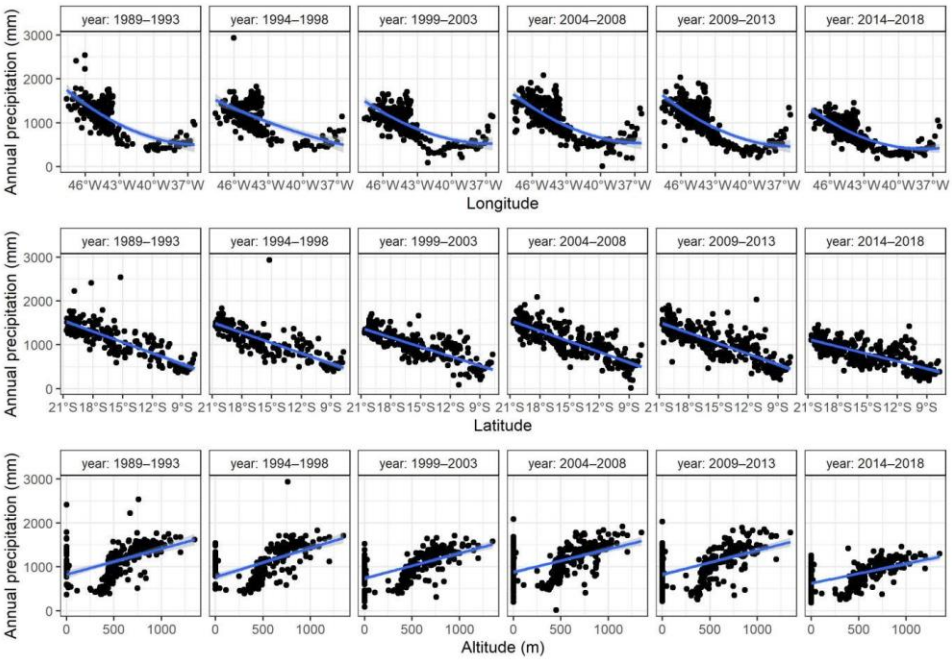

Figure 2. Annual precipitation data for the basin as a function of longitude, latitude and altitude.

Table 2 shows the estimates of the multiple regression model considering geographical coordinates as regressor variables. The variables were statistically significant ($P < 0.01$) in all six periods. The negative effects of latitude suggest that the accumulated annual precipitation decreases in the south-north direction in the study region. The high determination coefficients suggest that part of the spatial variability in accumulated precipitation within the SFRB can be explained by the trend component.

Table 2. Multiple linear regression model estimates of accumulated annual precipitation.

Variable	1989–1993	1994–1998	1999–2003	2004–2008	2009–2013	2014–2018
(Intercept)	6641**	6334**	5571**	6632**	6244**	3903**
Latitude	-0.5575**	-0.5742**	-0.4776**	-0.5771**	-0.5313**	-0.2874**
Longitude	-2.7376**	-1.8111**	-1.9654**	-2.0110**	-2.0965**	-1.9545**
Longitude²	0.0014**	0.0010**	0.0011**	0.0011**	0.0011**	0.0010**
Altitude	0.2358**	0.3185**	0.2544**	0.0884**	0.1235**	0.1776**
R^2	80.12%	73.69%	79.89%	78.56%	75.91%	75.14%

**Significant at 1% significance level by the t-test.

Table 3 shows the MAE, RMSE, and R^2 values obtained in the leave-one-out cross-validation for the interpolation methods IDW, Ordinary Kriging and Universal Kriging. In all scenarios, the methods based on geostatistics were superior to the deterministic IDW method, with the universal kriging interpolation presenting a better performance in four of the six time intervals. Ordinary Kriging presented the best interpolation in the periods comprising the years 2004 to 2013. Pirani and Modarres (2020) carried out a study in which they compared deterministic and geostatistical interpolation methods in rainfall data in the Zayandeh Rud Basin, Iran. In this study, the authors concluded that geostatistical interpolation methods produce better accuracies compared to deterministic methods, when considering a larger number of meters.

Table 3. Result of the leave-one-out cross-validation for the interpolation methods IDW, Ordinary Kriging and Universal Kriging.

Year	Variogram	Universal Kriging			Ordinary Kriging			IDW		
		MAE	RMSE	R^2	MAE	RMSE	R^2	MAE	RMSE	R^2
1989–1993	Spherical	100.47	167.58	81.6%	102.87	172	80.7%			
1989–1993	Exponential	99.92	166.82	81.8%	103.31	172.53	80.5%	121.21	177.62	79.3%
1989–1993	Gaussian	102.59	168.37	81.4%	126.5	197.28	75.4%			
1994–1998	Spherical	96.42	169.50	79.5%	97.06	172.47	78.8%			
1994–1998	Exponential	95.93	168.21	79.8%	97.09	172.53	78.8%	133.76	194.97	72.8%
1994–1998	Gaussian	96.13	165.41	80.4%	101.8	177.65	77.5%			
1999–2003	Spherical	78.50	115.87	87.8%	86.29	126.2	85.6%			
1999–2003	Exponential	78.97	116.19	87.8%	86.63	127.25	85.3%	112.48	152.38	79.0%
1999–2003	Gaussian	80.03	117.35	87.5%	110.31	152.35	80.3%			
2004–2008	Spherical	104.12	146.86	84.6%	102.04	141.14	85.7%			
2004–2008	Exponential	103.62	145.71	84.8%	101.61	140.86	85.8%	127.79	176.11	77.8%
2004–2008	Gaussian	105.30	147.05	84.5%	107.76	148.76	84.5%			
2009–2013	Spherical	104.58	157.65	83.4%	139.15	189.34	78.0%			
2009–2013	Exponential	102.05	155.71	83.8%	100.17	155.23	83.9%	135.14	193.66	75.0%
2009–2013	Gaussian	108.38	160.29	82.9%	158.55	207.56	73.6%			
2014–2018	Spherical	77.19	104.30	87.4%	77.43	104.5	87.4%			
2014–2018	Exponential	76.73	104.10	87.5%	77.46	104.5	87.4%	115.54	149.06	74.3%
2014–2018	Gaussian	78.39	106.01	87.5%	81.18	108.62	86.4%			

The exponential variogram model prevailed in four periods (1989–1993, 1994–1998, 2004–2008, 2009–2013 and 2014–2018), followed by the Gaussian and Spherical models from 1994–1998 and 1999–2003, respectively. Santos *et al.* (2017a) studied the rainfall seasonal behavior in the Brazilian semi-arid using geostatistical tools and observed that the spherical model had the best R^2 values for the analyzed variables. However, high R^2 values do not imply that the values fitted by the model are close to the observed ones, but that there is a strong linear relationship between them. Silva Neto *et al.* (2020) analyzed the annual maximum daily precipitation data for Tocantins state and the variogram models fitted were spherical, exponential, and Gaussian, with the spherical model being selected by mean absolute percentage error (MAPE).

Table 4 shows the highest sill estimate (74007.37) from 2009 to 2013, generating a range of 389 km. In the descriptive analysis, we verified that this was the period that presented the greatest variability of average annual precipitation, with a coefficient of variation of 37.3%. An inversion was observed from 1999 to 2003, reaching the lowest sill value (23285.90) and range of 368.81 km. A justification for this result is the fact that it was in this period that we observed one of the smallest variabilities of annual precipitation. Based on the spatial dependence index (SDI), it was noted that in all periods they presented a dependence classified as moderate, 25% < SDI < 75%, (Cambardella *et al.*, 1994). Similar results were found in a survey that modeled the spatial distribution of annual rainfall in the state of Paraná, between 1996 and 2015, estimating a moderate dependence in 16 of the 20 years analyzed (Gamero *et al.*, 2020).

Table 4. Estimates of the fitted variogram models for each of the six periods under study and spatial dependence index (SDI).

Year	Kriging	Model	Nugget	Sill	Range	SDI
1989–1993	Universal	Exponential	13865.66	49675.08	270.22 km	27.91%
1994–1998	Universal	Gaussian	13086.72	51637.18	180.32 km	25.34%
1999–2003	Universal	Spherical	10579.20	23285.90	368.81 km	45.43%
2004–2008	Ordinary	Exponential	13898.82	57729.62	176.46 km	26.36%
2009–2013	Ordinary	Exponential	24043.98	74007.37	471.89 km	32.49%
2014–2018	Universal	Exponential	8646.65	23335.71	155.36 km	37.05%

Figure 3 shows the rainfall distribution pattern along the hydrographic regions in the SFRB over the studied periods. The Upper São Francisco has high accumulated annual precipitation levels, which decrease mainly in the Sub-Middle region towards northeastern Brazil. The lowest precipitation indices were observed from 2014 to 2018 in all regions, with no rains above 1500 mm. The annual precipitation levels in the Sub-Middle decreased over time, with annual precipitation levels below 300 mm in the period from 2014 to 2018 in almost the entire region.

Assis *et al.* (2015) analyzed precipitation in the Sub-Middle of the SFRB from 1964 to 2014 and observed that, according to the rainfall anomaly index (RAI), the only dry years were between 1990 and 2000 and there was no positive RAI in 2012, which was classified as a dry and extremely dry year.

Furthermore, the Sobradinho Reservoir, with 320 kilometers of extension, is in the Sub-Middle of the SFRB, specifically within the municipalities of Sobradinho and Casa Nova, in the state of Bahia. This reservoir has a water surface of 4,214 km^2 and a storage capacity of 34.1 billion cubic meters at its nominal elevation of 392.50 m, making it the largest artificial lake in Brazil (CHESF, 2021). The useful volume (%) in the reservoir from 1999 to 2018, considering 5-year intervals, had a monthly mean of 67% of the useful volume from 2004 to 2008. However, this volume has decreased in the last decade, reaching a mean monthly percentage of 22% between 2014 and 2018 (ONS, 2021). Thus, our results reflect this worrying trend, as the period from 2014 to 2018 was the most critical regarding precipitation in the analyzed historical series.

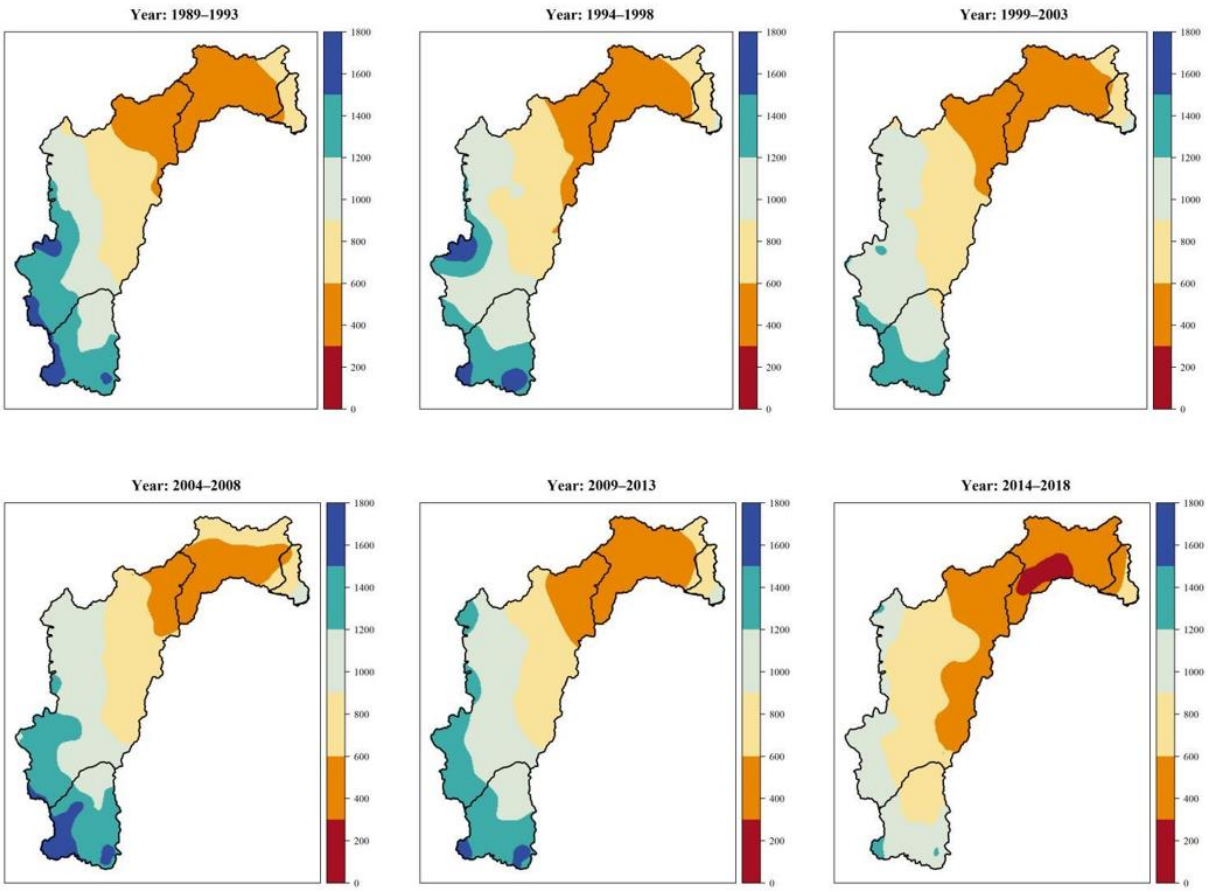

Figure 3. Map of accumulated annual precipitation (mm) in the São Francisco River Basin.

The variability of precipitation between the hydrographic regions of the SFRB is a result of the peculiar characteristics of each region. A comparison between Figure 1.b and Figure 3 makes it clear that regions with high altitudes tend to have high levels of precipitation. In addition, other factors contribute to this variability in precipitation, such as the climate in the SFRB and the proximity to the ocean in the region of the mouth of the São Francisco River. Upper São Francisco, in the part located in the state of Minas Gerais, has a high altitude, with a climate classified as humid. The middle São Francisco, as it represents the largest physiographic region of the basin, has different types of climate, with a climate similar to that of the Upper São Francisco; but the levels of precipitation decrease when entering the semi-arid region, and the climates are then classified as dry and sub-humid. semi-arid. The lower-middle of the basin is recognized as the driest part, with annual precipitation ranging from 350 to 800 mm and with an average annual temperature of 27ºC, being then defined as a semi-arid and arid climate. In the Lower São Francisco, due to its proximity to the ocean, the climate is a little milder, with an annual temperature of 25ºC and average annual precipitation ranging from 800 to 1,300 mm, with a climate ranging from semi-arid to sub-humid (Hermuche, 2002).

4. CONCLUSIONS

Geostatistical techniques allowed us to investigate the precipitation variability throughout the sub-regions within the São Francisco River Basin over 30 years. The sub-periods analyzed showed high variability, and the accumulated annual precipitation decreased over the years evaluated. The Sub-Middle region stands out as the most vulnerable in terms of rainfall shortages, which was mostly evident from 2014 to 2018.

The geographical coordinates were significant throughout the analyzed period, with latitude having a negative effect and signaling an annual decrease in precipitation towards the south-north direction in the São Francisco River Basin. In addition, the hydrographic regions that make up the basin have peculiar characteristics, thus justifying the difference in the spatial distribution of precipitation between these regions.

5. ACKNOWLEDGMENTS

The authors would like to thank the Federal University of Grande Dourados for financial support (Research Support Program (PAP) – PROPP Notice No. 02/2021) and for granting a Scientific Initiation scholarship to the first author of this research.

6. REFERENCES

ARAÚJO, H. L.; MONTENEGRO, A. A. A.; LOPES, I.; CARVALHO, A. A.; SILVA, E. C. E; GONÇALVES, G. E. Espacialização da precipitação na Bacia Hidrográfica do Rio Brígida no semiárido de Pernambuco. **Revista Brasileira de Geografia Física**, v. 13, n. 1, p. 391–405, 2020. https://doi.org/10.26848/rbgf.v13.1.p391-405f

ASSIS, J. M. O.; SOUZA, W. M.; SOBRAL, M. C. Climate analysis of the rainfall on sub‐medium part of the São Francisco River Basin based on the rain anomaly index. **Revista Brasileira de Ciências Ambientais (Online)**, v. 1, n. 36, p. 115–127, 2015. https://doi.org/10.5327/Z2176-947820151012

BARROS, T. H. S.; BENDER, F. D.; SILVA, F. R. B.; JOSÉ, J. V.; COSTA, J. O.; COELHO, R. D. Geoestatística como ferramenta para estudos da variabilidade da precipitação pluviométrica no estado de Pernambuco, Brasil. **Agrarian**, v. 13, n. 50, p. 513–520, 2020. https://doi.org/10.30612/agrarian.v13i50.11982

CAVALCANTI, L. C. S.; CORRÊA, A. C. B. Pluviosidade no parque nacional do Catimbau (Pernambuco): seus condicionantes e seus efeitos sobre a paisagem. **Geografia (Londrina)**, v. 23, n. 2, p. 133–156, 2015. http://dx.doi.org/10.5433/2447-1747.2014v23n2p133

CAMBARDELLA, C. A.; MOORMAN, T. B.; NOVAK, J. M.; PARKIN, T. B.; KARLEN, D. L.; TURCO, R. F. *et al.* Field-Scale Variability of Soil Properties in Central Iowa Soils. **Soil Science Society of America Journal**, v. 58, n. 5, p. 1501–1511, 1994. https://doi.org/10.2136/sssaj1994.03615995005800050033x

CBHSF. **Comitê da Bacia do Rio São Francisco**. 2021. Belo Horizonte, MG. Available in: https://cbhsaofrancisco.org.br/a-bacia/. Access at: 18 may 2021.

CHEN, F. W.; LIU, C. W. Estimation of the spatial rainfall distribution using inverse distance weighting (IDW) in the middle of Taiwan. **Paddy and Water Environment**, v. 10, n. 3, p. 209–222, 2012. https://doi.org/10.1007/s10333-012-0319-1

CHESF. **Sobradinho**: descrição do aproveitamento de sobradinho. 2021. Available in: https://www.chesf.gov.br/SistemaChesf/Pages/SistemaGeracao/Sobradinho.aspx. Access at: 15 may 2021.

CODEVASF. **São Francisco**. 2021. Available in: https://www.codevasf.gov.br/area-de-atuacao/bacia-hidrografica/sao-francisco. Access at: 19 may 2021.

DANTAS, G. D.; OLIVEIRA, L. A. Analysis of spatial continuity of precipitation in the são francisco river basin in its area of occurrence in the state of minas gerais-brazil, historical series 2004 to 2017. **Brazilian Journal of Development**, v. 7, n. 3, p. 23585–23595, 2021. https://doi.org/10.34117/bjdv7n3-190

GAMERO, P.; URIBE-OPAZO, M. A.; DE BASTIANI, F.; JOHANN, J. A.; GUEDES, L. P. C. Variabilidade espacial da precipitação no cultivo de milho segunda safra no Paraná utilizando o modelo Wave. **IRRIGA**, v. 25, n.3, p. 521–536, 2020. https://doi.org/10.15809/irriga.2020v25n3p521-536

GOOVAERTS, P. Geostatistical approaches for incorporating elevation into the spatial interpolation of rainfall. **Journal of hydrology**, v. 228, n. 1-2, p. 113–129, 2000. https://doi.org/10.1016/S0022-1694(00)00144-X

HERMUCHE, P. M. **O Rio de São Francisco.** Brasília: CODEVASF, 2002. 58 p. Available in: https://cdn.agenciapeixevivo.org.br/media/2019/06/Cartilha-sobre-o-Rio-S%C3%A3o-Francisco.pdf. Access at: 19 may 2021.

MEDEIROS, E. S.; LIMA, R. R.; OLINDA, R. A.; DANTAS, L. G.; SANTOS, C. A. C. Space–Time Kriging of Precipitation: Modeling the Large-Scale Variation with Model GAMLSS. **Water**, v. 11, n. 11, p. 1–16, 2019a. https://doi.org/10.3390/w11112368

MEDEIROS, E. S.; LIMA, R. R.; OLINDA, R. A.; SANTOS, C. A. C. Modeling Spatiotemporal Rainfall Variability in Paraíba, Brazil. **Water**, v. 11, n. 9, p. 1843, 2019b. https://doi.org/10.3390/w11091843

MONTEBELLER, C. A.; CEDDIA, M. B.; CARVALHO, D. F. D.; VIEIRA, S. R.; FRANCO, E. M. Variabilidade espacial do potencial erosivo das chuvas no Estado do Rio de Janeiro. **Engenharia Agrícola**, v. 27, p. 426-435, 2007. https://doi.org/10.1590/S0100-69162007000300011

MORIASI, D. N.; ARNOLD, J. G.; LIEW, M. W.; VAN; BINGNER, R. L.; HARMEL, R. D.; VEITH, T. L. Model Evaluation Guidelines for Systematic Quantification of Accuracy in Watershed Simulations. **Transactions of the ASABE**, v. 50, n. 3, p. 885–900, 2007. https://doi.org/10.13031/2013.23153.

ONS (Brasil). **Dados Hidrológicos**. 2021. Brasília, DF. Available in: http://www.ons.org.br/historico/geracao_energia.aspx. Access at: 14 may 2021.

PARKER, S. R.; ADAMS, S. K.; LAMMERS, R. W.; STEIN, E. D.; BLEDSOE, B. P. Targeted hydrologic model calibration to improve prediction of ecologically-relevant flow metrics. **Journal of Hydrology**, v. 573, p. 546–556, 2019. https://doi.org/10.1016/j.jhydrol.2019.03.081

PEBESMA, E. J. Multivariable geostatistics in S: the gstat package. **Computers & Geosciences**, v. 30, n. 7, p. 683–691, Aug. 2004. https://doi.org/10.1016/j.cageo.2004.03.012

PEREIRA FILHO, A. J.; PINTO, M. A. R. R. C.; MANFREDINI, L.; LIMA, F. A.; PINTO, A. C. E C.; MORIBE, C. H. *et al.* CESP Integrated Precipitation Estimation and Forecasting System for its Watersheds. **Revista Brasileira de Meteorologia**, v. 35, n. 4, p. 529–552, 2020. https://doi.org/10.1590/0102-7786352023

PEREIRA, S. B.; PRUSKI, F. F.; SILVA, D. D. DA; RAMOS, M. M. Study of the hydrological behavior of São Francisco River and its main tributaries. **Revista Brasileira de Engenharia Agrícola e Ambiental**, v. 11, n. 6, p. 615–622, 2007. https://doi.org/10.1590/s1415-43662007000600010

PETRUNGARO, A. C. N.; HORA, M. A. G. M. Avaliação das Secas Meteorológica e Hidrológica na Bacia Contribuinte à Barragem de Juturnaíba, Estado do Rio de Janeiro, Brasil. **Anuário do Instituto de Geociências**, v. 42, n. 4, p. 309–321, 2019. http://dx.doi.org/10.11137/2019_4_309_321

PIRANI, F. J.; MODARRES, R. Geostatistical and deterministic methods for rainfall interpolation in the Zayandeh Rud basin, Iran. **Hydrological Sciences Journal**, v. 65, n. 16, p. 2678–2692, 2020. https://doi.org/10.1080/02626667.2020.1833014

R CORE TEAM. **R: A language and environment for statistical computing.** Vienna, 2018.

SANTOS, W. M.; SOUZA, R. M. S.; SOUZA, E. S.; ALMEIDA, A. Q. DE; DANTAS ANTONINO, A. C. Spatial variability of rainfall seasonality in semi-arid region of Brazil. **Journal of Environmental Analysis and Progress**, v. 2, n. 4, p. 368–376, 2017a. https://doi.org/10.24221/jeap.2.4.2017.1466.368-376

SANTOS, C. A. G.; BRASIL NETO, R. M.; DE ARAÚJO PASSOS, J. S.; DA SILVA, R. M. Drought assessment using a TRMM-derived standardized precipitation index for the upper São Francisco River basin, Brazil. **Environmental Monitoring and Assessment**, v. 189, n. 6, p. 189–250, 2017b. https://doi.org/10.1007/s10661-017-5948-9

SILVA, B. C. DA; CLARKE, R. T. Análise estatística de chuvas intensas na bacia do rio São Francisco**. Revista Brasileira de Meteorologia**, v. 19, n. 3, p. 265–272, 2004.

SILVA NETO, V. L.; VIOLA, M. R.; MELLO, C. R.; ALVES, M. V. G.; SILVA, D. D.; PEREIRA, S. B. Heavy Rainfall Mapping for Tocantins State, Brazil. **Revista Brasileira de Meteorologia**, v. 35, n. 1, p. 1–11, 2020. https://doi.org/10.1590/0102-7786351017

SINGREH (Brasil). **Plano Nacional de Recursos Hídricos**. Diagnóstico das Regiões Hidrográficas – Versão 2: Bacia do Rio São Francisco. Brasília, 2002.

WANDERLEY, H. S.; AMORIM, R. F. C. DE; CARVALHO, F. DE O. Spatial interpolation of precipitation in the State of Alagoas utilizing technical geostatistics. **Campo Digital**, v. 8, n. 1, p. 34–42, 2013.

WEBSTER, R.; OLIVER, M. A. **Geostatistics for environmental scientists**. 2. ed. Chester: Wiley, 2007.

WICKHAM, H. **ggplot2: Elegant Graphics for Data Analysis**. New York: Springer, 2009

Ambiente & Água - An Interdisciplinary Journal of Applied Science
ISSN 1980-993X – doi:10.4136/1980-993X
www.ambi-agua.net
E-mail: ambi.agua@gmail.com

Decay process of free residual chlorine concentration affected by travel time in water distribution systems

ARTICLES doi:10.4136/ambi-agua.2830

Received: 21 Jan. 2022; Accepted: 18 Apr. 2022

Luciano de Oliveira[1]; Diana Rosa dos Reis[2]; Nora Katia Saavedra del Aguila Hoffmann[3*]

[1]Escola de Engenharia Civil e Ambiental. Programa de Pós-graduação em Engenharia Ambiental e Sanitária. Universidade Federal de Goiás (UFG), Avenida Universitária, n° 1488, CEP: 74605-220, Goiânia, GO, Brazil. E-mail: oliveira.luciano.eng@gmail.com
[2]Programa de Pós-graduação em Engenharia Agrícola. Universidade Estadual de Goiás (UEG), BR 153, Km 99, Zona Rural, CEP: 75132-903, Anápolis, GO, Brazil. E-mail: dianarosa22dr@gmail.com
[3]Departamento de Hidráulica e Saneamento. Programa de Pós-graduação em Engenharia Ambiental e Sanitária. Escola de Engenharia Civil e Ambiental da Universidade Federal de Goiás (EECA-UFG), Avenida Universitária, n° 1488, CEP: 74605-220, Goiânia, GO, Brazil.
[*]Corresponding author. E-mail: kasaavedra@ufg.br

ABSTRACT

Chlorination is the most widely used method for disinfecting water for human consumption. While the chlorinated water travels through a distribution system, the concentration of free residual chlorine (FRC) declines depending on the natural water characteristics. This study investigated FRC decay in two types of water sources – ground and surface water – with varied concentrations of organic compounds. The travel time variable depended on water consumption patterns of both distribution systems which attend low density populations and their initial project needs. Based on mathematical simulation techniques of water quality models, the study also investigated the effects of water temperature and total organic carbon (TOC) on the kinetic constants (k_b) of chlorine decay. Results show that travel time in the most critical locations in the water networks and the minimum disinfectant concentrations required at the entry points were 40 hours and 0.27-0.28 mg L^{-1} at Vale dos Pássaros housing complex, and 144 hours and 0.30-0.36 mg L^{-1} at Terras Alphaville housing complex.

Keywords: disinfection, TOC, water quality.

Decaimento da concentração de cloro residual livre influenciado pelo tempo de percurso nas redes de abastecimento de água

RESUMO

A cloração é o método mais utilizado para promover a desinfecção da água para consumo humano. Durante a passagem de água clorada em sistemas de abastecimento de água, a concentração de cloro residual livre (CRL) decai, cuja taxa de reação depende das características da água natural. Neste trabalho, foi avaliado a decadência da concentração de residual de cloro livre em dois tipos de água, subterrânea e superficial, com diferentes concentrações de matéria orgânica, sob a perspectiva da influência do tempo de deslocamento

This is an Open Access article distributed under the terms of the Creative Commons Attribution License, which permits unrestricted use, distribution, and reproduction in any medium, provided the original work is properly cited.

da água, dependente dos cenários de consumo nas redes de distribuição, cujos módulos de abastecimento são caracterizados por baixa adensamento populacional e operam sob as condições iniciais de demanda previstas nos projetos. Foi considerado o efeito da temperatura e do carbono orgânico total (COT) sobre os valores das constantes cinéticas de decaimento de massa (k_b), utilizadas nos modelos matemáticos que simulam a qualidade da água. Os tempos de viagem nos nós mais críticos e as concentrações mínimas de desinfetante na entrada do módulo de abastecimento para cumprir a legislação foram iguais a 40 horas e 0,27-0,28 mg L^{-1} para as redes de distribuição do condomínio Vale dos Pássaros e 144 horas e 0,30-0,36 mg L^{-1} para o condomínio Terras Alphaville.

Palavras-chave: COT, desinfecção, qualidade da água.

1. INTRODUCTION

Appropriate knowledge of the behaviour of FRC concentration as it travels through water distribution systems assists in meeting the minimum and maximum residual disinfectant levels allowed by regulations and also ensures the quality of the water reaching the population. According to the World Health Organization (WHO), water contamination can occur by viruses classified as moderately and highly harmful to health: Hepatitis A and E, rotavirus and more recently the coronavirus (García-Ávila *et al.*, 2021). Thus, public water systems are required to monitor the behaviour and the disinfectant concentration to maintain acceptable levels in more distant areas and to meet the minimum residual chlorine concentration throughout the day, ranging from 0.10 mg L^{-1} to 0.20 mg L^{-1} (Ozdemir and Buyruk, 2018; Ababu *et al.*, 2019).

From the moment it is applied at the chlorination or rechlorination points, chlorine reacts with the organic and inorganic matter present in the liquid mass, resulting in the decay of its residual concentration over time. Due to the reactions between chemical species present in the water in the runoff volume (mass degradation) and with the iron released by corrosion, deposits and biofilms at the interface of the tube wall (wall decay) the concentration of FRC decreases along the pipes of the distribution networks in supply systems (Rossman, 2000; Liu *et al.*, 2015; Monteiro *et al.*, 2017). The decay of free chlorine in the liquid mass occurs due to the reaction with many substances, mainly with dissolved organic matter.

On the other hand, chlorine reacts with natural organic matter present in the water, forming disinfection by-products, such as trihalomethanes (THMs), and exposure to them can pose risks to human health. For this reason, in many countries, regulatory agencies have imposed maximum THM concentration limits for drinking water (Abhijith *et al.*, 2021).

Generally, the monitoring of water quality parameters at specific points in the network, including residual chlorine, is determined by a sampling plan that becomes the main option in technical management, including to verify compliance with legislation. This form of monitoring may not be the most appropriate, as the periods and locations of sample collection are not representative and do not demonstrate the actual behavior of the disinfectant in the supply system. In order to satisfy regulatory requirements and consumer needs in relation to the quality of treated water, management entities feel the need to better understand the movements and transformations that water intended for human consumption is subject to within distribution systems.

According to Rossman (2000), the water quality simulation model allows monitoring the growth or decay of a substance due to reactions as it moves along the water distribution network. Chlorine decay models are useful for managers of drinking water supply systems to predict the residual chlorine concentration across the network under various hydraulic conditions (García-Ávila *et al.*, 2021). The degradation of the FRC can be modeled by some known computer software that simulates the hydraulic behavior and water quality in distribution networks.

Examples are EPANET, which is free to access, and WaterCAD, which is commercially available (Izinyon *et al.*, 2010).

Prior to the development of EPANET software, basic nonlinear equations were solved using the Hardy-Cross method, which makes successive approximations from a set of initial guesses (Ibarra-Berastegi and García-Arriba, 2017). To make such predictions, it needs to know both the bulk and wall reaction rates, as well as the manner in which these rates are affected by the residual concentration. Meanwhile, EPANET allows a modeler to treat these two reaction zones separately. The coefficient of the total decay reaction rate (k), for the specific study of the reactions that occur inside the pipes of supply networks is represented by the sum of the coefficients kb (mass degradation) and kw (wall decay) (Rossman, 2000).

Studies have shown that the increase in the concentration of total organic carbon (TOC) caused an increase in the values of the "kb" coefficient (Powell *et al.*, 2000; Al Heboos and Licskó, 2017; Saidan *et al.*, 2017). Another important point to be considered is that different types of natural water cause different behaviors in the decay of the concentration of residual free chlorine in the distributed water. Sanabria and De Julio (2013) carried out a study to adjust the kinetic models found in the bibliography and concluded that, from the chlorine decay tests, it was possible to observe that of the three samples collected in different springs, those of underground origin had lower levels of chlorine reaction with chlorine.

The decay of the FRC depends directly on the travel time of the water inside the system and the residence time in the reservoirs. This effect is mainly verified in the initial years of operation in which the number of connections can still be relatively low, characterizing consumptions lower than the dimensioned ones that will correspond to low flow velocities and longer travel times. When the pressure in the distribution network decreases, the corresponding flow will be lower and the hydraulic residence time (water age) will be longer. An increase in residence time allows the chlorine concentration to decrease (Coelho *et al.*, 2006; Olaia, 2012; Seyoum *et al.*, 2012).

Water temperature has an effect on the decay of chlorine content, according to what has been concluded in most studies to date (Ozdemir and Buyryk, 2018), being one of the factors that most influence decay rates in systems of drinking water (Monteiro *et al.*, 2017). Tests performed on samples of treated water showed lower residual chlorine values, for the same time t, at higher temperatures (Monteiro *et al.*, 2015), under the same conditions of flow velocity and water age (Eck *et al.*, 2016).

This study uses the EPANET software to model calibrated hydraulic calculations and water quality behaviour as a means of assessing FRC bulk decay rates in two existing water-distribution systems. One of them is a surface water source and the other a groundwater source. Moreover, organic compound concentrations, travel time according to water consumption patterns among the population, and water temperature were also analysed.

2. MATERIAL AND METHODS

2.1. Study sites

This study investigated FRC decay in water supply networks serving the Vale dos Pásssaros and Terras Alphaville housing complexes (Figures 1 and 2). The raw water features are determined, respectively, by the surface water source drawn from Ribeirão Caldas in the Agroindustrial District of Anápolis – DAIA's water supply system, and by the groundwater source from Terras Alphaville's independent supply system. These survey locations are part of the water distribution system (WDS) in the city of Anápolis, in the state of Goiás (Brazil), and were selected considering that the number of connections to the systems indicated consumption data values below the demand forecast. Additionally, they have clearly marked areas of distribution.

Figure 1. Critical nodes for data evaluation after simulation: Vale dos Pássaros (N1798).

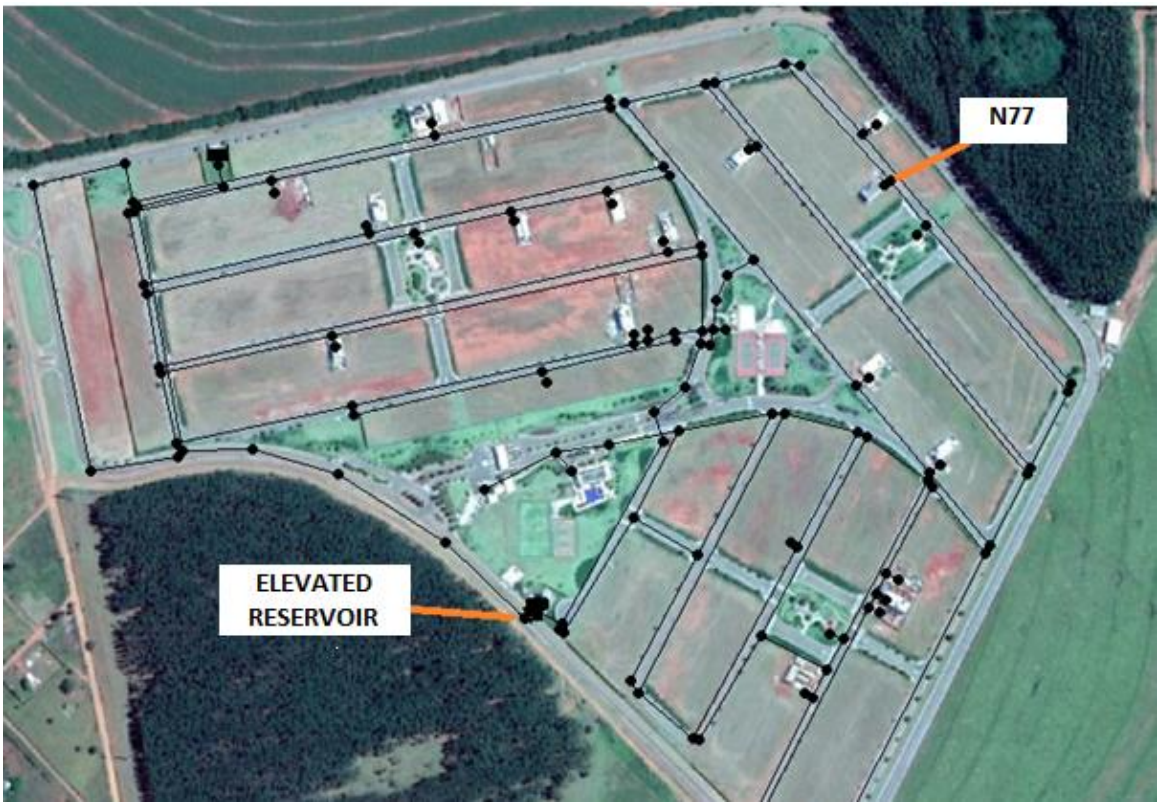

Figure 2. Critical nodes for data evaluation after simulation: Terras Alphaville (N77).

2.2. Scenarios to model

Scene 1: Simulation of travel time through each distribution system to identify the location receiving the last portion of water from the reservoir's exit point, considering consumer patterns.

Scene 2: Simulation of disinfectant decay in each distribution system, considering consumer patterns, to identify the initial chlorine concentration sufficient to ensure FRC of 0.2 mg L^{-1} in all nodes for different k_b coefficients obtained from bottle tests, depending on temperature variations.

2.3. Obtaining the kinetic coefficients "k_b" under the influence of temperature

Chlorine decay in the mass of water was evaluated by "bottle tests" (Monteiro *et al.*, 2017;

Ozdemir e Buyruk, 2018; Powell *et al.*, 2000; Saidan *et al.*, 2017; Sanabria and De Julio, 2013; García-Ávila *et al.*, 2021). Results were recorded onto forms and the measured data were processed by using Excel, which were then graphically represented. Decay rates in the mass of water were drawn from a graph value of $\ln(C_t/C_0)$ as a function of time recorded in hours.

Surface water samples were collected before chlorine application at the exit point of filter Number 1 in DAIA's treatment plant (16°25'32.63" S latitude and 48°54'41.60" O longitude), which serves the standing distribution reservoir at Vale dos Pássaros housing complex. The treatment process is of the conventional type.

Groundwater samples were collected from the discharge line of a submersible pump installed in a deep tube-well, before chlorine application, near the entry point of the standing reservoir at Terras Alphaville housing complex (16°21'4.11"S latitude and 48°52'50.56"O longitude), where the water is treated by simple disinfection process.

Samples were collected in 100 mL flasks, properly packed in a 1.5 L styrofoam box with ice and immediately sent to the laboratory of the Regional Center for Technological Development and Innovation - CRTI, located on the Samambaia Campus, of the Federal University of Goiás, in the city of Goiânia-GO (Brazil), for the analysis of the total carbon content using the Shimadzu TOC-L equipment. Measurements were performed in triplicate, with results equal to the average of the acquired values of organic and inorganic carbon present in the sample.

2.4. Model construction

2.4.1. Description of flows and consumption

The survey on the total volume of distribution involved the analysis of daily readings made by devices installed at the outlet of each water supply system. The study data also included microvolume levels and reference periods (base consumption) provided by reports from the company's commercial information system, which are consistent with the period of the macro network performance report, providing an oversight on physical losses within the sector.

2.4.2. Operational control

Information on operating conditions and routines of both distribution systems during simulations were obtained from technical record drawings, the information system for operation control, field study data, control charts and interviews with staff responsible for operating gate and pressure-relief valves as well as reservoir maintenance.

2.4.3. Model simulations

Reactions in the bulk flow (k_b) were the main input parameters during water quality simulations. Results show rates of water flow, velocity, mass deterioration, average reaction and FRC concentration along the tubes. Simulations have been modelled using EPANET 2.0, a reliable and free software used throughout the world.

2.4.4. Model calibration

The hydraulic model calibration used to simulate water quality and assess travel time and behaviour of FRC measured the amount of pressure in strategic points throughout the WDS, the water flow at the entry points (outlet of the water tanks) as well as consumption rates, aiming to define the consumption pattern and spatial distribution of demand.

Measurements of pressure within the distribution systems were recorded over a 24-hour period with a pressure gauge placed in key points of the network. Flow-through reservoir outlets were automatically measured and registered. Flow measurements were gathered at the entry point of the WDS between 01 February and 03 May 2018 at the Vale dos Pássaros complex and between 06 and 18 June 2018 at the Terras Alphaville complex.

In system areas with significant mass degradation or pressure, mean absolute errors

between observed and simulated values were ± 2.0 m. It was also observed that the simulated flow rates should be within the 5% range of measured flows (Walski, 2003). However, the absolute value of maximum deviation was recalculated according to the precision of measuring instruments and to the limitations identified during calibration.

2.5. Data analysis

Bulk values related to flow, pressure, consumption and physico-chemical parameters are presented as average values, including those in the system information reports.

3. RESULTS AND DISCUSSION

3.1. Values of kinetic coefficients "k_b" depending on TOC and temperature

Non-chlorinated water samples from DAIA's WDS at 20.2°C showed TOC measurements of 0.4798 mg L^{-1} after filtration. The raw water samples collected from the tubular well at the reservoir's entrance integrated to the Terras Alphaville WDS at 27.5°C show TOC measurements of 0.1740 mg L^{-1}.

For initial chlorine concentrations of 1 mg L^{-1} ± 0.05, the coefficient values of mass decay k_b as a function of temperature are presented in Table 1.

Table 1. Values of "k_b" (d^{-1}) depending on temperature (°C): a) Groundwater samples; b) Surface water samples.

(a)		
Temperature (°C)	Initial concentration of FRC (mg L^{-1})	k_b (d^{-1})
20 a 21	$C_0$20=0,97	0,0264
30 a 31	$C_0$30=1,04	0,0480
(b)		
Temperature (°C)	Initial concentration of FRC (mg L^{-1})	k_b (d^{-1})
20 a 21	$C_0$20=0,94	0,0888
30 a 31	$C_0$30=1,05	0,1200

3.2. Description of the physical components of the supply sectors

The WDS at the Vale dos Pássaros housing complex is formed by two integrated systems composed of PVC pipes with nominal diameters of 50-100 mm, measuring a total of 3,336.40 m in length. It also has five iron valves with nominal diameters of 50-75 mm. It is made up of fifty-nine singular characteristics such as curves, reductions and tees, including the valves made of PVC or iron.

The WDS at the Terras Alphaville housing complex is formed by three integrated systems composed of pipes with nominal diameters of 50-150 mm, all made of DeFoFo and PVC (with diameters equivalent to those of the iron pipes), measuring a total of 10,355.33 m in length. It also has three iron control valves with nominal diameters of 50 mm. It is made up of one hundred and six singular characteristics such as curves, reductions and tees, including the valves made of PVC or iron.

The standing metallic tank at Vale dos Pássaros measures 6.68 m in diameter, has a total storage capacity of 120 m^3, and maximum water depth and level of 1,098 m and 1,101.30 m respectively. Chlorine concentrations at the exit point of the reservoir are determined by the dosage applied to DAIA's WDS, varying in accordance to system operation.

The standing concrete tank at the Terras Alphaville complex measures 6.10 m in diameter, has a total storage capacity of 150 m^3, and maximum water depth and level of 1,056.85 and 1,062.25 m, respectively. Chlorine concentration at the exit point of the reservoir is determined by the dosage applied inside the standing tank, varying in accordance to system operation.

3.3. Survey of consumption

Results related to flow rates and physical degradation during the survey period are shown in Table 2 for Vale dos Pássaros complex and for the Terras Alphaville complex in Table 3.

Table 2. Losses in the supply system at the Vale dos Pássaros housing complex.

Month/year	Macromeasured volume (m^3)[1]	Micromeasured volume (m^3)[2]	Losses (m^3)	Loss index (%)
Oct/17	2003	1055	948	47.33
Nov/17	2370	886	1484	62.62
Dec/17	2995	805	2190	73.12
Jan/18	2551	883	1668	65.39
Feb/18	1126	1003	123	10.92
Mar/18	1038	933	105	10.12
Apr/18	997	922	75	7.52

Source: Saneago (2018).
[1]There were daily readings on the measuring equipment.
[2]There was a monthly reading on the measuring equipment between the days 01 and 05.

Table 3. Losses in the supply system at the Terras Alphaville housing complex.

Month/year	Macromeasured volume (m^3)[1]	Micromeasured volume (m^3)[2]	Losses (m^3)	Loss index (%)
Oct/17	349	255	94	26.93
Nov/17	245	170	75	30.61
Dec/17	212	167	45	21.23
Jan/18	298	261	37	12.42
Feb/18	232	206	26	11.21
Mar/18	231	201	30	12.99
Apr/18	296	262	34	11.49

Source: Saneago (2018).
[1]There were daily readings on the measuring equipment.
[2]There was a monthly reading on the measuring equipment between the days 08 and 10.

Analysis of reports on "Control and Leaks in Neighbourhood areas – RS382B" (Saneago, 2018) showed no significant leak occurrences at Vale dos Pássaros and no leakage at Terras Alphaville.

At Vale dos Pássaros, a total of 38 water bills are issued by the first system within its WDS, a total of 23 by its second system, and the bill of the administration area of the housing complex is linked to the main system. At Terras Alphaville, its three integrated systems issued a total of eleven (11), six (6) and seven (7) water bills, respectively.

Each water bill showed associated base consumption rates obtained during predetermined periods and were generated by reports which were also issued by the information system. Consumption data were recorded from 01 February 01 to 03 May 2018 at the Vale dos Pássaros complex, and from 11-18 June 2018 at the Terras Alphaville complex.

During these periods, flow rates at the exit points provided average consumption rates, which divided by the mean daily value, were able to determine multiple factors viewed as a

consumption pattern, then inserted in EPANET 2.0 for modelling. Flow rates obtained from the information system's database were illustrated in tables and graphs in 15-minute intervals.

The average consumption patterns that covered the working days of the week, Saturday and Sunday, within the periods considered and the average consumption patterns of Sunday and Monday used in the simulations in EPANET 2.0 are represented in Figures 3 and 4.

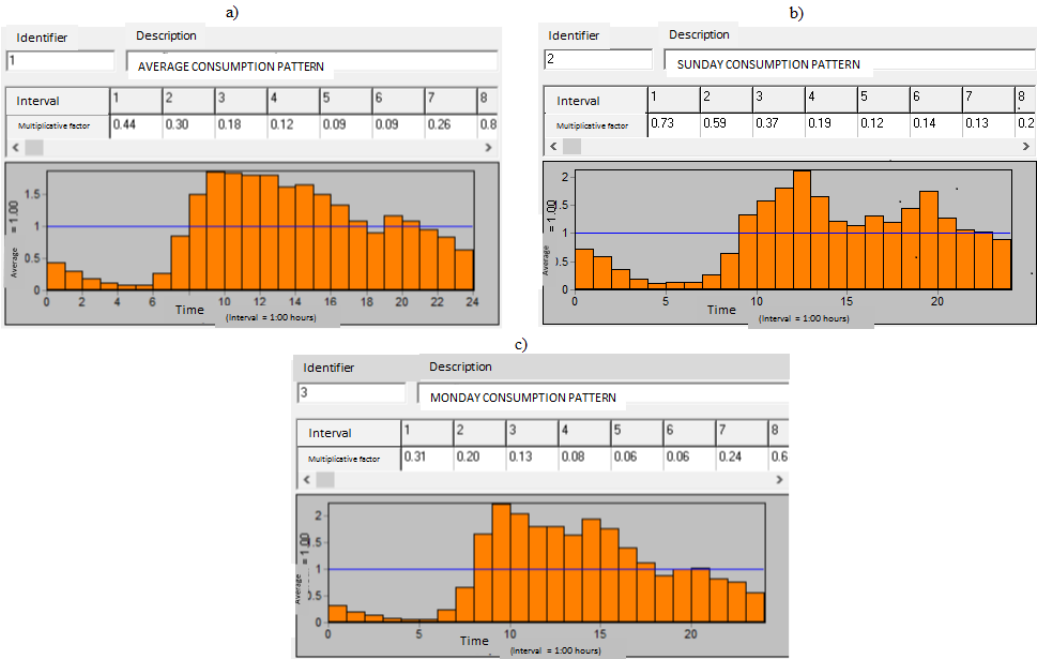

Figure 3. Consumption pattern in EPANET. Vale dos Pássaros in the period from 01/02/2018 to 03/05/2018: a) average consumption; b) Sunday consumption; c) Monday consumption. **Source:** EPANET.

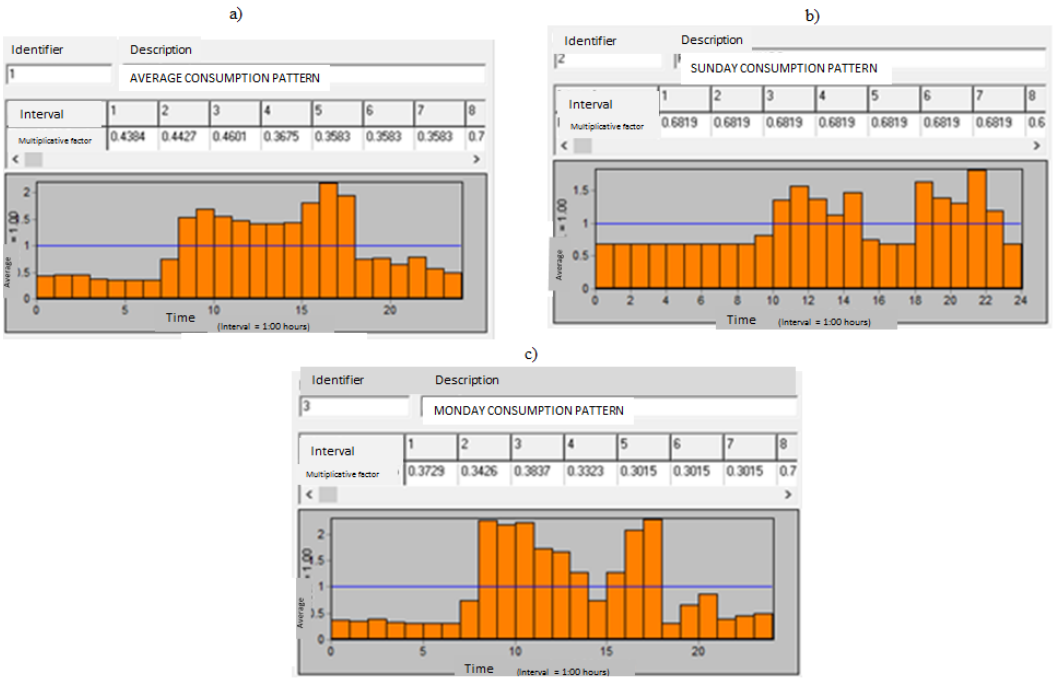

Figure 4. Consumption pattern in EPANET. Terras Alphaville in the period from 11/06/2018 to 18/06/2018: a) average consumption; b) Sunday consumption; c) Monday consumption. **Source:** EPANET.

It was found that the residences are of high constructive standard. During the field surveys, it was possible to perceive the high purchasing power of users, indicating that probably the high consumption on Monday is due to the fact that domestic services are preferably performed on this day of the week. The decrease in domestic activities is identified by Sunday consumption patterns.

3.4. Operational control detail

The inflow to the standing reservoir serving Vale dos Pássaros originates at the top. Its flow is controlled by a mechanical float level device in which the valve opens/closes the inlet pipe according to the level of the water.

The water serving the standing reservoir at Terras Alphaville is pumped up from a deep well through a pipe located at its top. The submersive pump works automatically, shutting down whenever the maximum and minimum water level points are reached.

Daily readings of both reservoir levels showed a relatively low variation of water level during the study period. Moreover, around 7.1 and 40.3% of all projected piped water connections for Terras Alphaville and Vale dos Pássaros were built, respectively. Both of these facts indicate low consumption rates, reduced flow velocity and long periods of water travel. Average hourly consumption rates were analysed between 25 January and 01 June 2018.

3.5. Simulations in EPANET

Hydraulic modelling results reproduced the behaviour of the existing WDS in terms of the flow and pressure variables. Similarly, water quality modelling results replicated FRC concentrations and travel time. EPANET 2.0 evaluated them as variable-level reservoirs. To carry out FRC decay simulations, each critical location was the basis for application of the initial quality parameter. Once network input data was incorporated by the software application along with consumption pattern information, pressure and flow calibrations were made. The results are described in Tables 4 to 7.

Table 4. Statistical treatment of pressure calibration data in the Vale dos Pássaros complex.

Localization	Observed number	Observed average (mca)	Simulated average (mca)	Absolute mean error (mca)	Standard deviation
2269563-0	24	34,33	32,99	1,344	1,447
2269528-1	24	35,13	37,93	2,805	3,380
Network	48	34,73	35,46	2,074	2,600

Table 5. Statistical treatment of calibration data for flow in the Vale dos Pássaros complex.

Localization	Observed number	Observed average (L s^{-1})	Simulated average (L s^{-1})	Absolute mean error (L s^{-1})	Standard deviation
Reservoir output	24	0,37	0,36	0,009	0,011
Network	24	0,37	0,36	0,009	0,011

Table 6. Statistical treatment of pressure calibration data in the Terras Alphaville complex.

Localization	Observed number	Observed average (mca)	Simulated average (mca)	Absolute mean error (mca)	Standard deviation
2314843-8	24	21,71	23,03	1,325	1,343
Network	24	21,71	23,03	1,325	1,343

Table 7. Statistical treatment of calibration data for flow in the Terras Alphaville complex.

Localization	Observed number	Observed average (L s^{-1})	Simulated average (L s^{-1})	Absolute mean error (L s^{-1})	Standard deviation
Reservoir output	24	0,17	0,17	0,001	0,001
Network	24	0,17	0,17	0,001	0,001

Mean absolute errors between observed and simulated values reached the initial prediction (± 2,0 m). There was no need to check the obtained data and there were no complications that required more complex critical analyses regarding the calibration results. The differences between observed and simulated values were satisfactory due to the fact that the study areas have a reliable technical record with traceable operation procedure information, such as accurate records of pressure within pressure-relief valves and low incidence of physical deterioration.

Adequate knowledge of users' consumption patterns and the adoption of these base consumptions as being at the water connection points themselves, without using the artifice of concentrating these consumptions at the ends of the stretches, combined with the fact that simplifications of the networks were also not adopted. Distribution in the model leads to the conclusion that this may also have significantly influenced the obtainment of observed and simulated values close together.

The hydraulic calibration models allowed simulations on EPANET 2.0 as described in Scene 1 as well as the assessment of travel time in average consumption on Sundays and Mondays.

Analysis of temporal series of results produced by the software application shows that travel time to the critical zone in the Vale dos Pássaros distribution system was 42 hours attending consumption patterns on Sundays, 40 hours on Mondays and 40 hours as the average consumption time.

The travel time in the Terra Alphaville distribution system reached a total of 144 hours attending consumption patterns on Sundays, Mondays and average consumption.

Pressure behaviour data in Terras Alphaville was measured on 13 June 2018 during a 24-hour period. Low variability pressure rates ranged between 20.81 and 22.07 mca, validating the simulated values. This indicated consumption rates below the predicted values, resulting in longer periods of travel time compared to those observed at Vale dos Pássaros, even though the latter serves a higher density population and has a shorter length of total distribution pipeline.

Residual chlorine decay simulations occurred in scenarios with various mass reaction coefficients (k_b) obtained as a function of temperature variation (Table 1). Additionally, other coefficients obtained from the bottle tests were used. These were chlorinated water samples gathered from the exit points of the reservoirs.

Considering that this study aims to investigate FRC in the water supply systems, analysis of the disinfectant behaviour was not compromised even though k_b values were obtained from samples gathered at the exit point of DAIA's WDS and from raw groundwater instead of other samples from the reservoirs' exit points.

K_b values were obtained from water samples submitted to progressive and controlled temperature variations in the laboratory, ranging between 25 and 30°C.

Once the model is calibrated in EPANET software, it can be used to predict chlorine concentrations for various water supply needs (Danieli *et al.*, 2006; Fischer *et al.*, 2016; Sharif *et al.*, 2017).

In Scenario 2, to ensure the minimum residual concentration of 0.20 mg L^{-1} required by Brazilian regulations, values were randomly inserted using a trial and error method.

By using various simulated mass reaction coefficient values (k_b), namely k_b = 0.0528 d^{-1},

k_b = 0.0888 d^{-1} and k_b = 0.1200 d^{-1}, the minimum required chlorine concentrations obtained from Vale dos Pássaros tested samples were C_0 = 0.27 mg L^{-1}, C_0 = 0.27 mg L^{-1} and C_0 = 0.28 mg L^{-1}, respectively.

TOC results are consistent with another study that investigated FRC kinetic behaviour in samples gathered from three raw surface water sources, which showed different values of 2.1 ± 0.3 mg L^{-1}, 5.0 ± 0.9 mg L^{-1} and 3.3 ± 0.6 mg L^{-1} (Ferreira Filho and Sakaguti, 2008). Researchers concluded that the higher the amounts of TOC removed by coagulation, the lower the chlorine demand values. This suggests water coagulation has a larger impact on chlorine decay in liquid mass whenever it maximizes the removal of natural organic compounds.

K_b values shown in Table 1 indicate a larger reaction to the disinfectant with the substances present in surface water and also with higher test temperatures in both water sources. Results show a direct proportion between temperature range and FRC decay kinetic coefficient, which is consistent with results obtained from other studies (Eck *et al.*, 2016; Fischer *et al.*, 2012; Powell *et al.*, 2000; Saidan *et al.*, 2017).

A similar correlation occurred regarding the temperature range of the bottle tests, which was the same as the one adopted in this research (between 20 and 30°C). Samples were submitted to pre-oxidation with ozone, coagulation, flocculation, sedimentation, rapid sand filtration and final disinfection with chlorine. For example, after 100 hours, samples measuring between 20 and 30°C with the same initial disinfectant concentrations showed FRC rates of 0.20 m L^{-1} and 0.05 mg L^{-1}, respectively (Monteiro *et al.*, 2017).

Notwithstanding the reaction coefficient with the mass of water or travel time, initial FRC rates below the minimum requirements (equal to zero) were only found in samples obtained from a section of the WDS interrupted by a cap, located just before the entry point of the housing complex. It suggests that the residence time was high at this point resulting in significant reduction in disinfectant concentration.

Analysis of data simulation of FRC behaviour in samples from Terras Alphaville's water supply system resulted in initial chlorine concentrations of 0.30 mg L^{-1}, 0.31 mg L^{-1} and 0.36 mg L^{-1} for simulated mass reaction coefficient k_b = 0.0216 d^{-1}, k_b = 0.0264 d^{-1} and k_b = 0.0480 d^{-1}, ensuring minimum residual disinfectant concentrations at the most critical locations in the water network.

García-Ávila *et al.* (2021) obtained the mean value of kb equal to 3.7 d^{-1} and used it to simulate the decay of free residual chlorine in a distribution network using the EPANET software. They found that at the outlet of the supply reservoir it was necessary to maintain a minimum concentration equal to 0.87 mg L^{-1} to comply with the minimum value allowed by local legislation. However, the minimum value of 0.5 mg L^{-1} allowed by the WHO to fight the coronavirus was not reached in 45% of the samples from the nodes evaluated. The authors also observed that the value of k_b was lower (0.12 h^{-1}) for samples collected in the month that presented lower temperatures and higher (0.19 h^{-1}) for higher temperatures.

Many locations along Terras Alphavilles's supply system showed values below the minimum concentration required, considering the simulations with the minimum dosage to ensure 0.20 mg L^{-1} in the critical zone. This may be due to the lack of demand along these locations, therefore showing a higher residence time.

Relatively low mass reaction coefficient were obtained for 20 and 30°C (Table 1, a and b) as well as for 25 and 30°C. Results from a research study carried out in 2010 showed k_b values of 0.0642 d^{-1}, 0.1316 d^{-1} and 0.1989 d^{-1} for 15, 20 and 30°C temperatures, respectively. Researchers considered them low coefficient values due to low TOC levels in the water (between 0.10 mg L^{-1} and 1.02 mg L^{-1} and average of 0.34 mg L^{-1}), which resulted in lower chlorine demand (Karadirek *et al.*, 2015; Al Heboos and Licskó, 2017; Madzivhandila and Chirwa, 2017).

Even though low k_b values were used to simulate FRC behaviour for both ground and

surface water samples, results show variations in disinfectant decay in some locations of the WDS.

Simulations developed in EPANET may be used to achieve initial target concentrations (C_0) necessary to obtain a specific product of disinfectant concentration-time (C_t) for primary disinfection, and also to study the minimum required concentration through every point in the system for secondary disinfection and the maximum acceptable concentration for aesthetic purposes.

4. CONCLUSION

The adopted methodology allowed analysis of the decay of the concentration of free residual chlorine during the course of water in supply networks. The results indicated the need for knowledge about the behavior of the disinfectant depending on the type of water, characterized by the concentration of organic matter and the temperature variation.

The variation in temperature ranges and concentrations of organic matter present in the samples used in the tests and the influences of these parameters demonstrated the need for detailed simulator studies in order to determine ideal values of the kinetic constants of chlorine decay in mass (k_b) in distribution networks to be used in simulation models, according to the characteristics of the waters that may vary throughout the year depending on seasonality.

EPANET successfully simulated the water travel times and the decay of residual chlorine in the supply networks. The results pointed to an efficient management tool that helps in decision-making when defining the sampling plan collection points for a given area and stipulates minimum values of FRC concentrations at the entry points of module supplies and consumption points, in this case, avoiding waste of chemical products for treatment. These technical assessments help to ensure public health and meet legal requirements.

5. REFERENCES

ABABU, T. T.; TESFAMARIAM Y. D.; STANLEY, J. N. Um Modelo Matemático para Taxas Variáveis de Decadência de Cloro. **Sistemas de Distribuição de Água, Modelagem e Simulação em Engenharia**, v. 2019, p. 1-11, 2019. https://doi.org/10.1155/2019/5863905

ABHIJITH, G. R.; KADINSKI, L.; OSTFELD, A. Modeling Bacterial Regrowth and Trihalomethane Formation in Water Distribution Systems. **Water,** v. 13, n. 4, 2021. https://doi.org/10.3390/w13040463

AL HEBOOS, S.; LICSKÓ, I. Application and Comparison of Two Chlorine Decay Models for Predicting Bulk Chlorine Residuals. **Periodica Polytechnica Civil Engineering,** v. 6, n. 1, p. 7-13, 2017. https://doi:10.3311/PPci.9273

COELHO, S. T.; LOUREIRO, D.; ALEGRE, H. **Modelação e análise de sistemas de abastecimento de água**. Manual, sperie IRAR-LNEC. Lisboa: Edições IRAR, 2006.

DANIELI, R. D.; GASTALDINI, M. C.; BARROSO, L. B. Modelagem do cloro residual em redes de distribuição – aplicação ao sistema de abastecimento de Santa Maria. **Revista Brasileira de Recursos Hídricos,** v. 11, n. 4, p. 201-208, 2006.

ECK, B. J.; SAITO, H.; MCKENNA, S. A. Temperature dynamics and water quality in distribution systems. **IBM Journal of Research and Development,** v. 60, n. 5-6, p. 1-8, 2016. https://doi:10.1147/JRD.2016.2594128

FERREIRA FILHO, S. S.; SAKAGUTI, M. Comportamento cinético do cloro livre em meio aquoso e formação de subprodutos da desinfecção. **Revista Engenharia Sanitária e Ambiental**, v. 13, n. 2, p. 198-206, 2008. https://doi.org/10.1590/S1413-41522008000200010

FISCHER, I.; KASTL, G.; SATHASIVAN, A. A suitable model of combined effects of temperature and initial condition on chlorine bulk decay in water distribution systems. **Water Research,** v. 46, n. 10, p. 3293-303, 2012. https://doi:10.1016/j.watres.2012.03.017

FISCHER, I.; KASTL, G.; SATHASIVAN, A. A comprehensive bulk chlorine decay model for simulating residuals in water distribution systems. **Urban Water Journal**, v. 14, n. 4, p. 361-368, 2016. https://doi:10.1080/1573062X.2016.1148180

GARCÍA-ÁVILA, F.; AVILÉS-AÑAZCO, A.; ORDOÑEZ-JARA, J. Modeling of residual chlorine in a drinking water network in times of pandemic of the SARS-CoV-2 (COVID-19). **Sustainable Environment Research**, v. 31, n. 12, 2021. https://doi.org/10.1186/s42834-021-00084-w

IBARRA-BERASTEGI, G.; GARCÍA-ARRIBA, R. Using open source software in engineering studies to teach water operation & management. *In:* IEEE GLOBAL ENGINEERING EDUCATION CONFERENCE (EDUCON), 25-28 Apr. 2017, Athens, Greece. **Documents[...]** IEEE, 2017. https://doi.org/10.1109/EDUCON.2017.7943030

IZINYON, O. C.; ANYATA, B. U. Modelling Water Age as Surrogate for Water Quality in a Distribution System: Modelling Water Age for Water Quality. **Ciências Biológicas - PJSIR**, v. 53, n. 4, p. 187-191, 2010.

KARADIREK, I. E.; KARA, S.; MUHAMMETOGLU, A.; MUHAMMETOGLU, H.; SOYUPAK, S. Management of chlorine dosing rates in urban water distribution networks using online continuous monitoring and modeling. **Urban Water Journal**, v. 13, n. 4, p. 345-349, 2015. https://doi.org/10.1080/1573062X.2014.992916

LIU, M. J.; CRAIK, S.; ZHU, D. Z. Determination of cast iron pipe wall decay coefficient for combined chlorine in a municipal water distribution system. **Canadian Journal of Civil Engineering**, v. 42, p. 250-258, 2015. https://dx.doi.org/10.1139/cjce-2014-0449

MADZIVHANDILA, V.; CHIRWA, E. M. N. Modeling Chlorine Decay in Drinking Water Distribution Systems using Aquasim. **Chemical Engineering Transactions**, v. 57, p. 1111-1116, 2017. https://doi.org/10.3303/CET1757186

MONTEIRO, L.; FIGUEIREDO, D.; COVAS, D.; MENAIA, J. Integrating water temperature in chlorine decay modelling: a case study. **Urban Water Journal**, v. 14, n. 10, 2017. https://doi.org/10.1080/1573062X.2017.1363249

MONTEIRO, L.; VIEGAS, R. M. C.; COVAS, D. I. C.; MENAIA, J. Modelling chlorine residual decay as influenced by temperature. **Water and Environment Journal**, v. 29, n. 3, p. 331-337, 2015. https://dx.doi.org/10.1111/wej.12122

OLAIA, A. I. S. **Gestão de Sistemas de Abastecimento de Água através de Modelação Hidráulica**. 2012. 120f. Dissertação (Mestrado em Engenharia do Ambiente – perfil Engenharia Sanitária) - Faculdade de Ciências e Tecnologia da Universidade de Nova Lisboa, Lisboa, 2012.

OZDEMIR, N. O.; BUYRUK, T. Effect of travel time and temperature on chlorine bulk decay in water Supply pipes. **Journal of Environmental Engineering**, v. 144, n. 3, 2018. https://doi.org/10.1061/(ASCE)EE.1943-7870.0001321

POWELL, J. C.; HALLAM, N. B.; WEST, J. R.; FORSTER, C. F.; SIMMS, J. Factors, which control bulk chlorine decay rates. **Water Research,** v. 34, n. 1, p. 117–126, 2000. https://doi.org/10.1016/S0043-1354(99)00097-4

ROSSMAN, L. A. **EPANET 2.0 – Users manual**. Cincinnati: USEPA, 2000.

SAIDAN, M. N.; RAWAJFEH, K.; NASRALLAH, S.; MERIC, S.; MASHAL, A. Evaluation of factors affecting bulk chlorine decay kinetics for the zai water supply system in Jordan. Case study. **Environment Protection Engineering**, v. 43, n. 4, p. 223-231, 2017. https://doi.org/10.5277/epe170417

SANEAGO. **Método ME08.0068** – Determinação da temperatura da água e do ar. Goiania, 2018. p. 2.

SHARIF, M. N.; FARAHAT, A.; HAIDER, H.; AL-ZAHRANI, M. A.; RODRIGUEZ, M. J.; SADIQ, R. Risk-based framework for optimizing residual chlorine in large water distribution systems. **Environmental Monitoring and Assessment**, v. 89, n. 7, p. 307- 314, 2017. https://doi.org/10.1007/s10661-017-5989-0

SANABRIA, J. M.; DE JULIO, M. Decaimento do cloro residual em águas de abastecimento do município de Campo Grande/MS. **Revista de Engenharia e Tecnologia**, v. 5, n. 4, p. 92-104, 2013.

SEYOUM, A. G.; TANYIMBOH, T. T.; SIEM, C. Assessment of water quality modelling capabilities of EPANET multiple species and pressure-dependent extension models. **Water Science & Technology: Water Supply,** p. 1161-1166, 2012. https://dx.doi.org/10.2166/ws.2013.118

WALSKI, T. **Advanced water distribution modeling and management.** Watertown: E. Hasted Press, 2003. p. 1-800.